Danian calcareous nannofossil evolution and taxonomy with focus on sites from the North Atlantic Ocean (IODP Expedition 342 Sites 1403 and 1407)

Paul Bown, Hojung Kim, Samantha Gibbs

Department of Earth Sciences, University College London, Gower Street, London, WC1E 6BT, UK; p.bown@ucl.ac.uk

Abstract Danian nannofossil taxonomy is problematic because many of the new taxa that appeared in the aftermath of the Cretaceous/Paleogene (K/Pg) mass extinction were exceptionally small (<3µm), simply constructed, morphologically similar, and inconspicuous when observed using cross-polarised light microscopy. As both identification and classification are challenging, this makes comparison of data from different workers difficult, and significantly hinders the analysis of broader questions regarding post-extinction evolutionary rates and the timing of ocean recolonisation and ecosystem recovery. Here we provide an illustrated account of Danian nannofossil taxonomy using two Integrated Ocean Drilling Program Expedition 342 sites - 1403 and 1407 - that together provide a complete Paleocene composite section with good calcareous nannofossil preservation. Site 1403 includes a K/Pg boundary section that has an intact spherule layer and appears to be stratigraphically complete. The Site 1407 section is incomplete across the boundary interval, due to a stratigraphic gap, but above this there is an almost complete Paleocene section with good nannofossil preservation. We describe the Danian nannofossil recovery succession recorded at both sites, focusing particularly on the survivorship record and emergence of new Cenozoic lineages. The sites reveal a succession of acme intervals, recording the incoming of new taxa and lineages, with *Neobiscutum*, *Cruciplacolithus*, *Praeprinsius*, *Coccolithus* and *Toweius* being especially notable. We attempt to bring consistency to the taxonomy of these groups and address the

practicality and logic of the higher taxonomy, especially the use of the genera *Prinsius*, *Praeprinsius*, *Futyania* and *Toweius*.

Keywords Danian, Cretaceous/Paleogene boundary, calcareous nannofossils, *Praeprinsius*

1. Introduction

Danian nannofossil taxonomy is especially difficult for reasons that are virtually unique to this time interval. First, the incoming Cenozoic lineages are almost all initially represented by very small coccoliths (2 μm or less) that share common morphological and crystallographic features, i.e., placoliths with V-unit shield elements and R-unit tube cycles, resulting in very similar bicyclic appearance in cross-polarised light (XPL). These include *Neobiscutum*, *Praeprinsius*, *Cruciplacolithus*, *Coccolithus, Prinsius* and *Toweius*. A number of these taxa are also virtually invisible in light microscope (LM) using XPL (*Neobiscutum* and early *Praeprinsius*) and can only be clearly seen using phase-contrast (PC) illumination. Second, their taxonomy has been obfuscated by type descriptions being largely based on scanning electron microscope (SEM) images, but which have later been questionably linked to LM observations, leading to usage that may not conform to the holotype images or original descriptions. Such problems are especially prevalent in the *Praeprinsius*-*Prinsius* group. For example, the species name *Prinsius dimorphosus* is often used for very small circular forms (Varol, 1989), despite the SEM holotype and original description highlighting an elliptical outline (Perch-Nielsen, 1969; see further discussion below). In addition, lowermost Danian sediments are often characterised by significant mixing and reworking, and determining which fossils are *in situ* and which are 'contamination' can be difficult, leading to uncertainty over survivorship *vs*. extinction (Pospichal, 1994; Minoletti et al. 2005; Bown, 2005a).

Due to these combined challenges of very small specimens and problematic taxonomy, it has become difficult to confidently compare the nannofossil results of different vintages and workers. This means that studies that aim to better understand Cretaceous/Paleogene (K/Pg) evolutionary rates, recovery histories and the timing of the post-extinction radiation may not be comparing equivalent taxonomies and/or stratigraphic records. Here, we describe the Danian nannoplankton recovery succession from Integrated Ocean Drilling Program Expedition (IODP Exp.) 342 sites 1403 and 1407, which provide good nannofossil preservation in a stratigraphically-complete Danian composite section. We focus on the survivorship record and new incoming Cenozoic lineages, providing a fully-illustrated description of the Danian nannofossil assemblages and laying out a consistent and logical taxonomic framework.

2. Material and methods

2.1 IODP sites 1403 and 1407: biostratigraphy and age models

Figure 1 here

IODP Exp. 342 cored two sites with K/Pg boundary sections, sites 1403 and 1407, located around 240 km apart on the J-Anomaly and Southeast Newfoundland ridges (SENR) in the NW Atlantic Ocean (Figure 1). Based on the shipboard data and age models, Site 1403 (4944.3 mbsl) has a relatively low sedimentation-rate Oligocene to Paleocene sequence, with minor hiatuses and intervals of low to no carbonate (Norris et al., 2014). A high-resolution cyclostratigraphic age-model has been developed for the Maastrichtian to lower Paleocene section, which appears to be stratigraphically complete, with an intact spherule layer at the K/Pg boundary and good nannofossil preservation in the lower Danian (Norris et al., 2014; Batenburg et al., 2018; Hull et al., 2020) (Figure 2). Site 1407 (3073.13 mbsl) has a relatively high sedimentation-rate Oligocene through Paleocene section and a lower sedimentation-rate Upper Cretaceous section (Norris et al., 2014). The Maastrichtian to Paleocene section at Site 1407

(3073.13 mbsl) is relatively complete but the K/Pg boundary itself is missing with an unconformity between uppermost Cretaceous nannofossil chalks of Subzone UC20c and lower Danian of Zone NP2, possibly due to coring disturbance (Norris et al., 2014) (Figure 2).

Figure 2: here

Herein, we use the cyclostratigraphic age model of Hull et al. (2020) for Site 1403 and present an updated age model for Site 1407, based on our higher-resolution nannofossil biostratigraphy. While this paper is concerned principally with improving taxonomic consistency for the main nannofossil groups encountered in the Danian, we should stress that this clarification of the taxonomy does not impact the biostratigraphy of the sections, for which we use well-established index species. Specifically, the nannofossil biozonation of Martini (1971) was applied using bioevent calibrations from Gradstein et al. (2012) (see Norris et al., 2014 fig. F5 for the Exp. 342 timescale). We use the terms Base for the first or lowest stratigraphic occurrence of a species, and Top for the last or highest stratigraphic occurrence. Note that we have followed previous reinterpretation of the taxonomic status of the Zone NP2 index species, applying Base *C. intermedius* as the marker, given the considerable uncertainty about the historic application of the name *C. tenuis sensu lato* (e.g., Perch-Nielsen, 1985; van Heck and Prins, 1987; Varol, 1989; Fornaciari et al., 2007; Thibault et al., 2018). *C. intermedius* is a large *Cruciplacolithus* (>7µm) with axial crossbars and *C. tenuis sensu stricto* has cross bars with disjunct terminal elements known as 'feet'. We also applied the CNP zones of Agnini et al. (2014) (Figures 3 and 5; Appendices 1 and 3) but this zonation is relatively untested in the Danian interval and there are taxonomic problems associated with several of the marker species, e.g., *P. dimorphosus* (Zone CNP3), *P. martinii* (Zone CNP4) and early *T. pertusus* (Zone CNP5) (see below). Our revised age model for Site 1407 is primarily based on our updated biostratigraphy, together with a new isotopic tie point (the late Danian event [LDE] carbon isotope excursion) identified by Yamaguchi et al. (2017). For Site 1403, the age model uses our updated nannofossil

biostratigraphy incorporated into the Hull *et al.* (2020) cyclostratigraphic model (see Section 3 below).

2.2 Nannofossil preparation and observation

Nannofossils were studied using both light and scanning electron microscopy. Samples were prepared for LM observation using standard smear slide techniques (Bown and Young, 1998) and for SEM observation, using both smear slide and raw rock-chip preparations (Gibbs et al., 2020; Lees et al., 2004). We used Olympus BX51 and Zeiss Axiophot LMs with XPL and PC at x1000, and a JEOL Digital JSM-6480LV SEM. Phase contrast was routinely applied to determine the distribution of *Neobiscutum* and early *Praeprinsius*. Forty-five samples were examined in the SEM to confirm the high-quality preservation that is evident in the LM, and to determine fine morphological structures and coccosphere morphologies.

2.3 Sampling strategy and assemblage data

Samples were taken at highest resolution through the lowermost Danian post-K/Pg recovery interval and at lower resolution through the remainder of the Danian. One hundred samples were studied from Site 1403 with a sampling interval of 2-10 cm (~4–20 kyr) in the lower Danian (66.02 to 64.71 Ma) and 30 cm (~50–60 kyr) for the rest of Danian (up to 63.02 Ma). Twenty-three samples were studied from Site 1407 with a sampling interval of 5-30 cm (~30–480 kyr) from 65.50 to 63.44 Ma and 40-110 cm (~35–100 kyr) for the rest of Danian (212.49–202.5 m core composite depth below sea floor [CCSF]). Samples were logged both semiquantitatively and quantitatively to determine diversity, biostratigraphic events and community compositions most effectively (see Bown and Young, 1998; Bralower, 2002). For semiquantitative analysis, every sample was examined over at least three transects (~200 fields of view [FOV]) and the abundance of each species was recorded using the following categories:

A - abundant >10 specimens/FOV, C - common 1-9 specimens/FOV, F - few 1 specimen/1-10 FOV, and R - rare 1 specimen/>10 FOV. This approach improves the likelihood of recording very rare taxa, because 10s of thousands of specimens are encountered, compared with quantitative count methods which tend to view far fewer specimens (1000s at most). For quantitative analysis, 22 samples were counted from Site 1403 with a sampling interval of 20 cm (~40–60 kyr) in the lowermost Danian (66.02–65.45 Ma) and of 40 cm (~80–100 kyr) through the remainder of the Danian (65.45–64.71 Ma). For Site 1407, the same samples were studied for both quantitative and semiquantitative analysis. A minimum of the first 300 nannofossil specimens were counted from randomly chosen fields of view with comparable particle density. In general, this required around 10–15 FOV but within the acme intervals (i.e., intervals dominated by one species) this was achieved after ~4–5 FOV. The number of calcisphere and planktonic foraminifera fragments were also counted but are not included in the relative abundance calculations and are plotted separately as specimens per FOV.

2.4 Morphometric data

Size measurement of coccoliths and coccospheres was carried out to help refine the taxonomy of the early Danian small Prinsiaceae taxa. This included >1500 measurements of *Praeprinsius vegrandis* sp. nov. coccoliths from 45 samples, >2000 measurements of *Praeprinsius tenuiculus* coccoliths from 60 samples, and 30 measurements of *Toweius selandianus* coccoliths (from sample 1407A-23-1, 59cm). From each sample, 50 *Praeprinsius* specimens were imaged in LM from randomly chosen FOVs for coccolith size measurement. A total of 144 coccospheres were measured mainly of *P. tenuiculus*. Measurements of *Prinsius dimorphosus* (5 specimens) and *Prinsius martinii* (6 specimens) were largely based on their coccosphere images from SEM (see Figure 11), as these were rare in our material and the former could not be definitively identified in LM. Images were taken using the Qcapture programme and lengths were measured using the

Image J programme (https://imagej.net). For individual coccoliths, maximum length was recorded (C_L) and for coccospheres, C_L of one coccolith per sphere, cell size (the internal dimension of the coccosphere, approximating to the size of the cell, Θ_{cell}), and the number of coccoliths that form the coccosphere (C_N) (see Gibbs et al., 2018).

2.5 Additional sample material

A small number of additional lower Danian samples (Zones NP1-3) from different locations were studied for comparative purposes. These included 21 samples from El Kef (Tunisia; 36°09'13.2"N and a longitude of 8°38'54.8"E), six samples from ODP Site 738 (Kerguelen Plateau, Southern Ocean; 62°42.54'S; 82°47.25'E), six samples from ODP Site 1049 (Blake Nose, North Atlantic Ocean; 30°08.5436'N; 76°06.7312'W), two samples from ODP Site 1262 (Walvis Ridge, South Atlantic Ocean; 27°11.15'S; 1°34.62'E), six samples from ODP Site 690 (Maud Rise, Weddell Sea, Southern Ocean; 65°9.629'S; 1°12.296'E) and six samples from the North Sea Basin. Where appropriate these samples are noted next to taxon images in the plates.

3. Results

3.1 Lithology, preservation and nannofossil biostratigraphy

3.1.1 Site 1403

Figure 3 and Table 1 summarise the stratigraphic distribution of nannofossils and key biohorizons recorded at Site 1403. A full stratigraphic range chart is given in Appendix 1 and count data in Appendix 3. The K/Pg boundary is marked at 247.69 m CCSF by a spherule layer and an abrupt colour change (Figure 2). The upper Maastrichtian sediment is greyish-green nannofossil clay and contains diverse Cretaceous nannofossil assemblages, including the uppermost Cretaceous marker species *Micula prinsii*. The spherule layer is ~0.5 cm thick and dark-green in colour (see also Loroch et al., 2016). Immediately above the spherule layer, is a

1 cm-thick dark-green chalk with abundant calcispheres, which is overlain by light-brown Danian nannofossil chalk (Norris et al., 2014). The lithological identification of the K/Pg boundary is confirmed by the nannofossil record, which shows an abrupt increase of calcispheres and presence of the first Paleogene taxon, *Biantholithus*, immediately above the spherule layer. *Neobiscutum parvulum* and the very small *Praeprinsius vegrandis* sp. nov. appeared successively within 20 kyr (+5 cm) of the K/Pg boundary at 247.64 m CCSF. *N. parvulum* rapidly increased in abundance and dominated the nannofossil assemblage for at least 80 kyr between +50 and +130 kyr, with peak relative abundance of over 90% within 60 kyr of its first occurrence (+79 kyr; +23 cm above boundary, 247.46 m CCSF) (Figure 6). This *acme* is the first of a series that characterises the Danian (see Section 3b), where we use the term acme to refer to an interval of dominance during which the relative abundance of a species reaches over 30-50% of the total assemblage.

Figure 3: here

Table 1: here

Nannofossil preservation is generally good throughout the Zone NP1-NP2 interval at Site 1403 but deteriorates in upper Zone NP2. Here the lithology shifts to red clay as the site came under the influence of the calcite compensation depth (CCD) and non-calcareous sediments dominate for much of the remainder of the Paleocene section (Norris et al., 2014). The Base of *Cruciplacolithus intermedius* and Base *Chiasmolithus danicus* mark the lower boundaries of zones NP2 and NP3, respectively, recorded in samples 1403A-26-4, 10 cm (246.18 m CCSF) and 1403A-26-1, 10 cm (241.68 m CCSF). Base *C. intermedius* is slightly lower than reported by the shipboard scientists. The base of Zone NP4 was not definitively identifiable due to the absence of the index species *Ellipsolithus macellus* at this level. Danian representatives of *Ellipsolithus* are small and fragile and tend to be sensitive to preservation state (Bown, 2016),

and are likely absent here due to the worsening preservation quality through this interval. The problems associated with the reliability of this biohorizon are well documented (Backman, 1986) and it was excluded from the recent Agnini et al. (2104) zonation scheme. The Base of *Fasciculithus magnicordis/magnus* has been suggested as an alternative indicator for the lower boundary of Zone NP4 (Backman, 1986), and its presence in sample 1403A-25-2, 35cm (234.57 m CCSF) is used here.

3.1.2 Site 1407

For Site 1407, we have revised the shipboard age model of Norris et al. (2014) using higher sampling resolution. This includes 12 additional samples from outside of the shipboard splice, from 1407A-23-2, 125 cm (215.68 m CCSF) to 1407A-22-5, 63 cm (211.08 m CCSF). Figure 5 and Table 4 summarise the stratigraphic distribution of nannofossils and key biohorizons recorded at Site 1407. A full stratigraphic range chart is given in Appendix 2 and count data in Appendix 3. The K/Pg boundary interval is missing at Site 1407 with an unconformity (details below) between the uppermost Cretaceous (Subzone UC20c) and lower Danian (Zone NP2). There is no obvious lithological change across the unconformity (Figure 2) and the lithology is dominated by light beige nannofossil chalk and ooze, which continues through the Danian. Nannofossil preservation is generally very good throughout the Danian, indicated by the presence of abundant coccospheres, very small coccoliths (<3 μm) and delicate structures such as central area grills (see Plates 2, 4 and 5). The oldest Danian sample falls near to the Zone NP1/NP2 boundary, indicated by the presence of *C. intermedius* alongside *N. parvulum* and *Futyania petalosa* (Figure 4). Zones NP3, NP4 and NP5 were identified by the incoming of *C. danicus*, *E. macellus* and *F. tympaniformis*, respectively. The level of the Base *E. macellus* event is uncertain in this section, as the species is very rare with sporadic distribution (Appendix 3). The species *Ellipsolithus pumex*, however, was identified more consistently and at the same

level as the first *E. macellus* specimen (~63.8 Ma), close to, but slightly older than, the current age calibration for the *E. macellus* biohorizon (Figure 4). Note also that *Sphenolithus* was not present in our Danian samples at Site 1403 and so the CNP6 Zone could not be applied. The Base of *Fasciculithus magnicordis/magnus* has been used as an approximation for the lower boundary of Zone NP4 (Backman, 1986), and its position in the Site 1407 section provides additional support for the identification based on the rare occurrence of the index species (Figure 4).

The new nannofossil data from the lowermost Danian samples (below 212.44 m CCSF) are not consistent with the shipboard splice correlations. For example, sample 1407C-20-5, 125cm (214.13 m CCSF) from the shipboard splice is from the *Futyania petalosa* acme interval, but sample 1407A-23-1, 125 cm from the equivalent CCSF-m in Hole A, is from the *Praeprinsius tenuiculus* acme, suggesting a slightly younger age. We have focused on samples from Hole A, as the interval between Sample 1407A-22-5, 63 cm (211.08 m CCSF) and 1407A-23-2, 125 cm (215.68 m CCSF, our oldest sample point) better captures the lower part of the *Praeprinsius vegrandis* acme, despite being outside of the shipboard splice. Using biostratigraphy, we have integrated the Hole A samples, providing revised depths (CCSFr) for the interval between 1407A-23-1, 0 cm (212.93 m CCSF–212.44 m CCSFr) and 1407A-23-2, 125 cm (oldest sample point, 215.68 m CCSF–215.19 m CCSFr) (Table 2).

The K/Pg boundary interval is missing at Site 1407 and our best estimate for the age of the oldest Danian section, where *C. intermedius* is already present (indicating Zone NP2), is based on *Cruciplacolithus* morphometric data comparison (100 specimens per sample) with Site 1403. The size profile of *Cruciplacolithus* liths in the oldest Danian sample at Site 1407 compares best with sample 1403A-26-4, 0-10 cm from Site 1403, which has an estimated age of 65.47

Ma and an average lith size of 4.67 µm (based on 100 specimens). *Cruciplacolithus* size increases very rapidly during this part of the Danian and we therefore consider coccolith size a useful supplementary tool for correlation here. As well as the revised biostratigraphic data we have also added a geochemical tiepoint, the LDE carbon isotope excursion (214.74 m), identified by Yamaguchi et al. (2017).

Table 2-3: here

Figures 4-5: here

Table 4: here

3.1.3 Correlating sites 1403 and 1407

The stratigraphically highest Danian nannofossil assemblages at Site 1403 are comparable with those of the lowermost Danian at Site 1407, and we estimate an interval of stratigraphic overlap equivalent to 65.5–64.7 Ma. Some aspects of the assemblages are slightly different, however, for example: 1) *Futyania petalosa* is rare at Site 1403 but forms a striking acme at Site 1407; 2) the *Praeprinsius tenuiculus* acme is observed at both sites but is relatively more prominent at Site 1407; and 3) *Braarudosphaera* and *Octolithus* are present in higher abundances at Site 1407 (the latter is virtually absent at Site 1403). These differences likely reflect poorer preservation at the deeper water Site 1403 (4944.3 mbsl *vs* 3073.13 mbsl at Site 1407), which became more strongly affected by the CCD towards the top of the Danian, with higher levels of dissolution removing smaller and more delicate taxa, such as *Futyania*, *Praeprinsius*, *Ellipsolithus* and holococcoliths (*Octolithus*). In addition, it is possible that Site 1407, though oceanic in setting, was also recording some neritic influence through the Danian, as indicated by the presence of *Braarudosphaera* (e.g., Hagino et al., 2015).

Figures 6-7: here

4. The Danian nannofossil recovery succession in the northwest Atlantic Ocean

4.1 Survivor species

Whether Cretaceous nannofossil specimens found above the K/Pg boundary are true survivors or reworked/mixed specimens has long been a topic for debate (Pospichal, 1994). There is now relatively clear consensus around the group of survivor species, which has largely been determined through analysis of biogeography, abundance patterns and geochemical fingerprinting (Pospichal, 1994; Gartner, 1996; Bown, 2005a; Minoletti et al. 2005; Alvarez et al. 2019). Many survivor taxa are absent from late Cretaceous open ocean sites or are very rare below the K/Pg boundary but increase in abundance above it and subsequently display variable abundance trends (Bown, 2005a). Disappearing species may occur above the boundary but decrease rapidly above it, displaying trends of decline that are consistent with reworking (e.g., Pospichal, 1994, 1996). Around 11 survivors within 9 genera are definitively recognised and all these survivor taxa were seen in this study (Table 5; Figure 8; Plate 1).

Figure 8: here

Genus	Species	Cretaceous distribution
Biscutum	*B. harrisonii* (other names also applied)	Rare, coastal, high latitude
Braarudosphaera	*B. bigelowii* + other species?	Very rare, coastal
Calciosolenia	*C. fossilis*	Very rare, coastal?
Cyclagelosphaera	*C. reinhardtii*	Very rare, coastal
Goniolithus	*G. fluckigeri*	Very rare, coastal
Lapideacassis	Species-level taxonomy not well constrained but could be 1-5 species	Very rare, coastal
Markalius	*M. aperta*	Rare, coastal-shelf
	M. inversus	Rare, coastal-shelf
Neocrepidolithus	*N. cruciatus*	Rare, shelf?
	N. neocrassus	Rare, shelf?
Octolithus	*O. multiplus* (there may be more holococcolith survivors, but their fossil record is poor)	Rare, shelf?
Zeugrhabdotus	*Z. sigmoides*	Shelf

292 **Table 5**: List of Cretaceous survivor species based on stratigraphic ranges that continue
293 significantly into the Paleogene, diagnostic Late Cretaceous biogeographic distributions, and
294 distinct abundance patterns above the K/Pg boundary (e.g., Bown, 2005a; Hagino et al., 2015;
295 Alvarez et al. 2019).
296
297 *Braarudosphaera, Cyclagelosphaera, Markalius* and *Zeugrhabdotus* are typically absent in the
298 Maastrichtian at sites 1403 and 1407 but increase to relatively high and variable abundances
299 immediately above the K/Pg boundary. *Goniolithus*, *Lapideacassis* and *Neocrepidolithus* are
300 rare but conspicuous in the Danian assemblages and absent below the boundary.
301 *Cyclagelosphaera reinhardtii* was common (up to 10%) for the initial 13 kyr after the K/Pg
302 boundary at Site 1403 but decreased rapidly thereafter. Relative abundance of *Markalius* was
303 low (<5%) but it persisted throughout the Danian, especially during the initial 2 Myr, after
304 which it gradually decreased in abundance. *Zeugrhadotus sigmoides* showed a similar pattern
305 to this, but with higher relative abundances (>20% at Site 1403) and a longer 'acme' interval
306 of ~3 Myr. Pentaliths of *Braarudosphaera*, as well as of other rare species of
307 Braarudosphaeraceae, are common in the lowermost two samples at Site 1407 (215.19–215.14
308 m CCSFr; between +522 and +552 kyr), initially accounting for >5% relative abundance, but
309 gradually decreased thereafter.
310
311 New species of *Cyclagelosphaera* (*C. colorata* sp. nov.) and *Zeugrhabdotus* (*Z. recens* sp. nov.)
312 appear in the Danian interval, indicating limited diversification within survivor lineages above
313 the boundary. *C. colorata* was relatively short-lived (between +112 and +843 kyr) while *Z.*
314 *recens* persisted for longer, from +1 Myr (64.99 Ma), continuing through the rest of Danian
315 with its Top recorded around + 6.54 Myr (59.5 Ma) (Fig. 8). The emergence of these new
316 species occurred around the end of the 'acme' intervals of their ancestral forms,

317 *Cyclagelosphaera reinhardtii* and *Zeugrhabdotus sigmoides*. Limited post-K/Pg diversification
318 is also seen in *Neocrepidolithus* and *Calciosolenia*, and much more significant Paleocene and
319 Eocene diversification is seen in *Braarudosphaera* (Bown, 2005b).
320
321 Planktonic foraminifera and calcispheres are also unusually common in the lowermost Danian
322 nannofossil smear slides (Figures 6, 7), but are very rare in the Upper Cretaceous samples. They
323 are present both as fragments and as whole specimens and are consistently observed during the
324 initial 2 Myr. Foraminifera are most abundant (5–7 fragments/FOV) between +122 and +322
325 kyr (Site 1403 247.26-246.58 m CCSF) and gradually decreased above this level. The size of
326 the foraminifera found in this interval is significantly smaller than that of the typical Cretaceous
327 species size range. Calcispheres are most abundantly found (8–10 fragments/FOV)
328 immediately above the K/Pg boundary, between +272 and +422 kyr (Site 1403 246.88–246.08
329 m CCSF) but are conspicuous (~5-10/FOV) up to around +1.1 Myr.
330
331 **4.2 Incoming Danian taxa**
332 The first appearing Danian taxon at Site 1403 is *Biantholithus sparsus*, which is present in our
333 first sample above the K/Pg boundary (+13 kyr) and continues rarely but consistently through
334 the Danian. *Neobiscutum parvulum* and *Praeprinsius vegrandis* sp. nov. (Family Prinsiaceae)
335 appear at +20 kyr, followed soon after by *Cruciplacolithus primus* (Family Coccolithaceae)
336 (+109 kyr). These form part of a series of acmes that characterise the Danian nannofossil
337 succession, alongside *Praeprinsius tenuiculus, Futyania petalosa, Coccolithus pelagicus* and
338 *Toweius selandianus* (Plate 2; Figures 8, 9). These Danian acmes have relatively short durations
339 of 0.1–1.0 Myr, and typically occur within 200 kyr of the origination of the species.
340 **Figure 9:** here
341

342 **4.2.1 Family Prinsiaceae**

343 The incoming first representatives of the Family Prinsiaceae, *Praeprinsius vegrandis* sp. nov.
344 and *Neobiscutum*, are exceptionally small (<2 μm) at their first appearance and the coccoliths
345 are dark and inconspicuous in XPL because their shields are predominantly formed of V-unit
346 crystals (Plate 2, figs 1–9). They are often only visible using PC illumination and this relative
347 'invisibility' may explain their inconsistent documentation in the literature.
348
349 *Neobiscutum parvulum* is generally considered an incoming Cenozoic taxon (e.g., Perch-
350 Nielsen, 1985; Jiang and Gartner, 1986) and is tentatively included within the Prinsiaceae here
351 (see Taxonomy section). It forms the first significant post K/Pg acme, persisting for 80 kyr
352 between +50 and +130 kyr (>50% relative abundance), and dominates the depauperate earliest
353 Danian nannoplankton communities (maximum 91.7% relative abundance at +79 kyr). It is
354 both common (often 10s of specimens per FOV) and extremely high in relative abundance. An
355 alternative interpretation of *N. parvulum* is that it is a survivor species, which is rare or difficult
356 to differentiate in diverse Upper Cretaceous assemblages, although it has occasionally been
357 reported from Maastrichtian sediments (e.g., Mai et al., 2003). Its morphology is simple and
358 similar if not indistinguishable from Cretaceous *Biscutum* coccoliths and its stratigraphic
359 distribution, forming one of the first acmes alongside other Cretaceous survivors such as
360 *Cyclagelospheara reinhardtii*, is consistent with survivorship. Reports of an earlier
361 *Neobiscutum* species, *N. romeinii*, which has a distinctive central-area grill, has led others to
362 consider the group a distinct incoming lineage (Perch-Nielsen, 1985).
363
364 Two short-lived acmes follow *Neobiscutum*, the first being *Praeprinius vegrandis* sp. nov.
365 (maximum relative abundance 50.3% at +380 kyr) and then *Futyania petalosa* (maximum
366 relative abundance 62% at +550 kyr) (Figure 9). Both species have coccoliths that are very

small (1-2 μm) and relatively fragile, and so they are easily overlooked and sensitive to preservation quality. The base of the *F. petalosa* acme is not well represented in our samples and as *P. vegrandis* is described here for the first time, the precise temporal relationship between these two acmes is uncertain.

The next Danian acme is *Praeprinsius tenuiculus* (named *P. dimorphosus* by some authors – see Section 5.2 and Taxonomy) (Figure 9), which lasted over 1 My at Site 1407 with very high relative abundances (maximum relative abundance 89.7% at +990 kyr). This is the most conspicuous Danian acme because the species is extremely common and the coccoliths are slightly larger than the previous acme taxa. For these reasons, both the Base and Base acme events have been identified as a biostratigraphically useful and applied as zonal markers (e.g., *Prinsius dimorphosus* Zone of Romein, 1979; *Praeprinsius dimorphosus* group acme Zone of Agnini et al., 2014; Base used by Varol, 1989; Fornaciari et al., 2007; Dallanave et al., 2012). *P. tenuiculus* coccospheres are also frequently preserved and so 10s-100s of coccoliths and coccospheres may be present per FOV (Plate 2, figs 21–26; Figure 10). Towards the end of the *P. tenuiculus* acme, the genera *Prinsius* and *Toweius* appear and at Site 1407, very small *Toweius* (*T. selandianus*) rise to dominance to form another acme. This *T. selandianus* acme (maximum relative abundance 66% at +2.6 Myr) is sustained for over 1 My until it gradually gave way to increasing *Toweius pertusus* dominance (maximum relative abundance 43% at 61.77 Ma).

Base *Praeprinsius tenuiculus* occurs at 65.28 Ma at Site 1403 and Base common at 65.13 Ma, which are estimates consistent with Tethyan and South Atlantic calibration ages for the *P. dimorphosus* group (Fornaciari et al., 2007; Dallanave et al., 2012; Agnini et al., 2014). Note that Fornaciari et al. (2007) and Dallanave et al. (2012) show separate abundance records for *P.*

392 *dimorphosus* and *P. tenuiculus* (distinguishing elliptical and circular forms) but they are very
393 similar in timing and structure, potentially suggesting variability within one taxon. As circular
394 to subcircular forms overwhelming dominate this acme in our material, we consider *P.*
395 *tenuiculus* to be the appropriate name for the species and acme.
396 **Figure 10:** here
397
398 **4.2.2 Family Coccolithaceae**
399 The incoming Danian Coccolithaceae taxa include *Cruciplacolithus, Chiasmolithus,*
400 *Coccolithus* and *Ericsonia* (Figures 8, 11). *Cruciplacolithus primus* was the first species to
401 appear at +112 kyrs at Site 1403 (65.91 Ma) and the earliest representatives are relatively small
402 (3-5 μm), forming an acme that peaks ~+420 kyr (maximum relative abundance 47.3% at +460
403 kyr). It is possible there are earlier *Cruciplacolithus* of even smaller size, but they are difficult
404 to differentiate from co-occurring *Neobiscutum* and their central structures are indistinguishable
405 in LM.
406
407 The main evolutionary trends in the *Cruciplacolithus* lineage are an early, rapid increase in
408 coccolith size between + 0.2 Myr and +1.1 Myr (giving rise to *C. intermedius* >7 μm), and a
409 rotation of the central area crossbars from axial orientation (*C. primus, C. intermedius, C. tenuis*)
410 to asymmetric (*Cr. asymmetricus, Cr. edwardsii, Cr. frequens*) and then to diagonal
411 orientations (*Chiasmolithus* spp.) (Romein, 1979; van Heck and Prins, 1987; Thibault *et al*.,
412 2018). *Coccolithus* appeared shortly after *Cruciplacolithus* (+571 kyr, herein), through
413 reduction of the central area opening width, increase in shield width and reduction or loss of
414 crossbars. Again, it is possible that there are earlier, smaller forms, but these could not be
415 differentiated from *Cruciplacolithus* in this study. This may explain why our Base *C. pelagicus*
416 age of ~65.45 is slightly younger than previous estimates (e.g., Fornaciari et al., 2007;

Dallanave et al., 2012; Agnini et al., 2014). *Coccolithus* is common in the Danian with peak relative abundance of 62% at +0.88 Myr (65.14 Ma) at Site 1403 (Figures 6, 11).

The divergence of circular Coccolithaceae forms with broad tube-cycles, classified here as *Ericsonia*, is an additional conspicuous morphological trend and occurred around +1.24 Myr (64.78 Ma).

Figure 11: here

4.2.3 Order Discoasterales, Family Fasciculithaceae

Nannoliths of the Order Discoasterales first appear in the upper Danian with the successive appearance of fasciculiths and then sphenoliths (Figures 3–5). *Fasciculithus magnicordis*/*magnus* (placed in the genus *Gomphiolithus* by some authors) is the first taxon to appear (63.37 Ma), followed closely by *Diantholitha* and *Lithoptychius* (Figures 5, 8). All these forms occur in low abundance and each taxon is short lived. The appearance of the Discoasterales is significant, however, because they are considered to be the first oligotrophic-adapted nannoplankton taxa in the aftermath of the mass extinction (Fuqua et al., 2008), suggesting the emergence of greater specialisation in nannoplankton ecological strategies as communities became more diverse and stable (Alvarez et al., 2019).

5. The Prinsiaceae (*Praeprinsius*-*Prinsius*-*Toweius*) lineage

5.1 Prinsiaceae taxonomy

The Prinsiaceae evolutionary lineage originated with the earliest Danian small placoliths, such as *Praeprinsius vegrandis* sp. nov. and *Futyania petalosa*, followed by slightly larger and morphologically more-complex forms, such as *Praeprinsius tenuiculus*, *Prinsius dimorphosus* and *Prinsius martinii*, and finally larger *Toweius* species with open central areas and perforate

grills (Figures 8, 12). The lineage was first recognised by Romein (1979, fig. 38) and broadly remains the consensus view with minor additions and revisions (e.g., Gallagher, 1989; Alvarez et al., 2019). In detail, however, the application of species concepts and generic terminology across the lineage is far from stable or consistent, and species such as *F. petalosa* and *P. dimorphosus* have been switched between three or four different genera, including *Biscutum*, *Prinsius*, *Toweius* and *Praeprinsius*.

The genera *Prinsius* and *Toweius* were originally proposed by Hay and Mohler (1967) but were not clearly defined and differentiated. *Prinsius* was described as elliptical placoliths with a solid distal shield (type species *P. bisulcus*) and *Toweius* as circular to subcircular placoliths with reticulate central-area grills (type species *T. craticulus*, a junior synonym of *T. pertusus*). Romein (1979) stressed the importance of the closed central-area in *Prinsius* and Perch-Nielsen (1985) emphasised the possession of reticulate grills in *Toweius*, while conceding that these also existed in *Prinsius*, e.g., *P. africanus* Perch-Nielsen 1981. These two authors also recognised the presence of unicyclic and bicyclic R-unit tube-cycles across the lineage but did not apply this as a diagnostic generic- or even species-level character. A new genus, *Praeprinsius*, was later proposed by Varol and Jakuboski (1989) to include the early, small forms that have a single R-unit tube-cycle (type species *P. tenuiculus*, plus *P. africanus*). They also included *P. dimorphosus*, which has one or two tube cycles. Romein (1979) had earlier used "*Prinsius dimorphosus*-type 1" for these small circular forms with one tube cycle (conforming to the *P. tenuiculus* concept applied herein) and "*Prinsius dimorphosus*-type 2" for more elliptical forms with two tube cycles (the *P. dimorphosus* concept applied herein). The presence of one or two R-unit tube-cycles cannot be determined from LM observation and though this feature has been widely applied as a taxonomic criterion it has generally not been validated by SEM observations.

5.2 The *Praeprinsius* genus

Our observations suggest that the *Praeprinsius* taxonomic concept is well supported by evolutionary history, stratigraphic range and morphology (Figure 12). These very small forms:

- occur early in the Prinsiaceae lineage – mostly restricted to the first 2 Myr of the Danian (nannofossil biozones NP1–NP3),
- are predominantly circular to subcircular in outline – a relatively unusual morphological feature in coccolithophores,
- possess a maximum of one R-unit tube-cycle, and
- are simply constructed with low numbers (10–12) of shield elements/segments.

The original *Prinsius dimorphosus* type description specifically noted the occurrence of both single and double tube-cycles on the same coccosphere and this may represent preservational modification or a truly transitional form (Perch-Nielsen, 1969). However, the elliptical outline, closed/narrow central area and two tube cycles of the type material is closer to the defined concept of *Prinsius*, and in essence the *P. dimorphosus* type-images show small (holotype coccolith length 3.5 µm) *Prinsius martinii*-like coccoliths (holotype coccolith length 5.5 µm), but with the low number of rim elements seen in *Praeprinsius*. Our SEM observations at sites 1403 and 1407 failed to uncover unequivocal *P. dimorphosus* coccospheres but we have seen specimens from North Sea core material, which have coccoliths that look similar to *P. tenuiculus*, i.e., small, circular-subcircular with ~12 rim elements, but with two clear tube cycles (Plate 5, fig. 5–9). Several of these coccospheres show a mix of coccoliths with one and two tube cycles (Plate 5, figs 5, 8). These observations suggest that *P. dimorphosus* represents a transitional form between the *Praeprinsius tenuiculus* and *Prinsius-Toweius* rim morphology.

Figure 12: here

492 *Prinsius* and *Toweius* coccoliths are typically larger and more complexly constructed than the
493 *Praeprinsius* species, with higher numbers of shield elements and complex scissoring in the
494 growth of the tube elements, resulting in the apparent double cycle of R-unit tube elements
495 (Plate 5). Coccolith outline also becomes predominantly elliptical (Plates 2, 4, 5). The
496 differentiation of *Prinsius* and *Toweius* using closed central-area *versus* open central-area,
497 respectively, depends on user interpretation of what this means in detail, plus the observation
498 technique applied (i.e., LM *vs* SEM) and preservation quality. The earliest *Toweius*-type
499 coccoliths in our record are very small, with correspondingly narrow central areas and grills
500 (Plate 2, figs 37–44; Plate 5, figs 20–25). Coccolith lengths and central-area openings gradually
501 increase in size and become more obvious in LM, but this leads to subjectivity over the
502 taxonomic threshold between 'closed' and 'open' central areas, and therefore between *Prinsius*
503 and *Toweius*. Our SEM work shows that early, very small *Toweius* forms have narrow central
504 areas spanned by grills and therefore conform to the *Toweius* concept (Plate 5, figs 20–25). We
505 have attempted to strictly adhere to the closed central area definition for *Prinsius*, but this
506 requires careful observation, e.g., rotation of the specimen in XPL, and may be made more
507 difficult when preservation is moderate or poor. Using this definition at sites 1403 and 1407,
508 the dominant forms in the Prinsiaceae lineage throughout the upper Danian are *Praeprinsius*
509 *tenuiculus* followed by *Toweius selandianus*, although the first appearance of the latter species
510 includes morphologies that are transitional, i.e., with narrow central areas. *Prinsius*
511 *dimorphosus* and *Prinsius martinii* are rare at sites 1403 and 1407 but these taxa may be more
512 common at higher latitudes (Pospichal and Wise, 1990). It is also possible that our species
513 concept of *T. selandianus* overlaps with the *P. dimorphosus* concept of other authors.
514
515 The published images and reported stratigraphic ranges of *P. dimorphosus* and *P. tenuiculus*
516 indicate that species concepts vary significantly between specialists, leading to a long duration

and early stratigraphic range for *P. dimorphosus*, especially when relying on LM observations alone. According to Varol (1989) both *P. dimorphosus* and *P. tenuiculus* range from Zone NP2 to NP4, but elliptical *P. dimorphosus* becomes dominant in Zone NP3, above the *P. tenuiculus* acme and immediately prior to the appearance of *P. martinii.* Both Romein (1979) and Agnini et al. (2014) use *P. dimorphosus* as a zonal index in a position within lower Zone NP2, i.e., just above the appearance of *C. intermedius*, but Romein (1979) included forms with both one and two tube cycles in his definition and Agnini et al. (2014) include both circular and elliptical forms (i.e., *P. dimorphosus* and *P. tenuiculus*). In the lower Zone NP2 interval we only encountered circular to subcircular forms, i.e., *P. tenuiculus*, which form a striking acme with a duration of around 1.2 million years between 65.3 and 64.1 Ma. Our SEM observations suggest that the appearance of forms with two cycles, i.e., *P. dimorphosus*, occurs later, at around 63.7 Ma in Zone NP3 (Plate 5, figs 13–15). Notably, the holotype of *P. dimorphosus* is from the upper Danian, most likely Zone NP3 (Perch-Nielsen, 1969).

5.3 Prinsiaceae coccospheres

5.3.1 Coccosphere morphology

Coccospheres of the Prinsiaceae family are relatively frequently preserved (e.g., Plates 2, 4, 5; also, Bown et al., 2014) and this is especially the case for the Danian representatives *Praeprinsius* and *Futyania*. The opportunity to document coccosphere geometries from the Prinsiaceae family provides important additional morphological information in support of the taxonomic concepts discussed herein (Figures 13, 14; Plates 2, 4, 5).

Figure 13: here

Figure 14: here

Coccospheres of the earliest species, *P. vegrandis* sp. nov., show very high numbers of coccoliths (>30) forming small coccospheres (<5 μm) with very small lith size ranges (<2 μm) (Figure 13B–C; Plate 2, figs 10–12; Plate 4, figs 6–10). Similarly, *Futyania* has very high numbers of very small liths (>60) but forming larger coccospheres (up to ~8 μm) (Figure 13B–C; Plate 2, figs 15–18; Plate 4, figs 20, 22, 23; Plate 5, fig. 4).

The coccosphere geometry of *P. tenuiculus* changes significantly through its stratigraphic range, displaying increasing lith and cell sizes but with variable lith numbers (Figures 13 B–C, 14). Two distinct size populations of *P. tenuiculus* can be differentiated by coccolith length *vs* cell-size (Figure 14B), which we differentiate as *P. tenuiculus* type 1 and *P. tenuiculus* type 2 (see also Plate 4, figs 11–14 and 15–19), and these broadly correspond to older and younger specimens. Compared with *P. vegrandis* and *Futyania*, the coccospheres of early *P. tenuiculus* (*P. tenuiculus* type 1, prior to +1.0 Myr) have fewer coccoliths (~19) with slightly larger lith sizes (1.5–2.5 μm) on small coccospheres (3.0–4.5 μm). *P. tenuiculus* coccospheres then almost double in size (up to 8μm; *P. tenuiculus* type 2, + 1.0-1.5 Myr) but show only minor increases in lith size and are formed from only slightly higher numbers of coccoliths (~20).

Coccosphere geometry shifts more abruptly with the appearance of *Prinsius* (*P. dimorphosus* and *P. martinii*), which has similar lith and cell size ranges but with half the number of coccoliths (11–12), compared with the preceding *Praeprinsius* populations (~20) (Figure 13B–C; Plate 5, figs 5–11). This shows that the packing of coccoliths on the coccospheres in *Prinsius* is significantly different to that of *Praeprinsius*, with greater overlapping of the shields in *Prinsius* producing relatively smaller, more compact spheres. *Toweius* maintains this geometry of tightly packed coccoliths with similar-sized spheres formed from slightly fewer (7–8) coccoliths.

These distinct coccosphere morphologies provide further support for the differentiation of *Praeprinsius* and *Prinsius* and confirm the similarity of the *Prinsius* and *Toweius* morphologies, at least early in their evolutionary history. The trends in Prinsiaceae coccosphere evolution however are in some ways counterintuitive, with increasing lith sizes not necessarily resulting in larger coccospheres/cells. These coccospheres are therefore not predictable from the typical geometries seen in other Cenozoic placolith taxa (Henderiks, 2008; Gibbs et al., 2018) and require the elucidation of taxon-specific geometric relationships to reconstruct coccosphere sizes from disarticulated liths (Gibbs et al., 2013, 2018)

5.3.2 Coccosphere openings and mixotrophy

Early representatives of the Prinsiaceae have distinct coccosphere geometries but their spheres also include openings, which are rarely if ever seen in other fossil placolith taxa (Gibbs et al., 2020). These openings have been observed in thousands of LM and SEM specimens and occur in ~60% of the specimens within populations, which indicates that all are likely to have them, given we can only observe around 60% of the surface area in any given LM specimen (Gibbs et al., 2020, Fig. S6). Further, these openings are consistent in shape and size and in the case of *Futyania*, they are surrounded by coccoliths with modified morphology, having significantly smaller size (Plate 4, figs 22–23). With reference to modern coccosphere morphologies, these holes are most likely flagellar openings surrounded by circumflagellar coccoliths, marking the place where flagella and haptonema emerge from the cell/sphere. We have observed these flagellar openings in five Prinsiaceae species: *P. tenuiculus*, *P. vegrandis*, *P. dimorphosus*, *F. petalosa* and *P. dimorphosus* (Plates 4–5).

These coccosphere openings indicate that the cells were motile, probably haploid, and likely mixotrophic, as flagella beating and the prehensile haptonema act together to capture and ingest prey particles in modern haptophytes (i.e., phagotrophy) (Houdan et al., 2006; Supraha et al., 2014). The occurrence of motile placolith forms as the dominant taxa, as seen in these Danian acme assemblages, is unique in the coccolithophore fossil record. Other time intervals are characterised by taxa with imperforate coccospheres that were therefore non-motile in that life cycle phase, e.g., *Watznaueria* in the Mesozoic and *Toweius* and reticulofenestrids (*Reticulofenestra*, *Cyclicargolithus*, *Gephyrocapsa*, *Emiliania*) in the Cenozoic. The dominance of motility and the ability to employ mixotrophy, i.e., both ingestion (phagotrophy) and/or photosynthesis (autotrophy), is a trophic strategy closely linked with mass extinction survivorship and the early success of these acme taxa in the post-extinction oceans (Gibbs et al., 2020). This physiology may also explain the atypical coccosphere geometries in these taxa (i.e., with small coccoliths but relatively large cells), reflecting the need to accommodate a phagotrophy-related food vacuole in addition to the more typical chloroplasts and coccolith-forming vesicles.

5.4 Prinsiaceae summary

Our Prinsiaceae records indicate that the earliest incoming representatives are very small, subcircular to circular *Praeprinsius* coccoliths that appear along with the elliptical *Neobiscutum parvulum* forms. These early *Praeprinsius* coccoliths are inconspicuous and tend to lack visible birefringent tube-cycles. Their presence is dependent on good preservation and their observation requires the use of phase contrast illumination. We propose a new name for the early forms, *P. vegrandis,* but probably some authors have included these in the early range of '*P. dimorphosus*' *sensu lato*. Coccoliths of the *Praeprinsius* lineage increase in size around 0.7 Myr above the K/Pg boundary (Figure 14) and they become far more conspicuous, with

birefringent tube cycles and small central openings (Plate 2). These forms have tended to be classified as *P. dimorphosus* in the older literature, but this is not consistent with the original type-material (elliptical, with one and two tube cycles, upper Danian) and we have instead applied the name *P. tenuiculus*. The *Futyania* acme occurs prior to the *P. tenuiculus* acme, with the two forms likely closely related, but distinguished by the height of the tube cycle and coccosphere morphology. In the North Atlantic, the next acme is the incoming of very small, elliptical *Toweius selandianus* but they are accompanied by transitional forms similar to *P. dimorphosus sensu stricto* and small *P. martinii*. The long stratigraphic range for *P. dimorphosus* reported in the literature therefore likely includes more than one species, i.e., the small early forms (*P. vegrandis*, *P. tenuiculus*) and later forms that are precursors to *P. martinii*, and possibly also *T. selandianus* and *P. martinii*. Both *Cruciplacolithus* and *Coccolithus* appear during the early stages of the Prinsiaceae evolution and are initially also very small, and identification of their first occurrence is difficult and, as for *Praeprinsius*, is probably preservation- and user-dependent.

6. Systematic Palaeontology

This section provides a comprehensive description of Danian nannofossil taxa with images drawn from our study of IODP Exp. 342 sites 1403 and 1407, with additional images from other sections, where necessary. The LM images are reproduced at constant magnification and a 2 µm scale bar is provided beside at least one of the images on each plate. Brief descriptions are provided for all taxa, with more detailed comments for notable or problematic taxa. Sample information is provided using standard IODP notation (Hole-Core-Section, depth in cm in section). The descriptive terminology (including size classes) follows the guidelines of Young et al. (1997). The higher taxonomy generally follows Young et al. (2003) for extant coccolithophores and Young & Bown (1997) and *Nannotax* (ina.tmsoc.org/Nannotax3) for the

extinct taxa. Range information is given for stratigraphic distributions at the Exp. 342 sites, unless stated otherwise. Variants are listed where appropriate, referring to names that we consider represent intraspecific morphological variability rather than distinct taxonomic units, such as varieties or subspecies (see Young, 1998, p. 239). The following abbreviations are used: LM – light microscope, XPL cross-polarised light, PC – phase-contrast illumination, L – length, H – height, W – width, D – diameter. Type material and images are stored in the Department of Earth Sciences, University College London.

INCOMING CENOZOIC TAXA

Cenozoic placolith coccoliths

Family **PRINSIACEAE** Hay & Mohler, 1967 emend. Young & Bown, 1997

Plates 2, 4, 5. **Description:** Placoliths with R-units forming the proximal shield-element and normally one or two tube-elements, and V-units forming an upper layer to the proximal shield, an outermost tube and the distal shield. Central-area structures, if present, are conjunct and typically net-like. **Remarks:** See Discussion in Section 5 above.

Genus ***Futyania*** Varol, 1989

Futyania petalosa (Ellis & Lohmann, 1973) Varol, 1989

Pl. 2, figs 13–18; Pl. 4, figs 20–23; Pl. 5, fig. 4. **Description:** Very small (usually <2µm) subcircular to elliptical placoliths with a narrow or closed central area; R-unit tube-elements extend distally to form an elevated flower-like distal structure. Commonly preserved as coccospheres that resemble calcispheres in LM (Pl. 2, figs 15–18). The tube cycle is birefringent and has a ragged appearance in XPL (Pl. 2, fig. 13). Side views are especially diagnostic, looking like Stonehenge's trilithons (Pl. 2, fig. 14). The coccospheres are 5.5–8.5 µm in diameter and have ~50–60 coccoliths. A flagellar opening (width ~2 µm) may be

665 visible and surrounded by slightly modified circumflagellar coccoliths that are smaller than
666 the body coccoliths with fewer tube elements (shaded orange in Pl. 4, figs 22–23; Pl. 5, fig.
667 4). **Remarks:** May be present in high abundances and considered an acme forming species
668 (>50% of assemblage), e.g., Turkey (Varol, 1989), Tunisia (Gardin, 2002; Bown, pers. obs.),
669 southern USA (Ellis and Lohmann, 1973; Jiang and Gartner, 1986). **Occurrence:** NP1 to
670 NP2. **Variant:** *F. attwellii* Varol, 1989 – circular.
671
672 Genus ***Neobiscutum*** Varol, 1989
673 *Neobiscutum parvulum* (Romein, 1979) Varol, 1989
674 Pl. 2, figs 1–5; Pl. 4, figs 1–5. **Description:** Very small, elliptical placoliths with narrow to
675 closed central area. Inconspicuous in XPL, although the narrow R-unit tube cycle is slightly
676 birefringent. May only be clearly visible in PC. Coccospheres are small (2–4 μm) with
677 relatively few coccoliths (11–15) and we have not found flagellar openings (Pl. 4, figs 1–5).
678 **Remarks:** One of the first new Danian species to appear after the K/Pg, around 20 kyr above
679 the boundary (lowermost Zone NP1) at Site 1403, and often abundant and dominant (e.g.,
680 Elles and El Kef, Tunisia – Gardin, 2002; Bown, pers. obs.; Brazos River, USA - Jiang and
681 Gartner, 1986; Shatsky Rise, Pacific Ocean – Bown, 2005a). The acme had a duration of
682 around 80 kyr (see Section 3.1.1 and Figures 6, 8). The morphology of these coccoliths is
683 simple, and practically indistinguishable from Mesozoic *Biscutum*; some have argued that this
684 may be a survivor form (see Section 4.2; Mai et al., 2003). **Occurrence:** NP1 to lower NP2.
685
686 *Neobiscutum romeinii* (Perch-Nielsen, 1981) Varol, 1989
687 Not figured. **Description:** Very small (~2μm), elliptical placoliths with central area spanned
688 by a net. Originally described from SEM. **Remarks:** Documented as acme-forming prior to
689 the *N. parvulum* acme in several studies (e.g., Jiang and Gartner, 1986; Pospichal, 1996), but

otherwise rarely reported. In LM around the type level, these coccoliths appears very similar to, and are difficult to distinguish from, *N. parvulum* (Bown, per obs.). It is likely that the two species concepts overlap and in LM studies *N. parvulum* and *N. romeinii* are probably often reported as one taxon. **Occurrence:** NP1; not seen in this study.

Genus ***Praeprinsius*** Varol & Jakubowski, 1989

Description: Very small to small, circular to subcircular placoliths, typically with one R-unit tube cycle and a narrow or closed central area. See further discussion in Section 5.2.

Praeprinsius tenuiculus (Okada & Thierstein, 1979) Perch-Nielsen, 1984

Pl. 2, figs 21–26; Pl. 4, figs 11–19; Pl. 5, figs 2–3. **Description:** Very small to small, circular to subcircular placoliths with a single R-unit tube cycle and small central opening. The number of rim elements is around 10. Coccospheres are relatively large and spherical (Figure 13) with a small flagellar opening (~1 μm) (Figure 10; Pl. 2, fig. 22; Pl. 4, figs 13–14, 17–18) (Section 5.3.2 and Gibbs et al., 2020). **Remarks:** *P. tenuiculus* shows significant size increase through its stratigraphic range with average lith length increasing from <2 μm to >3 μm (Figures 13–14). Some later forms have raised tube cycles (Pl. 4, fig. 19), perhaps heralding more complex intergrowth and the development of the two R-unit tube cycles, seen in *Prinsius*. The *P. tenuiculus* species concept as currently applied by other authors overlaps with *Prinsius dimorphosus sensu lato* and the two names are likely virtually interchangeable in some published work (e.g., Fornaciari et al., 2007; Dallanave et al., 2012), or are grouped together by others (e.g., Romein, 1979; Pospichal, 1996; Agnini et al., 2014). This is also shown by records of similar stratigraphic ranges and abundance trends (Fornaciari et al., 2007; Dallanave et al., 2012). We consider *P. tenuiculus* to be the earlier appearing species, forming the most conspicuous *Praeprinsius* acme, which ranges from ~65.3–64.1 Ma (Zone

NP2 to NP3). **Occurrence:** NP2 to NP3. **Synonyms:** *Prinsius africana* Perch-Nielsen, 1981 – with a net and raised tube cycle; *Prinsius rosenkrantzii* Perch-Nielsen, 1979.

Praeprinsius vegrandis sp. nov.

Pl. 2, figs 6–12; Pl. 4, figs 6–10; Pl. 5, fig. 1. **Derivation of name:** From *vegrandis*, meaning 'diminutive', referring to the smaller size of this species compared with other *Praeprinsius*. **Diagnosis:** Very small (1.5–2.5 μm), circular to subcircular placoliths with around 8 rim elements and a very narrow central area. **Description:** These placoliths are dark and inconspicuous in XPL and an R-unit tube cycle is usually not visible. The coccoliths are typically only visible using PC illumination. Coccospheres are around 5–6 μm in diameter with 32–34 coccoliths (Pl. 4, figs 6–10). A small flagellar opening (~1 μm) may be visible (Pl. 2, figs 11, 20; Pl. 4, figs 6, 8). **Differentiation:** Distinguished from other species of *Praeprinsius* by their smaller size and absent or reduced R-unit tube cycle. **Remarks:** One of the first new Danian species to appear after the K/Pg, around 20 Ky above the boundary at Site 1403. Due to its very small size, its presence and identification may depend on good preservation. **Dimensions:** Holotype coccolith L = 0.8 μm, Paratype coccolith L = 0.9 μm. **Holotype:** Pl. 2, fig. 6. **Type locality:** IODP Hole U1403A, NW Atlantic Ocean. **Type level:** Danian, Sample U1403A-26X-4, 130cm (Zone NP1). **Paratypes:** Pl. 2, fig. 8 (LM); Pl. 4, fig. 6 (SEM). **Occurrence:** NP1 to NP3; IODP Sites U1403, U1407 and ODP Sites 1209 and 1210 (Pacific).

Genus ***Prinsius*** Hay and Mohler, 1967

Description: Elliptical with central areas that are closed, although the taxonomic concept has been extended by some authors to include forms with a narrow opening and plate/net. The R-unit tube cycle is bicyclic and conspicuous (i.e., bright) in XPL. **Remarks:** This genus

concept overlaps with *Toweius*, with the two only differentiated by the width of the central area (Figure 12). As most early *Toweius* species have narrow central areas, the distinction is difficult to apply consistently in the Danian, especially if only relying on LM observations.

Prinsius bisulcus (Stradner, 1963) Hay & Mohler, 1967

Pl. 2, fig. 36. **Description:** Length >5.5 µm (Bown, 2016) with broad R-unit tube cycle/central area characterised by two grooves along the longitudinal axis. Several pores may be visible when preservation is good. Like *P. martinii* but larger (see also Wei & Liu, 1991). **Occurrence:** NP3 to NP9.

Prinsius dimorphosus (Perch-Nielsen, 1969) Perch-Nielsen, 1977

Pl. 2, figs 27–34; Pl. 5, figs 5–9, 13–15. **Description:** Very small to small (~<4 µm), elliptical to subcircular placoliths with well-developed R-unit tube cycle and narrow to closed central-area. The coccospheres are relatively small and compact (Figure 13; Pl. 5, figs 5–9). **Remarks:** Rare in our material (see Section 5). Holotype and original description refer to an elliptical coccolith with both single and double tube-cycles, but some of the type images may be more subcircular. The original description also mentions 12-15 rim elements, coccospheres with 8-14 coccoliths and an upper Danian type level (likely Zone NP3). Similar in overall species concept to *P. martinii* but slightly smaller (~<4 µm). The small size and small number of rim elements (~12–20 in our material – Pl. 5, figs 5–9) indicate the transitional nature of this form, sitting between *Praeprinsius tenuiculus* and small *Prinsius martinii*. We have included it within the *Prinsius* genus because of the elliptical outline, greater number of rim elements and more complex tube cycle element intergrowth.

764 The species concept as applied in the literature, based almost exclusively on LM observations,
765 is broad and likely includes several species, most notably including *Praeprinsius tenuiculus*
766 but probably also *Prinsius martinii* and possibly *Toweius selandianus*. Some authors do
767 explicitly state the grouping of *P. dimorphosus* and *P. tenuiculus* (e.g., Pospichal, 1996;
768 Agnini et al., 2014). We have definitive SEM observations of *P. dimorphosus* from upper
769 Zone NP3 (63.7–63.4 Ma) but its first and last occurrence is difficult to determine using the
770 LM. The reported literature range is therefore likely to be significantly extended by the
771 inclusion of these different taxa. **Occurrence:** ?NP3 to NP4 (type material is from upper
772 Danian – Perch-Nielsen, 1969).
773
774 *Prinsius martinii* (Perch-Nielsen, 1969) Haq, 1971
775 Pl. 2, fig. 35; Pl. 5, figs 10–11, 16–19. **Description:** Elliptical, length <5.5µm (Bown, 2016)
776 with broad R-unit tube cycle and closed central area. The overall size range using this species
777 concept is ~4.0–5.5µm. **Differentiation:** The closed central area is an important character and
778 allows differentiation from small *Toweius* species, such as *T. selandianus*. Similar in overall
779 species concept to *P. dimorphosus* but differentiated on slightly larger size, which is
780 undefined but likely approximated by a lith length >4 µm. *P. martinii* is also clearly elliptical.
781 **Occurrence:** NP3 to NP9.
782
783 Genus ***Toweius*** Hay & Mohler, 1967
784 **Description:** Elliptical to circular with central areas typically spanned by a proximal net
785 and/or distal conjunct net or bars. **Remarks:** See *Prinsius* and discussion in Section 5, above.
786
787 *Toweius pertusus* (Sullivan, 1965) Romein, 1979

Pl. 2, figs 45–47; Pl. 5, fig. 12, 26. **Description:** Elliptical to subcircular with finely perforate central-area net, but the perforations may be difficult to resolve in LM. **Remarks:** First appeared around 63.6 Ma (Zone NP3) at Site 1407, shortly after *T. selandianus* (64.0 Ma). The earliest forms are elliptical, similar to *Toweius selandianus* but are larger (> 5.5 μm) and become gradually more rounded with increasingly conspicuous perforations. This gradual change in size and outline likely explains the varying reports of it first appearance level (see also Agnini et al., 2014). Common. **Occurrence:** NP3 to NP14. **Synonym:** *Toweius craticulus* Hay and Mohler, 1967.

Toweius selandianus Perch-Nielsen, 1979

Pl. 2, figs 38–44; Pl. 5, figs 20–25. **Description:** Very small to small (<5.5 μm), elliptical with narrow central area spanned by a net. **Remarks:** First appeared around 64.1 Ma (Zone NP3) at Site 1407. Very abundant (relative abundance 25-66 %) to dominant between 63.61 and 61.57 Ma (upper Zone NP3 to NP4), just after the *P. tenuiculus* acme. Similar to *Prinsius martinii* but central area is not completely closed. Typically, smaller and more narrowly-elliptical than *T. pertusus*. The first appearance was used as a North Sea subzonal marker (Subzone NNTp7B) by Varol (1989). **Occurrence:** NP3 to NP6.

Order COCCOLITHALES **Haeckel, 1894 emend. Young & Bown, 1997**

Family **CALCIDISCACEAE** Young & Bown, 1997

Genus ***Umbilicosphaera*** Lohmann, 1902

Umbilicosphaera bramlettei (Hay & Towe, 1962) Bown *et al*., 2007

Pl. 3, fig. 34. **Description:** Circular, ring-like with narrow bicyclic rim and wide central-area. **Remarks:** Small (3.0–4.5 μm), ring-like forms appear ~64.0 Ma (Zone NP3) and most closely resemble *U. bramlettei*, although they appear to be sensitive to preservation state and

often appear to be incomplete, i.e., without a visible R-unit tube cycle. Eocene *U. bramlettei* are larger and more robust. **Occurrence:** NP3 to NP21.

Family **COCCOLITHACEAE** Poche, 1913 emend. Young & Bown, 1997

Plate 6. **Description:** Placoliths with *Coccolithus*-like rim structure: V-unit forms distal shield and lower cycle of central-area; R-unit forms proximal shield and upper cycle of central-area.

***Coccolithus* Group**

Pl. 3, figs 19–29; Pl. 6, figs 1–12. **Description:** *C. pelagicus* and similar, with broad centro-distal cycles and narrow central areas, which are vacant or spanned by transverse bars or crossbars. Includes *Coccolithus* and *Ericsonia.*

Genus ***Coccolithus*** Schwartz, 1894

Coccolithus pelagicus (Wallich, 1877) Schiller, 1930

Pl. 3, figs 19–21; Pl. 6, figs 1–4. **Description:** Broadly elliptical with narrow central area. Small to very large, and may represent more than one species. **Remarks:** First appeared around +571 kyr (65.5 Ma) at Site 1403 (lower Zone NP2) with lith size ranging between 4.0 to 8.5 μm. It is possible that there are smaller, earlier, representatives but these could not be differentiated from *Cruciplacolithus* in LM. Common. **Occurrence:** Lowermost NP2 to Present. **Variant/Synonym:** *C. tenuiforatus* (Clocchiatti & Jerkovic, 1970) Wise, 1983 – with narrow, fragile axial crossbars.

Genus ***Ericsonia*** Black, 1964

Pl. 3, figs 22–29; Pl. 6, figs 5–12. **Description:** Subcircular to circular Coccolithaceae coccoliths with a broad R-unit upper-tube cycle that is just narrower than the shield width and

so dominates the LM XPL image, resulting in a moderately bright appearance (see Bown, 2016 for further discussion). Central areas usually vacant. Almost exclusively Paleocene but note that some authors use this genus for the Eocene species *Coccolithus formosus* (Kamptner, 1963) Wise, 1973. **Remarks:** The type species of *Ericsonia* (*E. occidentalis* Black, 1964) is unfortunately an Eocene coccolithacean SEM specimen in proximal view, but it is subcircular with a wide central opening and so broadly conforms with the concept of *Ericsonia* we apply here. This is an ambiguous specimen, and we note that it could be a *Coccolithus* but we use the *Ericsonia* name to maintain nomenclatural stability.

Ericsonia media Bown, 2016

Pl. 3, figs 22–24; Pl. 6, fig. 12. **Description:** Medium to large (~6–11 μm), subcircular to circular with a moderately broad upper-tube cycle and narrow central area. The upper-tube cycle is narrower than that seen in most *Ericsonia* coccoliths but broader than that seen in *C. pelagicus*. The outer edge of the upper-tube cycle shows a diagnostic beaded appearance at certain focus levels. **Differentiation:** Distinguished by the prominent beading around the outer edge of the tube cycle. **Occurrence:** NP3/4 to NP8/9?

Ericsonia orbis Bown, 2016

Pl. 3, figs 25–26; Pl. 6, figs 7–11. **Description:** Small (<5 μm), circular with relatively wide central area. **Remarks:** Much smaller than other *Ericsonia* (and *Coccolithus*) species but distinctive in LM. **Occurrence:** NP3 to Eocene. **Variant:** *E. staerkeri* Bown, 2005 – with narrow, fragile crossbars.

Ericsonia subpertusa Hay & Mohler, 1967

Pl. 3, figs 27–29; Pl. 6, figs 5–6. **Description:** Medium to large, subcircular to circular with narrow central area. **Differentiation:** Similar to *E. media* but lacking the prominent beading around the outer edge of the tube cycle. **Occurrence:** NP3 to NP9.

***Chiasmolithus-Cruciplacolithus* Group**

Pl. 3, figs 1–18; Pl. 6, figs 14–18. **Description:** Coccolithacean coccoliths with central area spanned by crossbars that are normally broad and robust. Includes *Bramletteius, Campylosphaera, Chiasmolithus* and *Cruciplacolithus.*

Genus ***Bramletteius*** Gartner, 1969

Description: Small coccoliths with narrow rim and axial crossbars supporting tall, thin, blade-like spines.

Bramletteius cultellus Bown, 2016

Pl. 3, fig. 30. **Description:** Placolith coccoliths with long, flat, narrow, blade-like spine. **Occurrence:** NP4 to NP5.

Genus ***Chiasmolithus*** Hay et al., 1966

Description: Central areas spanned by diagonal crossbars; often with broad, birefringent centro-distal cycle.

Chiasmolithus bidens (Bramlette & Sullivan, 1961) Hay & Mohler, 1967

Pl. 3, figs 16–18; Pl. 6, fig. 18. **Description:** Narrow central area and broad bars, one straight and one curved/offset where they meet. May show two small conjunct projections (teeth) into the central area along the short axis. *C. solitus* and *C. edentulus* are similar but lack the 'teeth'

and are considered synonyms by some. **Occurrence:** NP5/6 to NP11. **Variant:** *Chiasmolithus edentulus* van Heck & Prins, 1987 – without the central area projections.

Chiasmolithus danicus (Brotzen, 1959) Hay & Mohler, 1967

Pl. 3, fig. 15. **Description:** Small to medium sized with narrow centro-distal cycle and curving diagonal crossbars. Highly variable (van Heck & Prins, 1987). **Occurrence:** NP3 to NP6 (Perch-Nielsen, 1985).

Genus ***Cruciplacolithus*** Hay & Mohler in Hay et al., 1967

Description: Central areas spanned by axial to slightly rotated (up to 20 degrees) crossbars; typically narrow, birefringent centro-distal cycle.

Cruciplacolithus asymmetricus van Heck & Prins, 1987

Pl. 3, figs 9–10; Pl. 6, figs 16–17. **Description:** Slightly rotated (<20 degrees) crossbars. **Occurrence:** NP2 to NP4.

Cruciplacolithus edwardsii Romein, 1979

Pl. 3, figs 11–12. **Description:** Rotated (>20 degrees) crossbars but not diagonal. **Occurrence:** NP3 to NP15?

Cruciplacolithus intermedius van Heck & Prins, 1987

Pl. 3, figs 5–8. **Description:** Length >7 μm with axial crossbars. Variable and further subdivided by some (e.g., Thibault et al., 2018). **Remarks:** Considered to be the correct taxonomic concept and name applied to the Zone NP2 index species (e.g., Perch-Nielsen, 1985; van Heck and Prins, 1987; Varol, 1989; Fornaciari et al., 2007; Thibault et al., 2018).

Differentiation: Distinguished by large size (>7 µm) and axial crossbars that lack disjunct elements or 'feet' where they meet the rim. **Occurrence:** NP2 to NP4?

Cruciplacolithus primus Perch-Nielsen, 1977

Pl. 3, figs 1–4; Pl. 6, figs 14–15. **Description:** Small to medium (<7 µm) with axial crossbars. The smaller forms (<5 µm) are similar in overall morphology to the extant *C. neohelis* (McIntyre & Bé 1967) Reinhardt 1972. **Occurrence:** Typically, NP1 to NP9, but documented from the Eocene to Miocene in Tanzania (Bown, 2010; Hagino et al., 2015), so this may indicate a long pseudo-ghost range for *C. neohelis*.

Cruciplacolithus subrotundus Perch-Nielsen, 1969

Pl. 3, fig. 14. **Description:** Circular to subcircular with narrow central area and broad crossbars. **Occurrence:** Rare, NP3 to NP5.

Cruciplacolithus tenuis (Stradner, 1961) Hay & Mohler *in* Hay et al., 1967

Pl. 3, fig. 13. **Description:** Medium to large (>7 µm) with axial crossbars that have disjunct, birefringent blocks ('feet') where they meet the rim. Re-examination of the Stradner material has refigured *C. tenuis* without the birefringent feet (Stradner et al., 2010). Therefore, arguably *C. intermedius* is a junior synonym of *C. tenuis*, which can be reinstated as the zonal fossil for NP2. The name *C. notus* Perch-Nielsen, 1977 can be used for the form with birefringent feet. For consistency, we continue with the usage that has stabilized over the last 30 years or so. **Occurrence:** (for *C. tenuis* with 'feet') NP3 to NP9.

Genus ***Hornibrookina*** Edwards, 1973

Description: Elliptical with bicyclic distal shields and central-area grill formed from robust radial/lateral bars. At least eight species have been described but several are similar and may be synonyms or variants (Self Trail et al., 2022). May be common in Danian high-latitude settings (Pospichal, 1996).

Hornibrookina teuriensis Edwards, 1973

Pl. 2, fig. 48. **Description:** Narrowly elliptical with central area grill formed from ~10 pairs of lateral bars meeting at a longitudinal bar. **Remarks:** Not seen in this study, but image from ODP Site 690 (Weddell Sea, Southern Ocean) included here for comparison. **Occurrence:** NP1 to NP10. **Synonym/variant:** *H. edwardsii* Perch-Nielsen, 1977 – smaller than *H. teuriensis*.

Placolith coccoliths *Incertae Sedis*

Genus ***Biantholithus*** Bramlette & Martini, 1964

Pl. 1, figs 46–48. **Description:** Large, circular to stellate placoliths with distal shield constructed from 6-12, large, radial elements. In LM they typically have the appearance of stellate nannoliths with low birefringence. Forms large, spherical coccospheres (Mai et al., 1997; Bown et al., 2014). **Remarks:** Considered to be the first occurring new Danian species, but usually rare. **Occurrence:** NP1 to NP10.

Biantholithus sparsus Bramlette & Martini, 1964

Pl. 1, fig. 48. **Description:** *Biantholithus* with 8-12 visible elements in LM. **Occurrence:** NP1 to NP10. **Variants:** *Biantholithus astralis* Steinmetz & Stradner, 1984 – with 7–8 visible elements/rays in LM, which are not in contact in their outer part (Pl. 1, figs 46–47);

Biantholithus hughesii Varol, 1989 – with 6 visible elements/rays in LM, which are not in contact in their outer part (Pl. 1, fig. 45).

Genus ***Ellipsolithus*** Sullivan, 1964

Description: Elliptical to oblong placoliths with shields formed from numerous narrow elements and central areas spanned by plates that may be perforate.

Ellipsolithus macellus (Bramlette & Sullivan, 1961) Sullivan, 1964

Pl. 3, fig. 36. **Description:** Medium to large with birefringent central area plate. **Remarks:** Early forms are small and fragile and highly susceptible to dissolution. **Occurrence:** NP4 to NP11.

Ellipsolithus pumex Bown, 2016

Pl. 3, fig. 35; Pl. 6, fig. 19. **Description:** Wide central area (central area width similar to rim width) spanned by a finely perforate plate; perforations are small and irregularly distributed but are broadly arranged in two to three cycles. **Occurrence:** NP4 to NP5.

Cenozoic murolith coccoliths

Order ZYGODISCALES **Young & Bown, 1997**

Description: Muroliths with an outer rim-cycle of V-units showing anticlockwise imbrication and an inner rim-cycle showing clockwise imbrication (the opposite imbrication sense to the Mesozoic Eiffellithales). Central-area structures include disjunct transverse bars, diagonal crossbars and perforate plates but no spines.

Family **ZYGODISCACEAE** Hay & Mohler, 1967

985 Genus ***Neochiastozygus*** Perch-Nielsen, 1971

986 **Description:** Muroliths with well-developed V- and R-units and diagonal central-area
987 crossbars. Predominantly Paleocene group.

988

989 *Neochiastozygus denticulatus* (Perch-Nielsen, 1969) Perch-Nielsen, 1971

990 **Description:** Small with asymmetric cross and additional radial bars. May be inconspicuous
991 in LM. **Occurrence:** NP1 to Eocene. **Synonyms:** A range of small, asymmetric
992 *Neochiastozygus* species have been described and may be synonyms, e.g., *Chiastozygus*
993 *ultimus* Perch-Nielsen, 1981; *Neochiastozygus primitivus* Perch-Nielsen, 1981;
994 *Neochiastozygus* 'asymmetrical species' of van Heck & Prins (1987).

995

996 *Neochiastozygus modestus* Perch-Nielsen, 1971

997 Pl. 3, fig. 31; Pl. 6, figs 20–21. **Description:** Small *Neochiastozygus* with relatively small
998 central area and broad bars which are diagonal or may be slightly rotated from diagonal.
999 Bright inner rim cycle prominent in XPL. **Occurrence:** NP2 to NP7.

1000

1001 *Neochiastozygus saepes* Perch-Nielsen, 1971

1002 Pl. 3, fig. 32; Pl. 6, fig. 22. **Description:** Narrowly elliptical with prominent bright inner cycle
1003 in XPL and broad crossbars. **Occurrence:** NP3 to NP5. **Variant:** *Neochiastozygus eosaepes*
1004 Perch-Nielsen, 1981 – small with non-imbricate outer wall cycle and a diagonal cross that is
1005 slightly rotated.

1006

1007 Genus ***Neococcolithes*** Sujkowski, 1931

1008 **Description:** Muroliths with diagonal to H-shaped crossbars. R-unit relict or absent and so
1009 LM image is unicyclic. Crossbars are low birefringence.

Neococcolithes protenus (Bramlette & Sullivan, 1961) Black, 1967

Pl. 3, fig. 33. **Description:** Small to moderately sized *Neococcolithes* with straight, diagonal crossbars. **Occurrence:** NP4 to NP14.

Cenzoic nannoliths

Order DISCOASTERALES **Hay, 1977 emend. Bown, 2010**

Description: Radially symmetrical nannoliths formed from one to several cycles of elements that radiate from a common centre or axis and including disc-like (discoasters), stellate (discoasters), cylindrical (fasciculiths, helioliths and sphenoliths) and conical (fasciculiths and sphenoliths) morphologies.

Family **FASCICULITHACEAE** Hay & Mohler, 1967

Description: Conical or cylindrical nannoliths consisting of one to several cycles of radially-arranged elements. **Remarks:** The taxonomy of this group, especially the early representatives, has been subject to considerable discussion and revision (e.g., Aubry et al., 2011; Monechi et al., 2013; Miniati et al., 2021), with the proposal of at least four new genera and the recombination of many existing species. We have taken a relatively conservative approach here, preferring to maintain taxonomic consistency with relatively broadly defined genera.

Genus ***Diantholitha*** Aubry *in* Aubry et al., 2011

Description: High, cylindrical nannoliths with distinct distal and proximal units. Slightly ragged in plan-view outline (Pl. 3, fig. 45) but most frequently seen in side-view (Pl. 3, fig. 48).

Diantholitha alata Aubry & Rodriguez *in* Aubry et al., 2011

Pl. 3, fig. 48. **Description:** Distal cycle is taller than the proximal cycle. **Occurrence:** NP4.

Diantholitha magnolia Rodriguez & Aubry *in* Aubry et al., 2011

Pl. 3, figs 43–47; Pl. 6, fig. 13. **Description:** Distal and proximal cycles of similar height. **Occurrence:** NP4. **Variant:** *Diantholitha mariposa* Rodriguez & Aubry *in* Aubry et al., 2011 – flares distally.

Genus ***Fasciculithus*** Bramlette & Sullivan, 1961

Description: Conical or cylindrical nannoliths consisting of one dominant cycle of radially-arranged elements but more cycles may be present.

Fasciculithus magnus Bukry & Percival, 1971 emend.

Pl. 3, figs 39–42. Large, simple fasciculith with a gently flaring/cylindrical column that narrows and tapers towards the top, forming a distinct 'shoulder'. **Remarks:** The proposal of the separate genus *Gomphiolithus* for this species (Aubry et al., 2011) was based on relatively minor morphological differences (reduced or absent distal cycle/calyptra) and the apparently disjunct stratigraphic range, compared with other fasciculith species. At sites 1403 and 1407, *F. magnus* ranges from 63.35 to 62.90 Ma, overlapping with species such as *D. mariposa*, suggesting that the proposed new generic name is not supported by a disjunct stratigraphic range. **Occurrence:** Rare, NP4.

Fasciculithus magnicordis Romein, 1979

Pl. 3, figs 37–38. **Description:** Large, simple fasciculith with a tapering column. **Remarks:** Specimens of this species do not have the distinct 'shoulder' of *F. magnus* but instead taper gradually. However, we have observed a range of forms between the two typical end-member morphologies (compare Pl. 3, figs 37–41) and so *F. magnicordis* may be a short/low variant of *F. magnus*. This is also supported by documentation of short and similar or identical stratigraphic ranges (Miniati et al., 2021), although these taxa are usually very rare. We have retained the species here pending further study. **Occurrence:** Rare, NP4.

Family **SPHENOLITHACEAE** Deflandre, 1952

Genus ***Sphenolithus*** Deflandre *in* Grassé, 1952

Description: Globular to dart-shaped, formed from a mass of elements radiating from a common origin. Typically comprise a basal column and an apical spine.

Sphenolithus moriformis (Brönnimann & Stradner, 1960) Bramlette & Wilcoxon, 1967

Not figured. **Description:** Dome-shaped with no spine and upper and lower quadrants of similar size. **Occurrence**: NP4 to NN10. **Synonym:** *S. primus* Perch-Nielsen 1971.

SURVIVOR LINEAGES

Mesozoic murolith lineages

Order EIFFELLITHALES **Rood et al., 1971**

Description: Loxoliths with a distal/outer cycle composed of clockwise imbricating elements, the opposite imbrication sense to that seen in the Cenozoic Zygodiscales.

Family **CHIASTOZYGACEAE** Rood et al., 1973

Description: Eiffellithids with central areas typically spanned by transverse, axial, non-axial, or diagonal bars.

Genus ***Neocrepidolithus*** Romein, 1979

Description: Eiffellithids with broad, high rims and narrow or closed central-areas. Predominantly Danian group.

Neocrepidolithus cruciatus (Perch-Nielsen, 1979) Perch-Nielsen, 1981

Pl. 1, figs 35–36. **Description:** Narrow central area filled with an axial cross. Clearly bicyclic in LM. **Occurrence:** Upper Cretaceous (Turonian?) to NP4.

Neocrepidolithus neocrassus (Perch-Nielsen, 1968) Romein, 1979

Pl. 1, fig. 34. **Description:** Bicyclic LM image, high rim with narrow to closed central area. **Occurrence:** Upper Cretaceous (Maastrichtian?) to NP5. **Synonyms:** *N. cohenii* (Perch-Nielsen, 1968) Perch-Nielsen, 1984; *N. dirimosus* (Perch-Nielsen, 1979) Perch-Nielsen, 1981.

Neocrepidolithus fossus (Romein, 1977) Romein, 1979

Pl. 1, fig. 37. **Description:** Low, broad rim and narrow to closed central area. No obvious central structures and unicyclic in LM. **Occurrence:** NP1 to NP4.

Neocrepidolithus grandiculus Bown, 2005

Pl. 1, fig. 38. **Description:** Medium to large with broad rim, unicyclic LM image and a narrow, vacant central area. **Occurrence:** NP5 to NP15.

Genus ***Zeugrhabdotus*** Reinhardt, 1965

Description: Eiffellithids with central-area spanned by a transverse bar.

Zeugrhabdotus recens sp. nov.

Pl. 1, figs 32–33; Pl. 6, figs 23–24. **Derivation of name:** From *recens*, meaning 'recent', referring to the Danian first appearance of this *Zeugrhabdotus* species. **Diagnosis:** Large with broad rim and central area spanned by a broad, birefringent transverse bar that bears a spine; bicyclic LM image. **Remarks:** A Danian homeomorph of the Mesozoic species *Z. embergeri*, appearing around 1.25 million years above the K/Pg boundary and likely descended from the survivor species *Z. sigmoides*. **Dimensions:** Holotype L =10.1 μm (Paratype L = 11.0 μm). **Holotype:** Pl. 1, fig. 33. **Paratype:** Pl. 1, fig. 32. **Type locality:** IODP Hole U1407A, NW Atlantic Ocean. **Type level:** Danian, Sample U1407C-23X-1, 5 cm (Zone NP4). **Occurrence:** NP3 to NP6. **Synonymy list:** *Zeugrhabdotus embergeri* (Noël 1959); Bown (2016), pp 8–9, Pl.4, figs 24–26.

Zeugrhabdotus sigmoides (Bramlette & Sullivan, 1961) Bown & Young, 1997

Pl. 1, fig. 31. **Description:** Relatively narrow rim with wide central area spanned by a spine-bearing bar that narrows at both ends. Narrow bright inner cycle in XPL that broadens where the bar meets the rim. **Occurrence:** Upper Cretaceous (Campanian) to NP10.

Family **GONIOLITHACEAE** Deflandre, 1957

Goniolithus fluckigeri Deflandre, 1957

Description: Pentagonal liths with narrow rim and granular central area plate. Dark, inconspicuous image in LM. Rarely reported but becomes more conspicuous in the lowermost Danian. Forms dodecahedral coccospheres (Mai et al., 1997). **Occurrence:** Upper Cretaceous to NP22.

Mesozoic survivor placolith lineages

Order PODORHABDALES **Rood et al., 1971 emend. Bown, 1987**

Family **BISCUTACEAE** Black, 1971

Genus ***Biscutum*** Black *in* Black & Barnes, 1959

Biscutum harrisonii Varol, 1989

Pl. 1, figs 13–14. **Description:** Medium sized, broadly elliptical, bicyclic placolith with a closed central area. The birefringent tube cycle is narrow but conspicuous in XPL. **Remarks:** Other names have been used for Danian *Biscutum* survivor species including *Biscutum melaniae* (Gorka, 1957) Reinhardt, 1969 and *Biscutum panis* (Edwards, 1973) Edwards & Perch-Nielsen 1975. Both are unsatisfactory, as the former is based on a very poor holotype drawing which is not obviously the species figured here, and there is uncertainty over the exact nature of the latter species with some including it within *Markalius* (e.g., Jiang and Gartner 1986). **Occurrence:** Upper Cretaceous (Turonian) to NP9 (Burnett, 1998; Varol, 1989).

Genus ***Markalius*** Bramlette & Martini, 1964

Description: Circular placoliths with moderately birefringent (grey) shields, bright inner tube cycle and open or closed central area.

Markalius apertus Perch-Nielsen, 1979

Pl. 1, figs 11–12. **Description:** *Markalius* with narrow to moderately wide, open central area. Central area width similar to rim width. **Occurrence:** NP1 to NP15?

Markalius inversus (Deflandre *in* Deflandre & Fert, 1954) Bramlette & Martini, 1964

Pl. 1, figs 7–10. **Description:** *Markalius* with very narrow to closed central area. **Remarks:** Usually rare, but common and conspicuous at Site 1403 in the samples immediately above the K/Pg. In this interval there is variability in morphology, including larger sizes, subcircular to broadly elliptical outlines, and pores or pits evident in the bright tube cycle in XPL (Pl. 1, fig. 8). In these latter forms there is usually one conspicuous pore in each tube cycle sector, but more may be present (4–6 in total). **Occurrence:** Cretaceous to NP22. **Synonym:** *M. astroporus* (Stradner, 1963) Hay & Mohler *in* Hay et al., 1967; **Variants:** *M. latus* Shamrock & Watkins, 2012 – wide birefringent cycle (>33%); *M. walvisensis* Bernaola & Monechi, 2007 – very narrow tube cycle.

Order WATZNAUERIALES **Bown, 1987**

Family **WATZNAUERIACEAE** Rood et al., 1971

Description: Placoliths with R-units forming proximal and distal shield elements; the V-unit typically forms a narrow distal cycle near the inner edge of the shield.

Genus ***Cyclagelosphaera*** Noël, 1965

Pl. 1, figs 15–23. **Description:** Circular watznaeurids.

Cyclagelosphaera alta Perch-Nielsen, 1979

Description: With central, plug-forming, inner tube-cycle that forms a high conical structure with 4–6 prominent rays. **Occurrence:** NP1 to NP3.

Cyclagelosphaera colorata sp. nov.

Pl. 1, figs 19–23. **Derivation of name:** From *colorata*, meaning ‘coloured’, referring to the high birefringence colours that characterise the appearance of this species in XPL. **Diagnosis:**

Large, circular to subcircular (8-11 µm) watznauaerid with an indistinct but diagnostic low central plug and overall yellow-orange birefringence. **Differentiation:** Distinguished from other species of *Cyclagelosphaera* (and *Watznaueria*) by its large size, yellow-orange birefringence colours and unusual central plug structure. **Remarks:** This species has a short stratigraphic range in the Danian (Zone NP1–2; +112 to +843 kyr) and is likely a descendant of *Cyclagelosphaera reinhardtii*. The slight variation in outline is unusual for a species of *Cyclagelosphaera* but circular forms are generally dominant. **Dimensions:** Holotype L = 11.2 µm (Paratype L = 8.8 µm). **Holotype:** Pl. 1, fig. 21. **Paratype:** Pl. 1, fig. 19. **Type locality:** IODP Hole U1407C, NW Atlantic Ocean. **Type level:** Danian, Sample U1407C-20X-5, 119cm (Zone NP2). **Occurrence:** Rare to frequent. NP1 to NP2; IODP Sites U1403, U1407 and ODP Sites 1209 and 1210 (Pacific).

Cyclagelosphaera reinhardtii (Perch-Nielsen, 1968) Romein, 1977

Pl. 1, figs 17–18. **Description:** *Cyclagelosphaera* with central, plug-forming, inner tube-cycle that is slightly raised above shield level. Very similar to extant *Tergestiella adriatica* Kamptner, 1940 (see Hagino et al., 2015). **Occurrence:** Albian (Burnett, 1998) to NP10 (Bybell and Self-Trial, 1995).

Cyclagelosphaera cf. *C. tubulata* (Grün & Zweili, 1980) Cooper, 1987

Pl. 1, figs 15–16. **Description:** Small to medium sized *Cyclagelosphaera* with narrow central opening. **Remarks:** Similar in overall morphology to the Jurassic species *C. tubulata*. **Occurrence:** Danian.

Holococcoliths

Family **CALYPTROSPHAERACEAE** Boudreaux & Hay, 1967

Remarks: Apart from a small number of larger and robust taxa, the presence of holococcoliths in the Danian and later Paleogene fossil record is usually dependent on good to exceptional preservation. Stratigraphic range estimates are often uncertain due to these preservation dependent records.

Genus ***Octolithus*** Romein, 1979

Octolithus multiplus (Perch-Nielsen, 1973) Romein, 1979

Pl. 1, figs 39–41. **Description:** Holococccolith with four main blocks and two smaller blocks at either end. **Occurrence:** Maastrichtian to NP4. **Synonyms:** *Lanternithus jawzii* Varol, 1989.

Mesozoic survivor nannolith lineages

Order BRAARUDOSPHAERALES **Aubry, 2013 emend. Lees & Bown, 2016**

Family **BRAARUDOSPHAERACEAE** Deflandre, 1947

Description: Pentaliths consisting of five segments, each of which behaves as a discrete crystal-unit with c-axis parallel to the edge of the pentalith (tangential). A lamellar substructure to the segments is consistently present. Outline may be pentagonal, stellate, scalloped or crenulated.

Genus ***Braarudosphaera*** Deflandre, 1947

Description: Pentaliths with sutures that go to the edges of the pentagon.

Braarudosphaera alta Romein, 1979

Pl. 1, fig. 29–30. **Description:** Tall braarudosphaerids, usually seen in side-view.

Braarudosphaera bigelowii (Gran & Braarud, 1935) Deflandre, 1947

Pl. 1, fig. 24. **Description:** Sutures show clockwise obliquity in distal view, running from the centre to approximately 3/8 of the way along the side of the pentalith. **Occurrence:** Aptian to Recent, but only recorded through a short interval at Site 1403 (NP1–2) and Site 1407 (NP2 to lower NP4).

Braarudosphaera perampla Bown, 2010

Pl. 1, fig. 26. **Description:** Very large (>14 μm) with slightly rounded corners and convex upper surface. **Occurrence:** NP2 to NN1, but only recorded through a short interval (NP2 to lower NP4) at Site 1407.

Genus ***Micrantholithus*** Deflandre *in* Deflandre & Fert, 1954

Description: Pentaliths with sutures that go to the vertices (points) of the pentagon.

Micrantholithus attenuatus Bramlette & Sullivan, 1961

Pl. 1, fig. 27. **Description:** Stellate with deeply indented sides and gracile, long rays. **Occurrence:** NP2 to NP23, but only recorded through a short interval (NP2 to lower NP4) at Site 1407. **Synonyms:** *M. inaequalis* Martini, 1961; *M. aequalis* Sullivan, 1964 – ?smaller.

Micrantholithus breviradiatus Bown, 2005

Pl. 1, fig. 28. **Description:** Shallowly indented sides and rounded apices. **Occurrence:** NP2 to NP16, but only recorded through a short interval (NP2) at Site 1407.

Micrantholithus discula (Bramlette & Riedel, 1954) Bown, 2005

Pl. 1, fig. 25. **Description:** Elevated with rounded outline and elliptical side views. **Occurrence:** NP2 to NP11, but only recorded through a short interval (NP2) at Site 1407.

Micrantholithus flos Deflandre *in* Deflandre & Fert, 1954

Description: Relatively straight edges. **Occurrence:** NP2 to NP23, but only recorded through a short interval (NP2 to lower NP4) at Site 1407.

Family **LAPIDEACASSACEAE** Bown & Young 1997

Pl. 1, fig. 42–44. **Description:** Dome-shaped to cylindrical nannoliths, with high walls constructed of one to several cycles of thin elements, enclosing a hollow central space; they taper distally and may have long apical spines or processes. Conspicuous in lowermost Danian assemblages but otherwise rarely seen and so stratigraphic ranges are very uncertain. The numerous species names are largely based on the number of apical spines present, but this is strongly influenced by preservation, and may not represent any real taxonomic significance. **Occurrence:** Lower Aptian to Eocene.

Genus ***Lapideacassis*** Black, 1971

Pl. 1, fig. 42–44. **Remarks:** Specimens within this group were generally not identified to species level during this study, but we broadly apply the two morphogroups below and provide a list of previously described species. **Synonyms:** *Scampanella* Forchheimer & Stradner, 1973; *Pervilithus* Crux, 1981 – plan view. The name *Mennerius* Luljeva, 1967 may be the senior synonym, but for taxonomic stability we continue to use *Lapideacassis*.

Lapideacassis glans Black, 1971

Description: Squat, dome-shaped with protruding ledge just above the base. **Occurrence:** Lower Aptian to Eocene.

Lapideacassis mariae Black 1971

Description: Narrow, tall, cylindrical in its lower half and tapers to a domed upper surface. Tall apical spines seen when well preserved. **Occurrence:** Aptian to Eocene. **Variants:** *L. asymmetrica* (Perch-Nielsen *in* Perch-Nielsen & Franz, 1977) Burnett, 1998 – asymmetric spines; *L. bispinosa* (Perch-Nielsen *in* Perch-Nielsen & Franz, 1977) Burnett, 1998 – two spines, one near-vertical and one at 45 degrees; *L. blackii* Perch-Nielsen *in* Perch-Nielsen & Franz, 1977 – single spine; *L. magnifica* (Perch-Nielsen *in* Perch-Nielsen & Franz, 1977) Burnett, 1998 – single spine with distal bifurcations; *L. multispinata* Perch-Nielsen *in* Perch-Nielsen & Franz, 1977 – >three spines; *L. trispina* Perch-Nielsen *in* Perch-Nielsen & Franz, 1977 – three, near-horizontally orientated spines; *L. wisei* Perch-Nielsen *in* Perch-Nielsen & Franz, 1977 – three, asymmetrically-arranged spines at about 45 degrees. All described from NP3 or NP4.

Acknowledgements

Thanks to Jim Pospichal, Matthew Hampton, Sarah Alvarez, Jeremy Young and Laia Alegret for sharing comparative sample material. Thanks to IODP Expedition 342 operational and technical staff and shipboard science party for facilitating such an enjoyable and successful drilling expedition. This research used samples and data provided by the Integrated Ocean Drilling Program (IODP). We thank UCL for providing HK with the Dean's Prize to part support this study. Funding for this research was provided to PB (Expedition participation) by the Natural Environment Research Council (NERC). Finally, thanks to Jean Self Trail and Claudia Agnini for thorough reviews of the manuscript.

FIGURE CAPTIONS

Figure 1: Location map of IODP Expedition 342 sites 1403 and 1407 (Site 1403 – 39°56.5997′N, 51°48.1998′W; Site 1407 – 41°25.4993′N 49 48.7987′W).

Figure 2: Core images of the K/Pg sections from sites 1403 and 1407 showing position of the boundary level and details of the spherule layer (core images from IODP).

Figure 3: Stratigraphic distribution of selected nannofossils from the Danian of Site 1403. Vertical lines indicate stratigraphic ranges: dashed lines are discontinuous ranges, solid lines are continuous ranges, and broad boxes are acme intervals, where abundance is typically >50% of the assemblage. Red triangles indicate biozonal events: solid triangles Martini (1971), open triangles Agnini et al. (2014).

Figure 4: Revised age model for Site 1407 (black line) and comparison with the shipboard age model (grey line) from Norris et al. (2014). Bioevent age calibrations are from Gradstein et al. (2012), except for the *Cruciplacolithus* size observation, which is from this study.

Figure 5: Stratigraphic distribution of selected nannofossils from the Danian of Site 1407. Vertical lines indicate stratigraphic ranges: dashed lines are discontinuous ranges, solid lines are continuous ranges, and broad boxes are acme intervals, where abundance is typically >50% of the assemblage. Red triangles indicate biozonal events: solid triangles Martini (1971), open triangles Agnini et al. (2014).

Figure 6: Relative abundance of key Danian taxa (% of total nannofossil abundance) from Site 1403. Species with <3% maximum relative abundance are not included. Foraminifera and calcisphere counts are given as fragments (Frags) per FOV.

Figure 7: Relative abundance of key Danian species (% of total nannofossil abundance) from Site 1407. Species with <3% maximum relative abundance are not included. Foraminifera and calcisphere counts are given as fragments (Frags) per FOV.

Figure 8: Stratigraphic distribution of calcareous nannoplankton across the K/Pg boundary and Danian. Species are grouped as survivor (green) and incoming (brown), with broader lines for acme occurrences and subhorizontal lines indicating likely evolutionary relationships. Inc. Sed.

= Incertae Sedis; Calcisdisc. = Calcidiscaceae; Watz. = Watznaueriaceae; Braar. = Braarudosphaeraceae; Hol. = holococcoliths; Bisc. = Biscutaceae.

Figure 9: Prinsiaceae relative abundance (% of total nannofossil abundance) from sites 1403 and 1407, combined to form a composite section. The initial ~+0.5 Myr of data is taken from Site 1403 and the upper part comes from Site 1407, to best show the *Praeprinsius* acme.

Figure 10: Rock surface scanning electron micrograph from the *P. tenuiculus* acme interval (Sample 1407A-23-2, 50 cm) showing the abundance of liths and coccosphere.

Figure 11: Coccolithaceae relative abundance (% of total nannofossil abundance) from sites 1403 and 1407 combined to form a composite section. The initial +1.2 Myr of data is taken from Site 1403 to best show the *Cruciplacolithus* and *Coccolithus* acmes. The sharp drop in *Coccolithus* abundance, where the record switches from Site 1403 to Site 1407, is due to the higher numbers of *P. tenuiculus* at Site 1407 through this interval, shown in the separate Site 1407 plot on the right (see also Figures 6 and 7).

Figure 12: Genus and species concepts across the *Praeprinsius*-*Prinsius*-*Toweius* lineage highlighting the diagnostic morphological and morphometric criteria.

Figure 13: Coccosphere geometry across the Prinsiaceae (taxa are colour coded), including cell diameter (Φ_{Cell}), coccolith length (C_L) and number of coccoliths per sphere (C_N). **(A)** Observed stratigraphic range for each taxon (black bars) and coccosphere data source range (coloured bars). Horizontal lines are drawn where first and last occurrences have been recorded. **(B)** All Prinsiaceae coccosphere data with the average number of coccoliths per coccosphere (C_n) given in square brackets for each taxon. **(C)** Prinsiaceae biometric data by timeslice from 0 to +0.9 Myr above the K/Pg boundary (lowermost panel), +0.9 to +1.5 Myr (middle panel) and +1.5 to +4 Myr (top panel). The black arrows on the coccolith size *versus* cell diameter plots indicate the general trends in size with age, getting younger towards the arrowheads, as well as providing an indication of evolutionary lineage.

Figure 14: (**A**) *Praeprinsius* coccolith size (length in μm) through time with each point representing a single measurement and showing the average (dashed line), median (solid line) and 5th–95th percentile range (grey envelope). Data from holes 1403A and 1407A (1403A-26-5-5cm to 1403A 25-5-4cm; 1407A-23-2-125cm to 1407A-23-1-95cm). **(B)** *Praeprinsius tenuiculus* coccosphere geometry sorted by coccolith length and cell diameter where two distinct populations (types 1 and 2) are distinguished using the size-frequency plots. Data are colour coded by age (upper panel) and number of coccoliths per coccosphere (C_N) (lower panel).

PLATE CAPTIONS

Plate 1. Light micrographs of Danian survivor group nannofossil taxa, calcispheres and *Biantholithus*.

Plate 2. Light micrographs of Danian incoming nannofossil taxa: Prinsiaceae and *Hornibrookina*.

Plate 3. Light micrographs of Danian incoming nannofossil taxa: Coccolithaceae, Zygodiscaceae, *Ellipsolithus* and Discoasterales.

Plate 4. Scanning electron micrographs of Danian incoming Prinsiaceae nannofossil taxa: *Neobiscutum, Praeprinsius* and *Futyania*. All images are the same magnification.

Plate 5. Scanning electron micrographs of Danian incoming Prinsiaceae nannofossil taxa: *Praeprinsius, Prinsius, Futyania* and *Toweius*.

Plate 6. Scanning electron micrographs of Danian incoming nannofossil taxa: Coccolithaceae, Zygodiscaceae, *Ellipsolithus,* Discoasterales and *Zeugrhabdotus recens*.

TABLE CAPTIONS

Table 1: Nannofossil bioevents for the Danian of Site 1403. Sample depth is core composite depth below seafloor (m CCSF) based on Norris et al. (2014) and ages are based on the Hull et

al. (2020) age model. Previously published bioevent calibration ages are from Gradstein et al. (2012) and Agnini et al. (2014)*.

Table 2: Revised CCSF (CCSFr) for samples outside the shipboard splice, with revised depths shaded. CCSF = Core composite depth below sea floor.

Table 3: Age-depth tie points used for the revised Site 1407 age model, with revised depths shaded. The nannofossil biohorizon ages are from Gradstein et al. (2012)* or the cyclostratigraphic age model of Hull et al. (2020)**. CCSFr = revised core composite depth below sea floor.

Table 4: Nannofossil bioevents for the Danian of Site 1407. CCSF = Core composite depth below sea floor. Previously published bioevent calibration ages are from Gradstein et al. (2012) and Agnini et al. (2014)*.

Table 5: List of Cretaceous survivor species based on stratigraphic ranges that continue significantly into the Paleogene, diagnostic late Cretaceous biogeographic distributions, and distinct abundance patterns above the K/Pg boundary (e.g., Bown, 2005a; Alvarez et al. 2019).

APPENDICES

Appendix 1. Stratigraphical range chart of calcareous nannofossils from IODP Site 1403. Biostratigraphical index species and other notable occurrences are shaded grey. Species abundance: A = >10 specimens per field of view (FOV), C = 1–9 specimens per FOV, F = 1 specimen per 2–10 FOV, R = 1 specimen per 11–100 FOV, counts are provided for very rare species, ? = questionable occurrence. Nannofossil preservation: G = good, M = moderate, P = poor. Base (B) and Top (T) are used in the Bioevents column. The NP biozones are from Martini (1971), CNP Zones from Agnini et al. (2014) and UC biozones from Burnett (1998). The chart shows all of the samples studied but some were used only for morphometric data collection and so are not as thoroughly logged as others.

Appendix 2. Stratigraphical range chart of calcareous nannofossils from IODP Site 1407. Biostratigraphical index species and other notable occurrences are shaded. Species abundance: A = >10 specimens per field of view (FOV), C = 1–9 specimens per FOV, F = 1 specimen per 2–10 FOV, R = 1 specimen per 11–100 FOV, counts are provided for very rare species, ? = questionable occurrence. Nannofossil preservation: G = good, M = moderate, P = poor. Base (B) and Top (T) are used in the Bioevents column. The NP biozones are from Martini (1971), CNP Zones from Agnini et al. (2014) and UC biozones from Burnett (1998).

Appendix 3. Charts showing raw data and calculated % relative abundance nannofossil count data from IODP sites 1403 and 1407.

References

Agnini, C., Fornaciari, E., Raffi, I., Catanzariti, R., Pälike, H., Backman, J., Rio, D. 2014. Biozonation and biochronology of Paleogene calcareous nannofossils from low and middle latitudes. *Newsletters on Stratigraphy*, **47**:131-181.

Alvarez, S.A., Gibbs, S.J., Bown, P.R., Kim, H., Sheward, R.M. & Ridgwell, A. 2019. Diversity decoupled from ecosystem function and resilience during mass extinction recovery. *Nature*, **574**: 242-245.

Aubry, M.-P., Bord, D. & Rodriguez, O. 2011. New taxa of the Order Discoasterales Hay 1977. *Micropaleontology*, **57**(3): 269-287.

Backman, J. 1986. Late Paleocene to middle Eocene calcareousnannofossil biochronology from the Shatsky Rise, Walvis Ridge and Italy. *Palaeogeography, Palaeoclimatology, Palaeoecology*, **57**: 43–59.

Batenburg, S.J., Friedrich, O., Moriya, K., Voigt, S., Cournède, C., Moebius, I., Blum, P., Bornemann, A., Fiebig, J., Hasegawa, T., Hull, P.M., Norris, R.D., Röhl, U., Sexton, P.F., Westerhold, T., Wilson, P.A. and the IODP Expedition 342 Scientists. 2018. Late

Maastrichtian carbon isotope stratigraphy and cyclostratigraphy of the Newfoundland Margin (Site U1403, IODP Leg 342). *Newsletters on Stratigraphy*, **51**(2): 245-260.

Bown, P. 2005a. Selective calcareous nannoplankton survivorship at the Cretaceous-Tertiary boundary. *Geology*, **33**(8): 653-656.

Bown, P.R. 2005b. Calcareous nannoplankton evolution: a tale of two oceans. *Micropaleontology*, **51**(4): 299-308.

Bown, P.R. 2010. Calcareous nannofossils from the Paleocene/Eocene Thermal Maximum interval of southern Tanzania (TDP Site 14). *Journal of Nannoplankton Research*, **31**: 11-38.

Bown, P.R. 2016. Paleocene calcareous nannofossils from Tanzania (TDP sites 19, 27 and 38). *Journal of Nannoplankton Research,* **36**: 1-32

Bown, P.R. & Young, J.R. 1998. Techniques. *In*: Bown, P.R. (Ed.). *Calcareous Nannofossil Biostratigraphy*. Kluwer Academic, London: 16–28.

Bown, P.R., Gibbs, S.J., Sheward, R., O'Dea, S. & Higgins, D. 2014. Searching for cells: the potential of fossil coccospheres in coccolithophore research. *Journal of Nannoplankton Research*, **34**: 5-21.

Bralower, T.J. 2002. Evidence of surface water oligotrophy during the Paleocene-Eocene Thermal Maximum: Nannofossil assemblage data from Ocean Drilling Program Site 690, Maud Rise: Weddell Sea. *Paleoceanography*, **17**: 1-13.

Burnett, J. A. 1998. Upper Cretaceous. *In*: Bown, P. R. (ed.) *Calcareous Nannofossil Biostratigraphy*. Kluwer Academic, London: 132-199.

Bybell, L. M. & Self-Trail, J. 1995. Evolutionary, biostratigraphic and taxonomic study of calcareous nannofossils from a continuous Palaeocene-Eocene boundary section in New Jersey. *U.S. Geological Survey, Professional Paper*, **1554**: 1-36.

1457 Dallanave, E., Agnini, C., Muttoni, G. & Rio, D. 2012. Paleocene magneto-biostratigraphy
1458 and climate-controlled rock magnetism from the Belluno Basin, Tethys Ocean, Italy.
1459 *Palaeogeography Palaeoclimatology Palaeoecology*, **337–338**: 130-142.
1460 Ellis, C. H. & Lohmann, W. H. 1973. *Toweius petalosus* new species, a Paleocene calcareous
1461 nannofossil from Alabama. *Tulane Studies in Geology and Paleontology*, **10**: 107-110.
1462 Fornaciari, E., Giusberti, L., Luciani, V., Tateo, F., Agnini, C., Backman, J., Oddone, M. &
1463 Rio, D. 2007. An expanded Cretaceous−Tertiary transition in a pelagic setting of the
1464 Southern Alps (central-western Tethys). *Palaeogeography Palaeoclimatology*
1465 *Palaeoecology*, **255**: 98-131.
1466 Fuqua, L.M., Bralower, T.J., Arthur, M.A. & Patzkowsky, M.E. 2008. Evolution of
1467 Calcareous Nannoplankton and the Recovery of Marine Food Webs After the Cretaceous-
1468 Paleocene Mass Extinction. *Palaios*, **23**(4): 185-194.
1469 Gallagher, L. T. 1989. *Reticulofenestra*: A critical review of taxonomy, structure and
1470 evolution. *In*: Crux, J. A. & van Heck, S. E. (eds) Nannofossils and their applications:
1471 Proceedings of the 2nd INA Conference, London 1987. *British Micropalaeontological*
1472 *Society Publication Series*: 41-75.
1473 Gardin, S. 2002. Late Maastrichtian to early Danian calcareous nannofossils at Elles
1474 (Northwest Tunisia). A tale of one million years across the K-T
1475 boundary. *Palaeogeography Palaeoclimatology Palaeoecology*, **178**: 211-231.
1476 Gartner, S. 1996. Calcareous nannofossils at the Cretaceous-Tertiary boundary. *In*: MacLeod,
1477 N., Keller, G. (eds) Cretaceous-Tertiary mass extinctions: biotic and environmental
1478 changes. W.W. Norton & Company: 27–47.
1479 Gibbs, S.J., Poulton, A.J., Bown, P.R., Daniels, C.J., Hopkins, J., Young, J.R., Jones, H.L.,
1480 Thiemann, G.J., O'Dea, S.A. & Newsam, C. 2013. Species-specific growth response of

coccolithophores to Palaeocene–Eocene environmental change. *Nature Geoscience*, **6**(3): 218-222.

Gibbs, S.J., Sheward, R.M., Bown, P.R., Poulton, A.J. & Alvarez, S.A. 2018. Warm plankton soup and red herrings: calcareous nannoplankton cellular communities and the Palaeocene-Eocene Thermal Maximum. *Phil. Trans. R. Soc. A*, **376**(2130).

Gibbs, S.J., Bown, P.R., Ward, B.A., Alvarez, S.A., Kim, H., Archontikis, O.A., Sauterey, B., Poulton, A.J., Wilson, J., Ridgwell. A. 2020. Algal plankton turn to hunting to survive and recover from end-Cretaceous impact darkness. *Science Advances* **6** no. 44: eabc9123, DOI: 10.1126/sciadv.abc9123.

Gradstein, F.M., Ogg, J.G., Schmitz, M., Ogg, G. (Eds) 2012. *The Geological Time Scale 2012*. Elsevier.

Hagino, K., Young, J.R., Bown, P.R., Godrijan, J., Kulhanek, D.K., Kogame, K. & Horiguchi, T. 2015. Re-discovery of a "living fossil" coccolithophore from the coastal waters of Japan and Croatia. *Marine Micropaleontology*, **116**: 28-37.

Hay, W.W. & Mohler, H.P. 1967. Calcareous Nannoplankton from Early Tertiary Rocks at Pont Labau, France, and Paleocene: Early Eocene Correlations. *Journal of Paleontology*, **41**(6): 1505-1541.

Henderiks, J. 2008. Coccolithophore size rules — Reconstructing ancient cell geometry and cellular calcite quota from fossil coccoliths. *Marine Micropaleontology*, **67**(1-2): 143-154.

Houdan, A., Probert, I., Zatylny, C., Véron, B. & Billard, C., 2006. Ecology of oceanic coccolithophores. I. Nutritional preferences of the two stages in the life cycle of *Coccolithus braarudii* and *Calcidiscus leptoporus*. *Aquatic Microbial Ecology*, **44**: 291-301.

Hull, P.M., Bornemann, A., Penman, D.E., Henehan, M.J., Norris, R.D., Wilson, P.A., Blum, P., Alegret, L., Batenburg, S.J., Bown, P.R., Bralower, T.J., Cournede, C., Deutsch, A.,

Donner, B., Friedrich, O., Jehle, S., Kim, H., Kroon, D., Lippert, P.C., Loroch, D., Moebius, I., Moriya, K., Peppe, D.J., Ravizza, G.E., Rohl, U., Schueth, J.D., Sepulveda, J., Sexton, P.F., Sibert, E.C., Sliwinska, K.K., Summons, R.E., Thomas, E., Westerhold, T., Whiteside, J.H., Yamaguchi, T. & Zachos, J.C. 2020. On impact and volcanism across the Cretaceous-Paleogene boundary. *Science*, **367**(6475): 266-272.

Jiang, M.J. & Gartner, S. 1986. Calcareous Nannofossil Succession across the Cretaceous/Tertiary Boundary in East-Central Texas. *Micropaleontology*, **32**(3): 232-255

Lees, J.A., Bown, P.R., Young, J.R. & Riding, J.B. 2004. Evidence for annual records of phytoplankton productivity in the Kimmeridge Clay Formation coccolith stone bands (Upper Jurassic, Dorset, UK). *Marine Micropaleontology*, **52**(1-4): 29-49.

Loroch, D., Deutsch, A., Berndt, J. & Bornemann, A. 2016. The Cretaceous/Paleogene (K-Pg) boundary at the J Anomaly Ridge, Newfoundland (IODP Expedition 342, Hole U1403B). *Meteoritics & Planetary Science*, **51**(7): 1370-1385.

Mai, H., von Salis, K., Willems, H. & Romein, A. J. T. 1997. Fossil coccospheres from the K/T boundary section from Geulhemmerberg, The Netherlands. *Micropaleontology*, **43**: 281-303.

Mai, H., Speijer, R.P. & Schulte, P. 2003. Calcareous index nannofossils (coccoliths) of the lowermost Paleocene originated in the late Maastrichtian. *Micropaleontology*, **49**(2): 189-195.

Martini, E. 1971. Standard Tertiary and Quaternary calcareous nannoplankton zonation. *In*: A. Faranacci (Ed.) *Proceedings of the Second Planktonic Conference Roma 1970.* Edizioni Tecnoscienza, Rome, **2**: 739–785.

Miniati, F., Cappelli, C. & Monechi, S. 2021. Revised taxonomy and early evolution of fasciculiths at the Danian–Selandian transition. *Journal of Micropalaeontology*, **40**: 101-144.

1531 Minoletti, F., De Rafelis, M., Renard, M., Gardin, S. & Young, J. 2005. Changes in the
1532 pelagic fine fraction carbonate sedimentation during the Cretaceous–Paleocene transition:
1533 contribution of the separation technique to the study of Bidart section. *Palaeogeography,*
1534 *Palaeoclimatology, Palaeoecology*, **216**: 119–137.
1535 Monechi. S., Reale, V., Bernaola, G. & Balestra, B. 2013. The Danian/Selandian boundary at
1536 Site 1262 (South Atlantic) and in the Tethyan region: Biomagnetostratigraphy,
1537 evolutionary trends in fasciculiths and environmental effects of the Latest Danian Event.
1538 *Marine Micropaleontology*, **98**: 28–40.
1539 Nannotax3 - Young, J.R., Bown P.R. & Lees J.A. (Eds): Nannotax website. International
1540 Nannoplankton Association. May 2014. URL: http://ina.tmsoc.org/Nannotax3
1541 Norris, R.D., Wilson, P.A., Blum, P. & the Expedition 342 Scientists. 2014. Paleogene
1542 Newfoundland Sediment Drifts and MDHDS Test. *Proceedings of the Integrated Ocean*
1543 *Drilling Program*, **342**: College Station, TX (Integrated Ocean Drilling Program). doi:
1544 10.2204/iodp.proc.342.2014 [http://publications.iodp.org/proceedings/342/342title.htm]
1545 Perch-Nielsen, K. 1969. Elektronenmikroskopische Untersuchungen der Coccolithophoriden
1546 der Dan-Scholle von Katharinenjof (Fehmarn). *Neues Jahrbuch für Geologie und*
1547 *Paläontologie, Abhandlungen*, **132**: 317-332.
1548 Perch-Nielsen, K. 1985. Cenozoic calcareous nannofossils. *In*: H.M. Bolli, J.B. Saunders &
1549 K. Perch-Nielsen (Eds.). *Plankton Stratigraphy*. Cambridge University Press, Cambridge:
1550 427–554.
1551 Pospichal, J.J. 1994. Calcareous nannofossils at the K-T boundary, El Kef: No evidence for
1552 stepwise, gradual, or sequential extinctions. *Geology*, **22**(2): 99-102.
1553 Pospichal, J.J. 1996. *Calcareous nannoplankton mass extinction at the Cretaceous/Tertiary*
1554 *boundary: An update*. *In:* Ryder, G., Fastovsky, D.E. and Gartner, S. eds., The Cretaceous-

1555 Tertiary event and other catastrophes in Earth history: *Geological Society of America*
1556 *Special Paper* **307**: 335–360.
1557 Pospichal, J. J. & Wise, S. W. 1990. Calcareous nannofossils across the K/T boundary, ODP
1558 hole 690C, Maud Rise, Weddell Sea. *Proceedings of the Ocean Drilling Program,*
1559 *Scientific Results*, **113**: 515-532.
1560 Romein, A.J.T. 1979. Lineages in early Paleogene calcareous nannoplankton. *Utrecht*
1561 *Micropaleontological Bulletins*, **22**: 1-230.
1562 Self-Trail, J.M., Watkins, D.K., Pospichal, J.J. & Seefelt, E.L. 2022. Evolution and taxonomy
1563 of the Paleogene calcareous nannofossil genus *Hornibrookina*. *Micropaleontology*, 68: 85-
1564 113.
1565 Stradner, H., Aubry, M. -P. & Bonnemaison, M. 2010. Calcareous nannofossil type
1566 specimens in the collection of the Geological Survey of Austria: A taxonomic and
1567 stratigraphic update. *Jahrbuch der Geologischen Bundesanstalt*, **150**(1-2): 9-84.
1568 Supraha, L., Ljubesic, Z., Mihanovic, H. & Henderiks, J. 2014. Observations on the life cycle
1569 and ecology of *Acanthoica quattrospina* Lohmann from a Mediterranean estuary. *Journal*
1570 *of Nannoplankton Research*, **34**: 49-56.
1571 Thibault, N., Minoletti, F. & Gardin, S. 2018. Offsets in the early Danian recovery phase in
1572 carbon isotopes: Evidence from the biometrics and phylogeny of the *Cruciplacolithus*
1573 lineage. *Revue de Micropaléontologie*, **61**(3-4): 207-221.
1574 van Heck, S. E. & Prins, B. 1987. A refined nannoplankton zonation for the Danian of the
1575 Central North Sea. *Abhandlungen der Geologischen Bundesanstalt*, **39**: 285-303.
1576 Varol, O. 1989. Palaeocene calcareous nannofossil biostratigraphy. *In*, Crux, J. A. & van
1577 Heck, S. E. (eds) Nannofossils and their applications: Proceedings of the 2nd INA
1578 Conference, London 1987. *British Micropalaeontological Society Publication Series*,
1579 Chapman and Hall: 265-310.

1580 Varol, O. & Jakubowski, M. 1989. Some new calcareous nannofossil taxa. *INA Newsletter*,
1581 **11**: 24-29.
1582 Wei, W. & Liu, L. 1992. Biometric and biochronologic study of the *Prinsius martinii - P.*
1583 *bisulcus* group. *Knihovnicka ZPN*, **14b**(2): 11-35.
1584 Yamaguchi, T., Bornemann, A., Matsui, H. & Nishi, H. 2017. Latest Cretaceous/Paleocene
1585 deep-sea ostracode fauna at IODP Site U1407 (western North Atlantic) with special
1586 reference to the Cretaceous/Paleogene boundary and the Latest Danian Event. *Marine*
1587 *Micropaleontology*, **135**: 32-44.
1588 Young, J. R. 1998. Neogene. *In*: Bown, P. R. (ed.) *Calcareous Nannofossil Biostratigraphy*.
1589 Kluwer Academic, London: 225-265.
1590 Young, J.R. & Bown, P.R. 1997. Cenozoic calcareous nannoplankton classification. *Journal*
1591 *of Nannoplankton Research*, **19**: 36-47.
1592 Young, J.R., Bergen, J.A., Bown, P.R., Burnett, J.A., Fiorentino, A., Jordan, R.W., Kleijne,
1593 A., van Niel, B.E., Romein, A.J.T. & von Salis, K. 1997. Guidelines for coccolith and
1594 calcareous nannofossil terminology. *Palaeontology*, **40**: 875-912.
1595 Young, J. R., Geisen, M., Cros, L., Kleijne, A., Probert, I. & Ostergaard, J. B. 2003. A guide
1596 to extant coccolithophore taxonomy. *Journal of Nannoplankton Research, Special Issue*, **1**: 1-
1597 132.

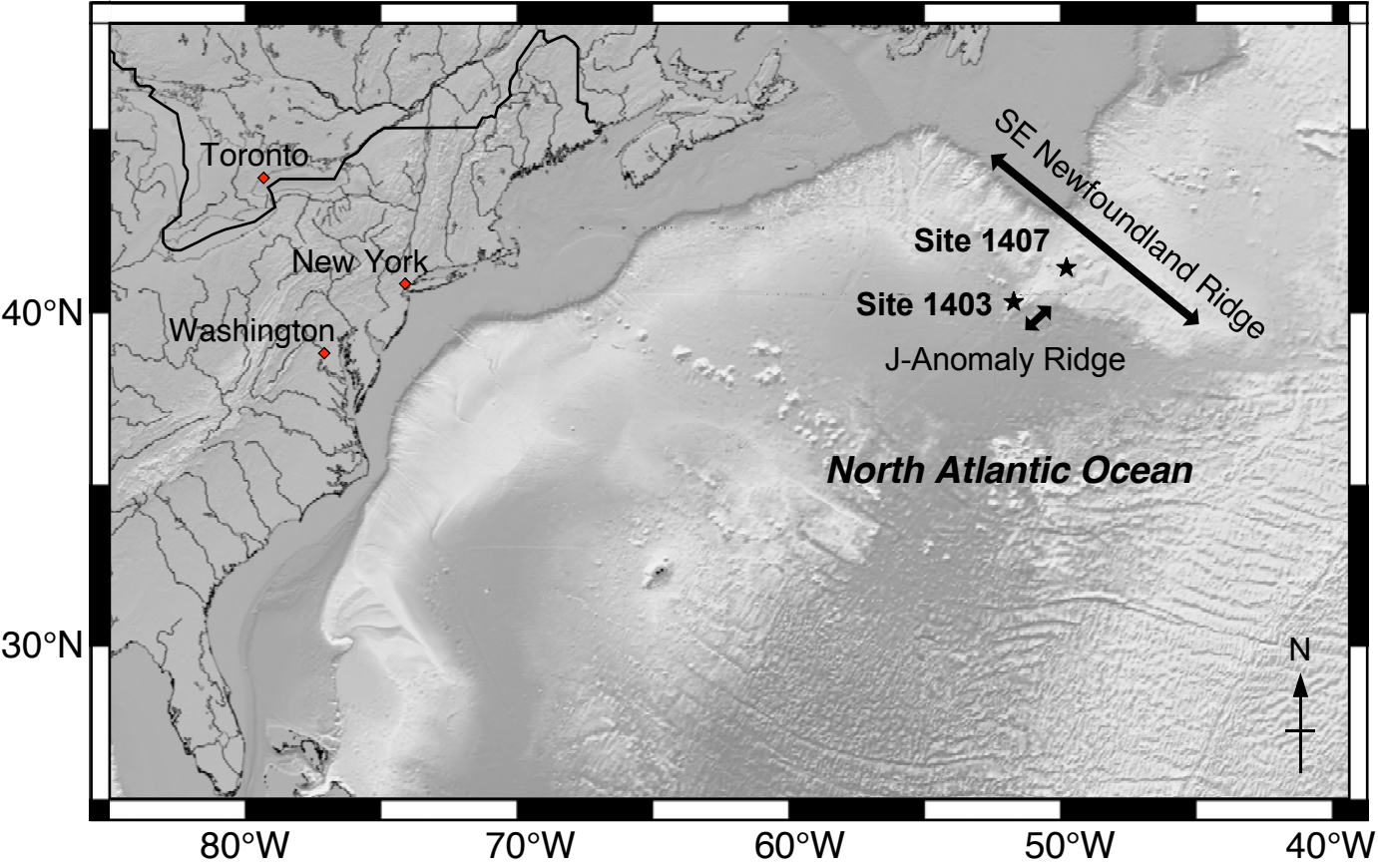
Toronto
New York
Washington
SE Newfoundland Ridge
Site 1407
Site 1403
J-Anomaly Ridge
North Atlantic Ocean
N
40°N
30°N
80°W
70°W
60°W
50°W
40°W

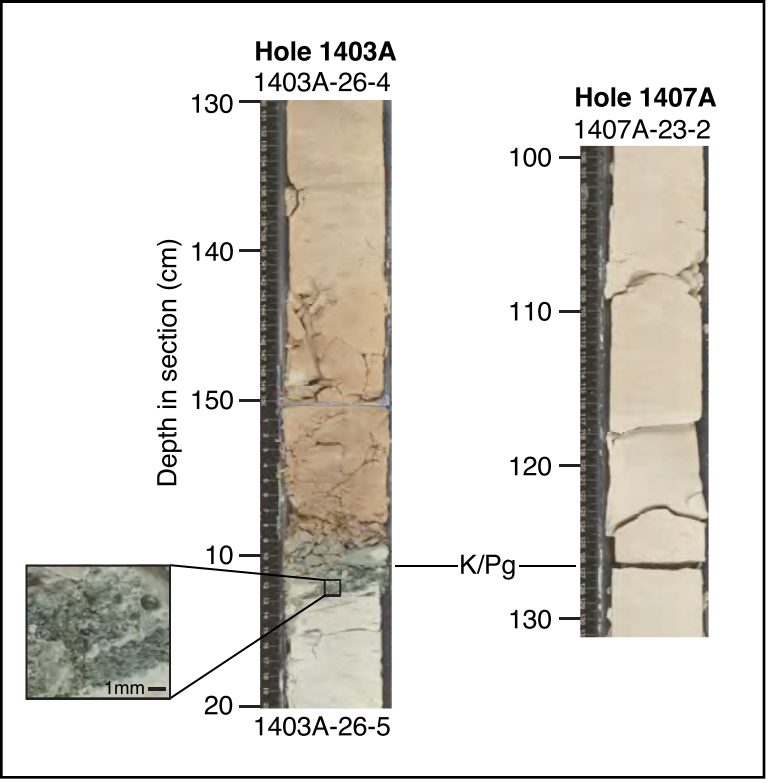
Hole 1403A
1403A-26-4
130
140
150
10
20
1403A-26-5
Depth in section (cm)
1mm
K/Pg
Hole 1407A
1407A-23-2
100
110
120
130

Site 1403

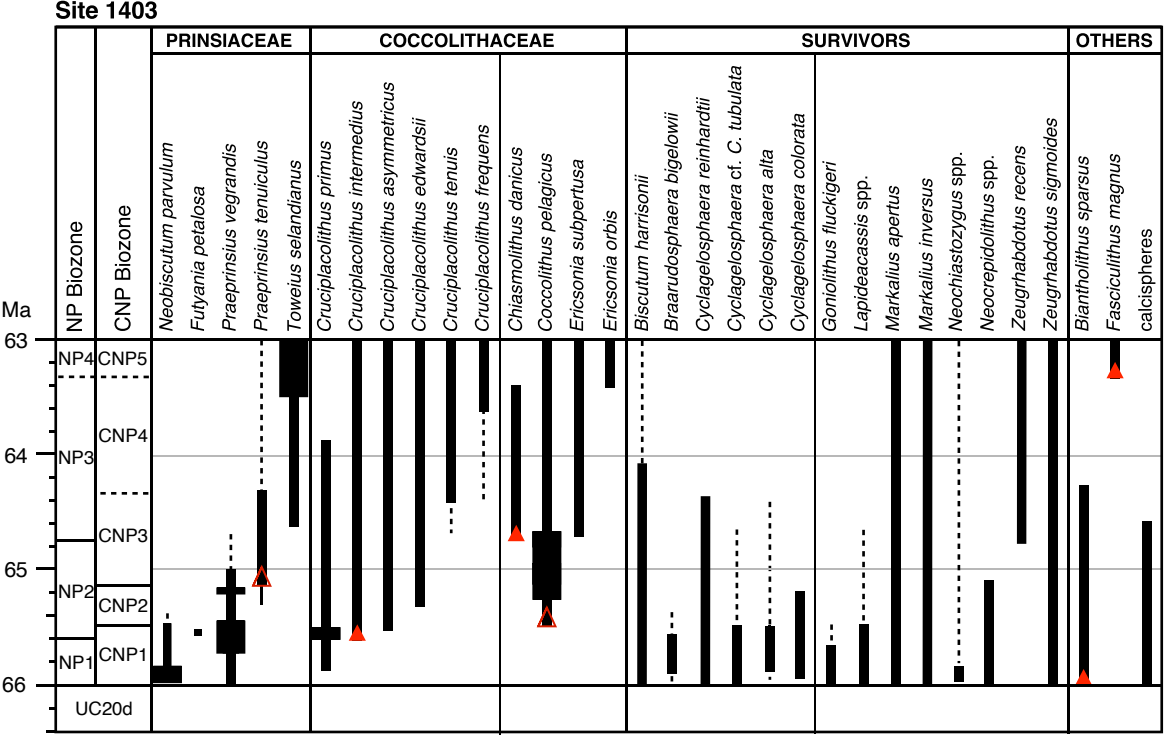
PRINSIACEAE
COCCOLITHACEAE
SURVIVORS
OTHERS
NP Biozone
CNP Biozone
Ma
63
64
65
66
NP4
NP3
NP2
NP1
CNP5
CNP4
CNP3
CNP2
CNP1
UC20d
Neobiscutum parvulum
Futyania petalosa
Praeprinsius vegrandis
Praeprinsius tenuiculus
Toweius selandianus
Cruciplacolithus primus
Cruciplacolithus intermedius
Cruciplacolithus asymmetricus
Cruciplacolithus edwardsii
Cruciplacolithus tenuis
Cruciplacolithus frequens
Chiasmolithus danicus
Coccolithus pelagicus
Ericsonia subpertusa
Ericsonia orbis
Biscutum harrisonii
Braarudosphaera bigelowii
Cyclagelosphaera reinhardtii
Cyclagelosphaera cf. C. tubulata
Cyclagelosphaera alta
Cyclagelosphaera colorata
Goniolithus fluckigeri
Lapideacassis spp.
Markalius apertus
Markalius inversus
Neochiastozygus spp.
Neocrepidolithus spp.
Zeugrhabdotus recens
Zeugrhabdotus sigmoides
Biantholithus sparsus
Fasciculithus magnus
calcispheres

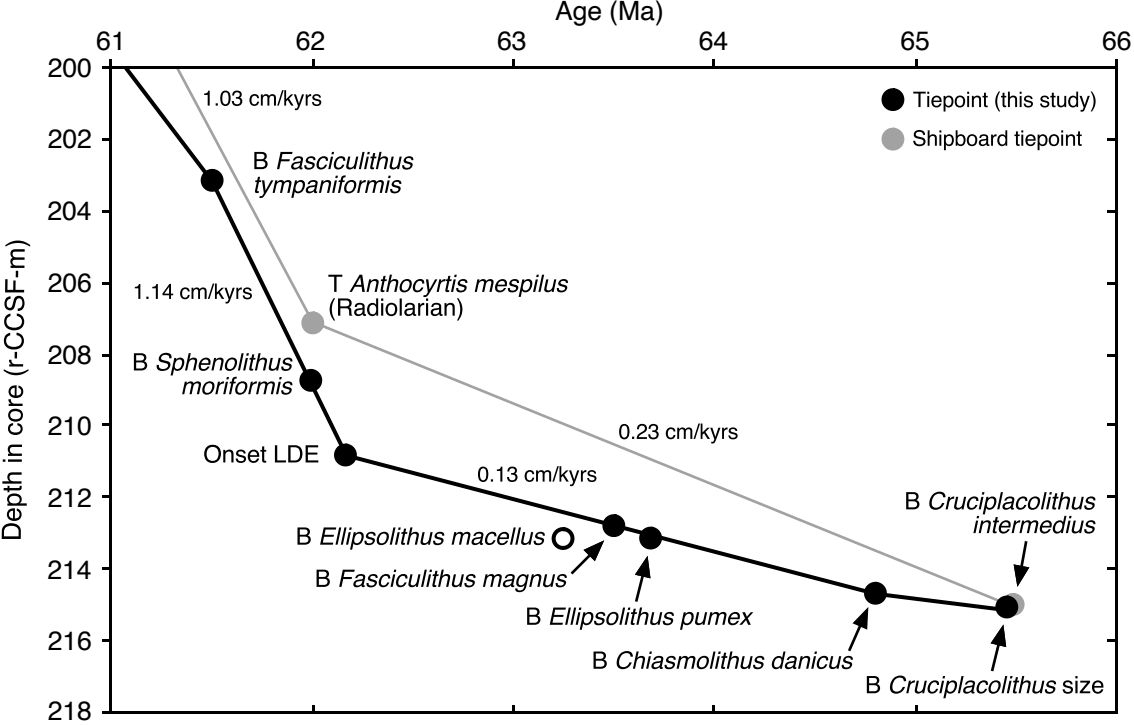
Age (Ma)
61
62
63
64
65
66
Depth in core (r-CCSF-m)
200
202
204
206
208
210
212
214
216
218
1.03 cm/kyrs
1.14 cm/kyrs
0.23 cm/kyrs
0.13 cm/kyrs
Tiepoint (this study)
Shipboard tiepoint
B Fasciculithus tympaniformis
T Anthocyrtis mespilus (Radiolarian)
B Sphenolithus moriformis
Onset LDE
B Ellipsolithus macellus
B Fasciculithus magnus
B Ellipsolithus pumex
B Chiasmolithus danicus
B Cruciplacolithus intermedius
B Cruciplacolithus size

Site 1407

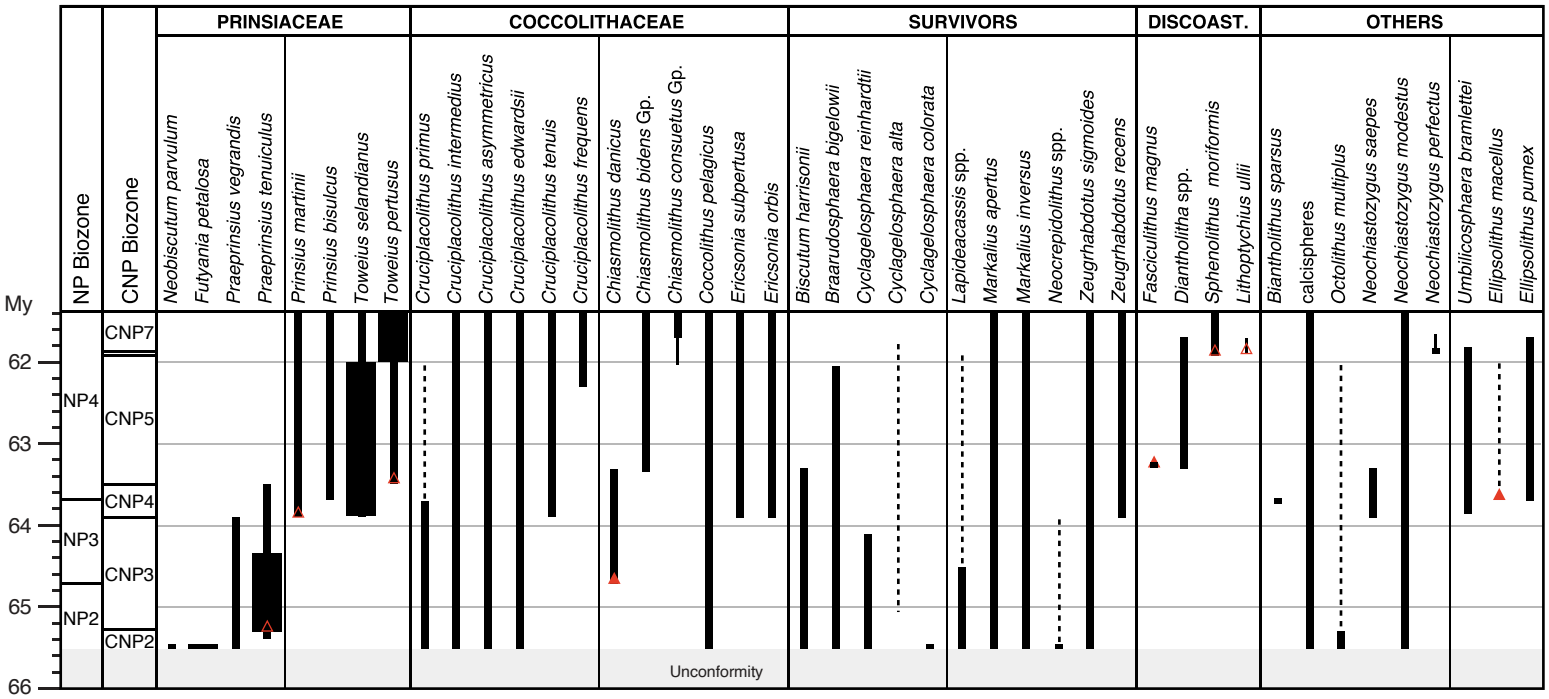
PRINSIACEAE
COCCOLITHACEAE
SURVIVORS
DISCOAST.
OTHERS
NP Biozone
CNP Biozone
Neobiscutum parvulum
Futyania petalosa
Praeprinsius vegrandis
Praeprinsius tenuiculus
Prinsius martinii
Prinsius bisulcus
Toweius selandianus
Toweius pertusus
Cruciplacolithus primus
Cruciplacolithus intermedius
Cruciplacolithus asymmetricus
Cruciplacolithus edwardsii
Cruciplacolithus tenuis
Cruciplacolithus frequens
Chiasmolithus danicus
Chiasmolithus bidens Gp.
Chiasmolithus consuetus Gp.
Coccolithus pelagicus
Ericsonia subpertusa
Ericsonia orbis
Biscutum harrisonii
Braarudosphaera bigelowii
Cyclagelosphaera reinhardtii
Cyclagelosphaera alta
Cyclagelosphaera colorata
Lapideacassis spp.
Markalius apertus
Markalius inversus
Neocrepidolithus spp.
Zeugrhabdotus sigmoides
Zeugrhabdotus recens
Fasciculithus magnus
Diantholitha spp.
Sphenolithus moriformis
Lithoptychius ullii
Biantholithus sparsus
calcispheres
Octolithus multiplus
Neochiastozygus saepes
Neochiastozygus modestus
Neochiastozygus perfectus
Umbilicosphaera bramlettei
Ellipsolithus macellus
Ellipsolithus pumex
My
62
63
64
65
66
NP4
NP3
NP2
CNP7
CNP5
CNP4
CNP3
CNP2
Unconformity

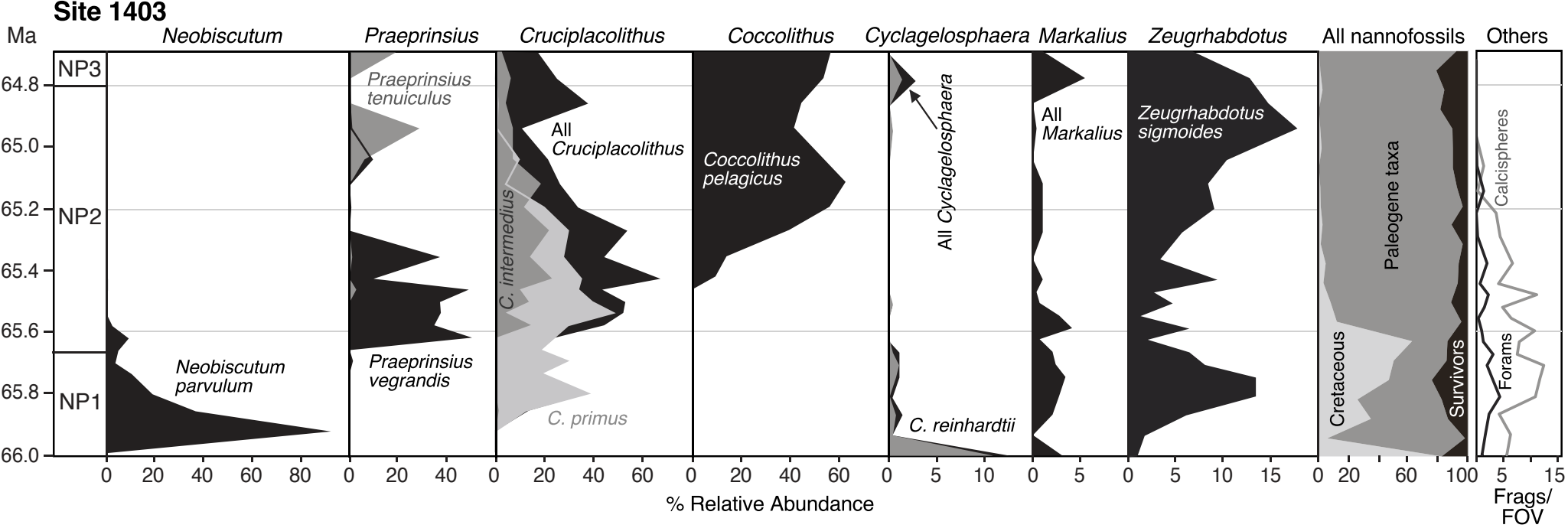
Site 1403
Ma
Neobiscutum
Praeprinsius
Cruciplacolithus
Coccolithus
Cyclagelosphaera
Markalius
Zeugrhabdotus
All nannofossils
Others
NP3
NP2
NP1
64.8
65.0
65.2
65.4
65.6
65.8
66.0
Neobiscutum parvulum
Praeprinsius tenuiculus
Praeprinsius vegrandis
C. intermedius
All Cruciplacolithus
C. primus
Coccolithus pelagicus
All Cyclagelosphaera
C. reinhardtii
All Markalius
Zeugrhabdotus sigmoides
Paleogene taxa
Cretaceous
Survivors
Calcispheres
Forams
0 20 40 60 80
0 20 40
0 20 40 60
0 20 40 60
0 5 10
0 5
0 5 10 15
0 20 60 100
0 5 15
% Relative Abundance
Frags/ FOV

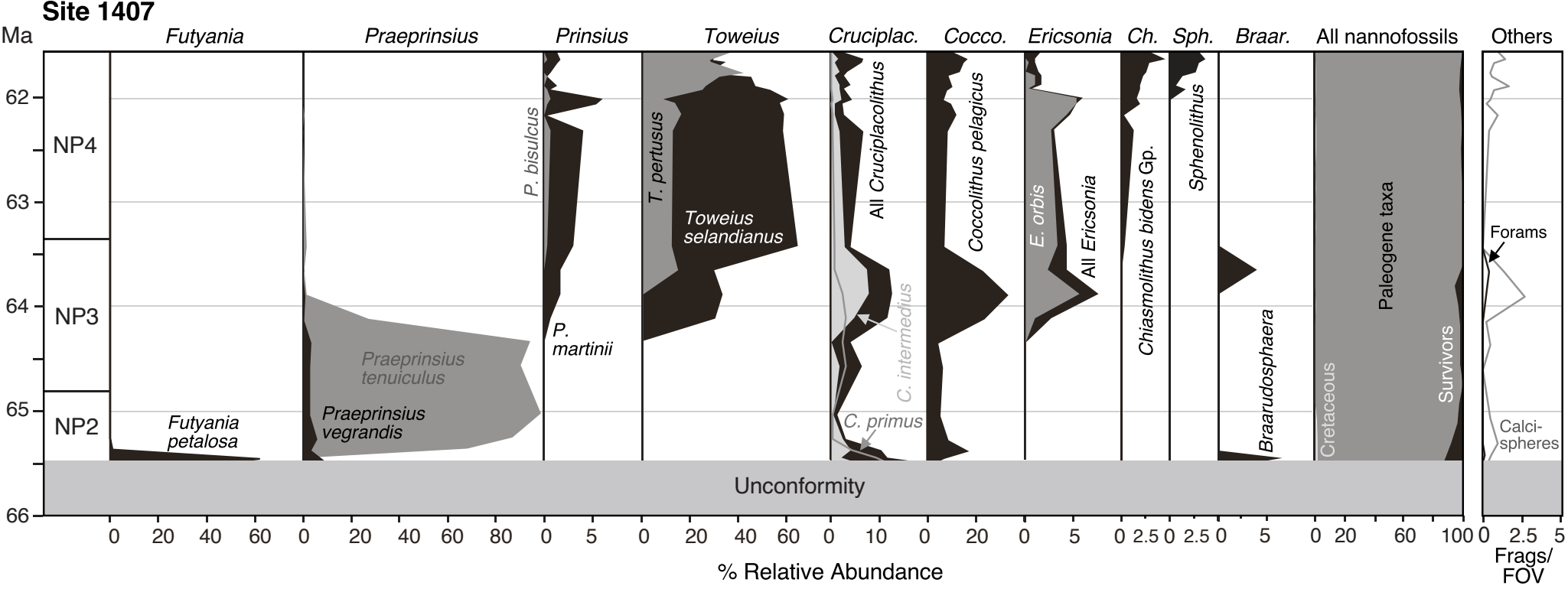
Site 1407
Ma
Futyania
Praeprinsius
Prinsius
Toweius
Cruciplac.
Cocco.
Ericsonia
Ch.
Sph.
Braar.
All nannofossils
Others
62
63
64
65
66
NP4
NP3
NP2
P. bisulcus
P. martinii
T. pertusus
Toweius selandianus
All Cruciplacolithus
C. intermedius
C. primus
Coccolithus pelagicus
E. orbis
All Ericsonia
Chiasmolithus bidens Gp.
Sphenolithus
Braarudosphaera
Cretaceous
Paleogene taxa
Survivors
Forams
Calci-spheres
Futyania petalosa
Praeprinsius tenuiculus
Praeprinsius vegrandis
Unconformity
0 20 40 60
0 20 40 60 80
0 5
0 20 40 60
0 10
0 20
0 5
0 2.5
0 2.5
0 5
0 20 60 100
0 2.5 5
% Relative Abundance
Frags/ FOV

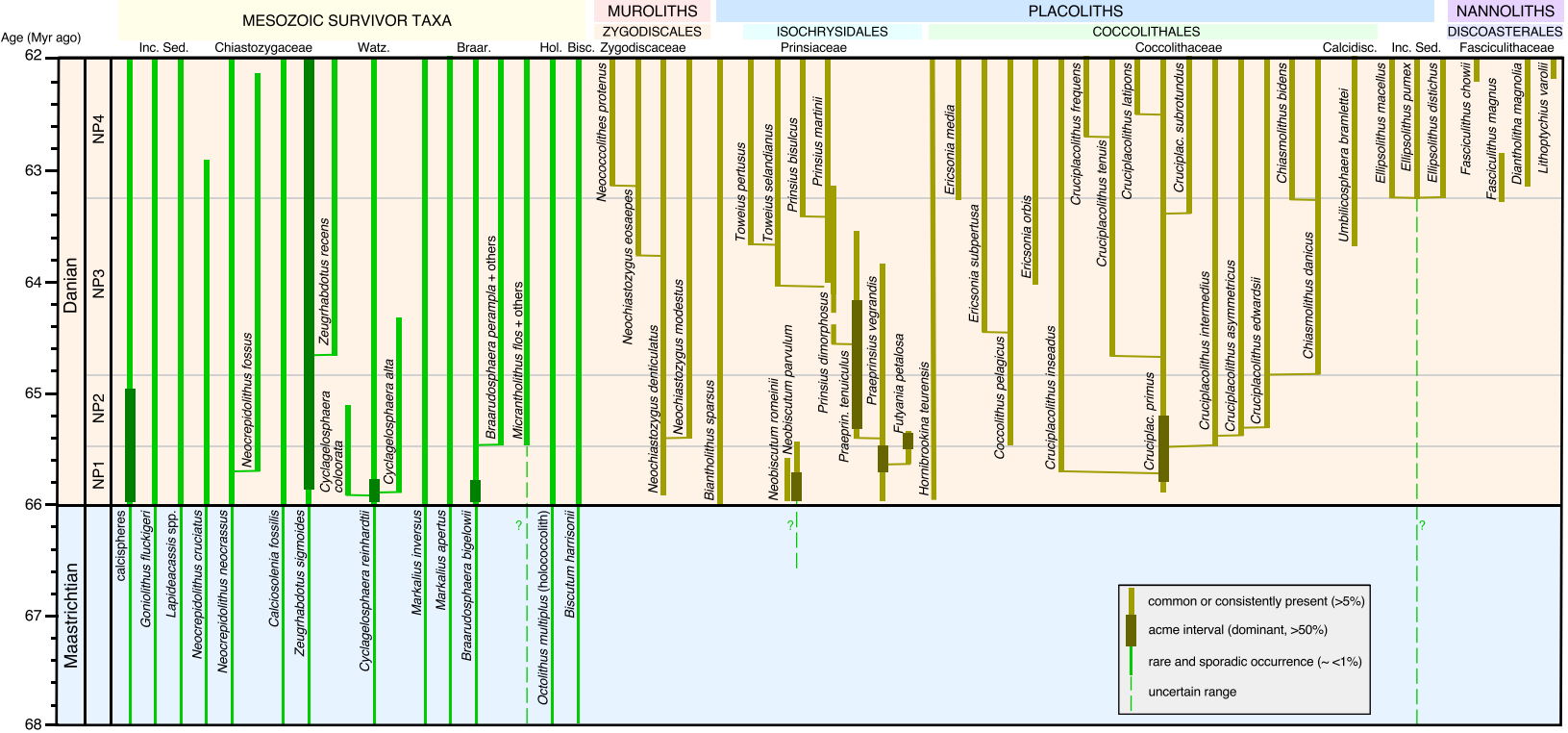
MESOZOIC SURVIVOR TAXA
MUROLITHS
PLACOLITHS
NANNOLITHS
ZYGODISCALES
ISOCHRYSIDALES
COCCOLITHALES
DISCOASTERALES
Age (Myr ago)
Inc. Sed.
Chiastozygaceae
Watz.
Braar.
Hol.
Bisc.
Zygodiscaceae
Prinsiaceae
Coccolithaceae
Calcidisc.
Inc. Sed.
Fasciculithaceae
62
63
64
65
66
67
68
Danian
Maastrichtian
NP4
NP3
NP2
NP1
calcispheres
Goniolithus fluckigeri
Lapideacassis spp.
Neocrepidolithus cruciatus
Neocrepidolithus neocrassus
Neocrepidolithus fossus
Calciosolenia fossilis
Zeugrhabdotus sigmoides
Cyclagelosphaera reinhardtii
Markalius inversus
Markalius apertus
Braarudosphaera bigelowii
Octolithus multiplus (holococcolith)
Biscutum harrisonii
Zeugrhabdotus recens
Cyclagelosphaera cohcorata
Cyclagelosphaera alta
Braarudosphaera perampla + others
Micrantholithus flos + others
Neococcolithes protenus
Neochiastozygus eosaepes
Neochiastozygus deniculatus
Neochiastozygus modestus
Biantholithus sparsus
Toweius pertusus
Toweius selandianus
Neobiscutum romeinii
Neobiscutum parvulum
Prinsius bisulcus
Prinsius martinii
Prinsius dimorphosus
Praeprin. tenuiculus
Praeprinsius vegrandis
Fulyania petalosa
Hornibrookina teurensis
Ericsonia media
Ericsonia subpertusa
Coccolithus pelagicus
Ericsonia orbis
Cruciplacolithus inseadus
Cruciplacolithus frequens
Cruciplacolithus tenuis
Cruciplacolithus latipons
Cruciplac. primus
Cruciplac. subrotundus
Cruciplacolithus intermedius
Cruciplacolithus asymmetricus
Cruciplacolithus edwardsii
Chiasmolithus bidens
Chiasmolithus danicus
Umbilicosphaera bramlettei
Ellipsolithus macellus
Ellipsolithus pumex
Ellipsolithus distichus
Fasciculithus chowii
Fasciculithus magnus
Diantholitha magnolia
Lithoptychius varolii
common or consistently present (>5%)
acme interval (dominant, >50%)
rare and sporadic occurrence (~ <1%)
uncertain range

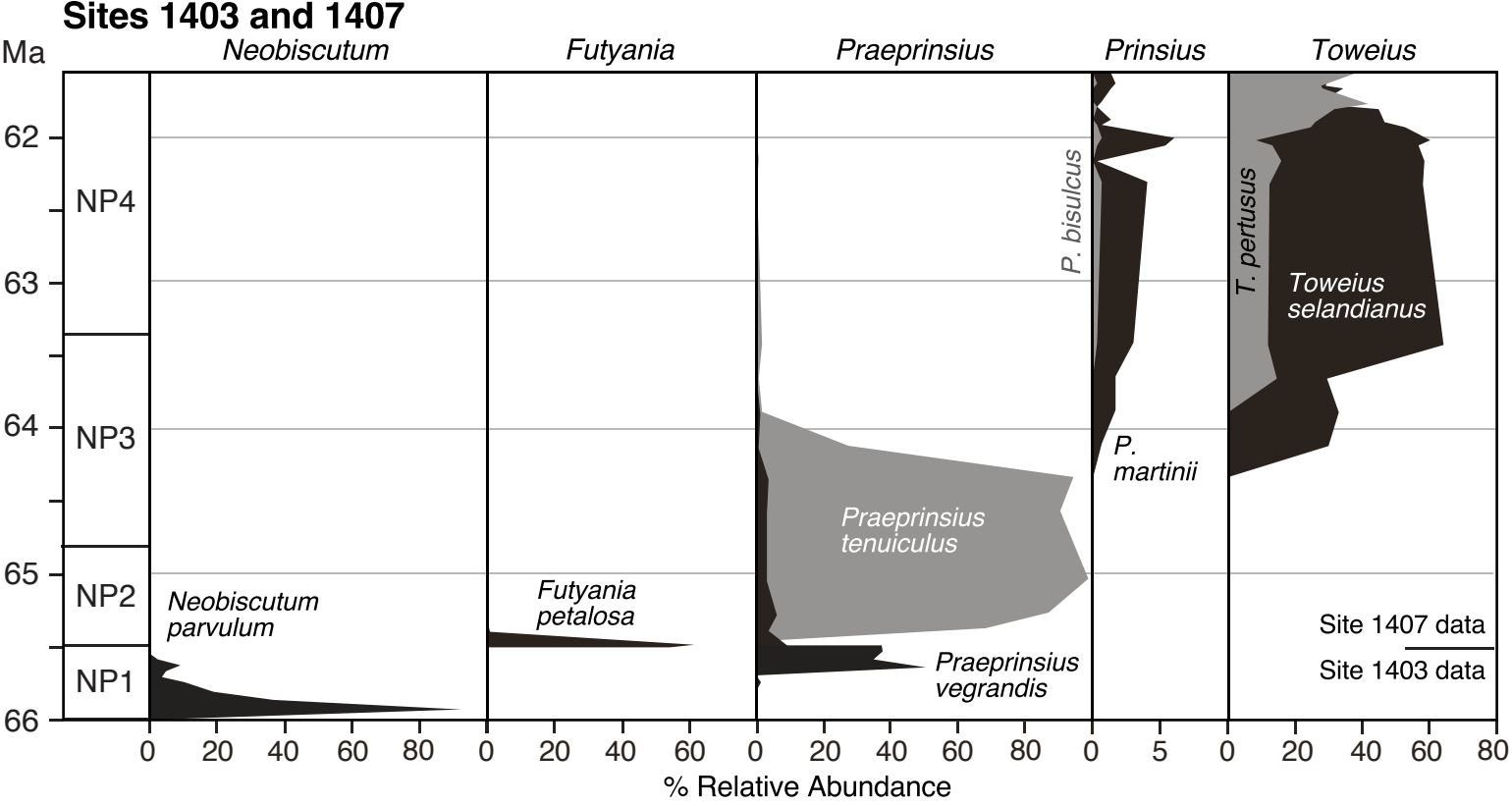
Sites 1403 and 1407
Ma
Neobiscutum
Futyania
Praeprinsius
Prinsius
Toweius
62
63
64
65
66
NP4
NP3
NP2
NP1
P. bisulcus
T. pertusus
Toweius selandianus
P. martinii
Praeprinsius tenuiculus
Neobiscutum parvulum
Futyania petalosa
Praeprinsius vegrandis
Site 1407 data
Site 1403 data
0 20 40 60 80
0 20 40 60
0 20 40 60 80
0 5
0 20 40 60 80
% Relative Abundance

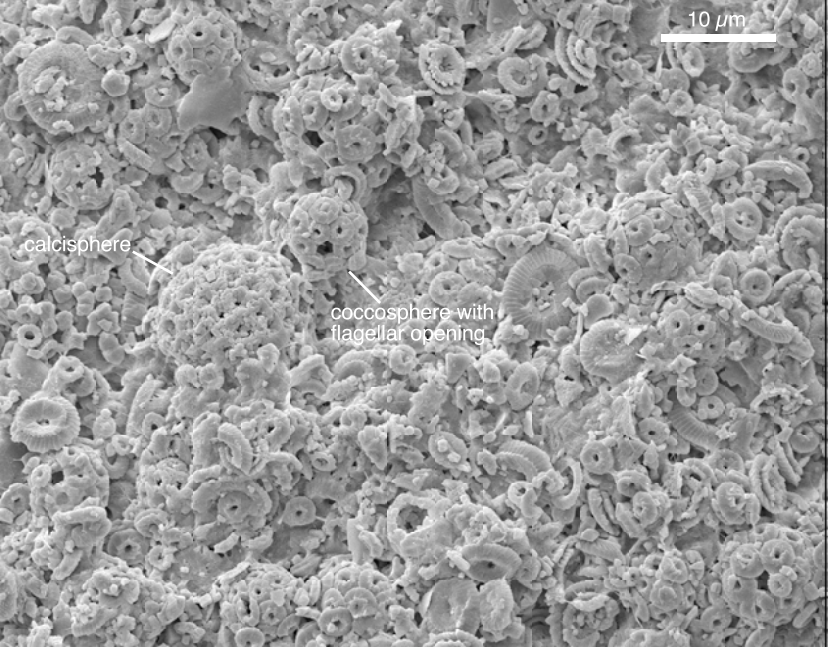
10 μm
calcisphere
coccosphere with
flagellar opening

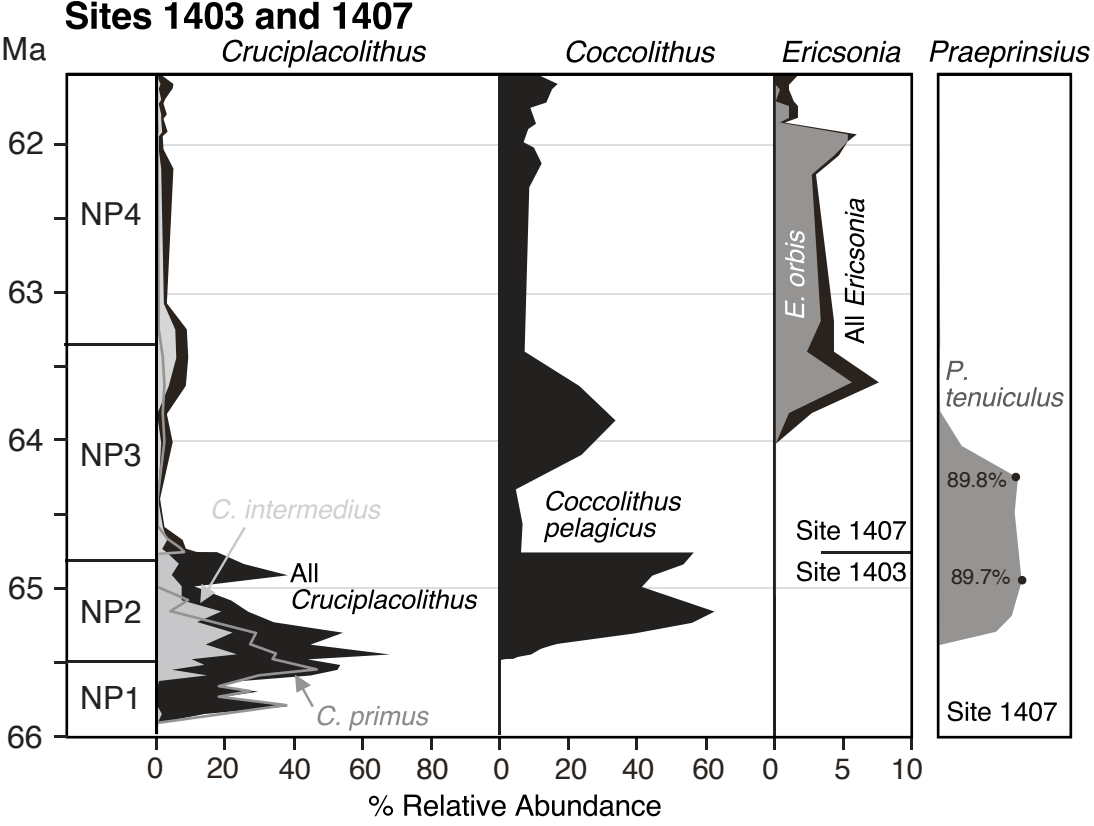
Sites 1403 and 1407
Ma
Cruciplacolithus
Coccolithus
Ericsonia
Praeprinsius
62
63
64
65
66
NP4
NP3
NP2
NP1
C. intermedius
All
Cruciplacolithus
C. primus
Coccolithus
pelagicus
E. orbis
All Ericsonia
Site 1407
Site 1403
P.
tenuiculus
89.8%
89.7%
Site 1407
0
20
40
60
80
0
20
40
60
0
5
10
% Relative Abundance

FAMILY PRINSIACEAE

Genera	Species

Genus *Toweius*

- Small to large size coccoliths
- Elliptical to broadly elliptical/circular outline
- Narrow to **broad central area**
- **Perforate central area grill**
- Two tube cycles (SEM)
- Standard geometry coccosphere
- No flagellar openings
- Zone NP3 to NP15, rare after NP12

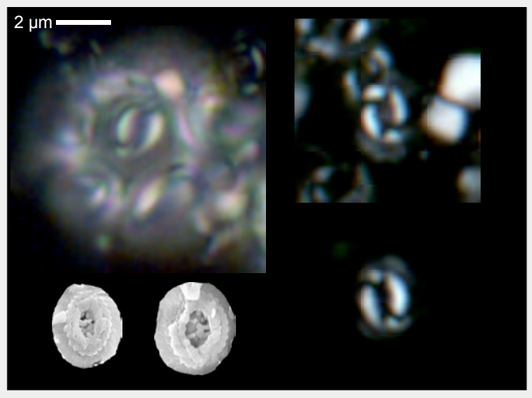

Toweius selandianus
small, elliptical, narrow central area with grill

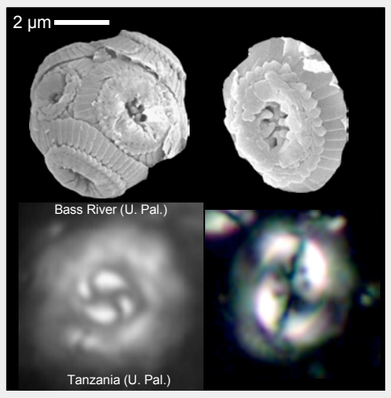

Toweius pertusus
small-medium, subcircular, broad central area with grill

Genus *Prinsius*

- Small to medium size coccoliths
- Subcircular to **elliptical** outline
- **Closed to narrow central area**
- **Two tube cycles** (SEM) (typically)
- Higher number of rim elements (~>12)
- Standard geometry coccosphere
- No flagellar openings (typically)
- Zone NP3 to NP10?, rare after NP4

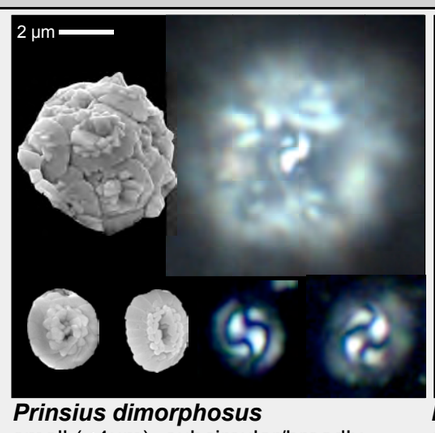

Prinsius dimorphosus
small (<4µm), subcircular/broadly elliptical, closed to narrow central area

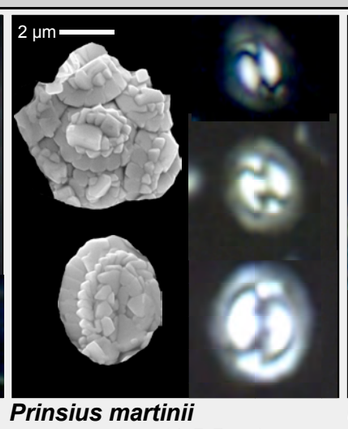

Prinsius martinii
small-medium (4-5.5µm), elliptical, closed central area

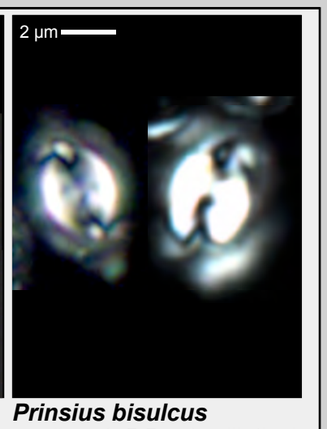

Prinsius bisulcus
medium (>5.5µm), elliptical, closed central area with perforations

Genus *Praeprinsius*

- **Very small to small** size coccoliths
- **Circular** to subcircular outline
- Narrow central area
- **One or no tube cycle** (SEM)
- Low number of rim elements (8-12)
- Large coccospheres, small liths
- Flagellar openings
- Zone NP1 to NP3

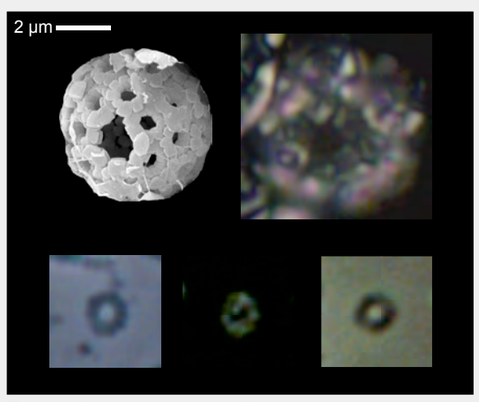

Praeprinsius vegrandis
very small (<2.5µm), circular to subcircular, no visible tube cycle

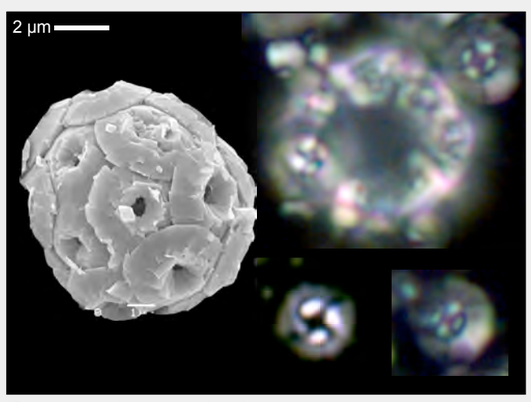

Praeprinsius tenuiculus
very small to small (1.5-4.0µm), circular to subcircular, one tube cycle

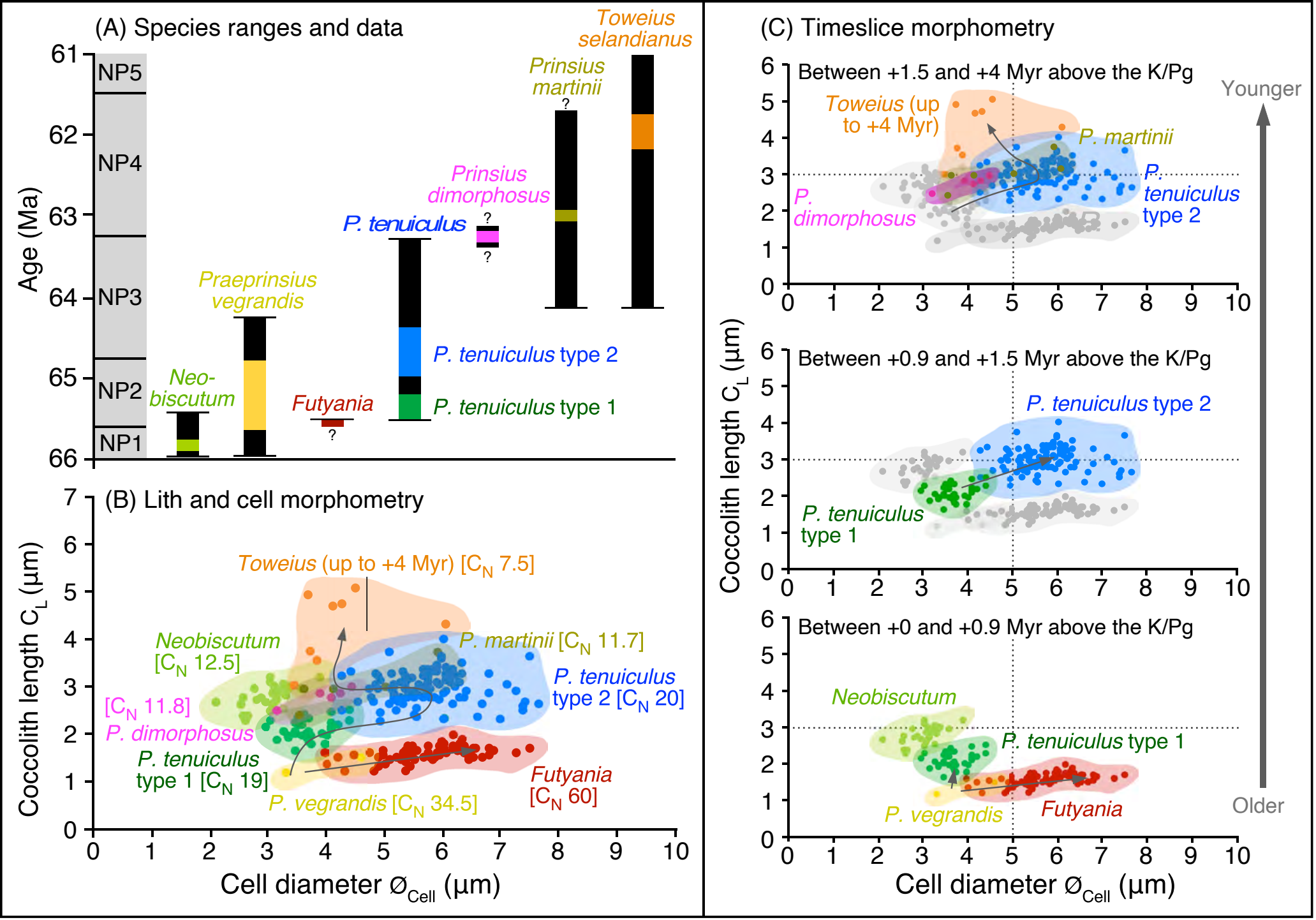
(A) Species ranges and data
Age (Ma)
61
62
63
64
65
66
NP5
NP4
NP3
NP2
NP1
Toweius selandianus
Prinsius martinii
Prinsius dimorphosus
P. tenuiculus
P. tenuiculus type 2
P. tenuiculus type 1
Praeprinsius vegrandis
Neo-biscutum
Futyania
(B) Lith and cell morphometry
Coccolith length C_L (µm)
Cell diameter Ø_Cell (µm)
Toweius (up to +4 Myr) [C_N 7.5]
Neobiscutum [C_N 12.5]
P. martinii [C_N 11.7]
P. tenuiculus type 2 [C_N 20]
[C_N 11.8]
P. dimorphosus
P. tenuiculus type 1 [C_N 19]
P. vegrandis [C_N 34.5]
Futyania [C_N 60]
(C) Timeslice morphometry
Between +1.5 and +4 Myr above the K/Pg
Toweius (up to +4 Myr)
P. martinii
P. tenuiculus type 2
P. dimorphosus
Between +0.9 and +1.5 Myr above the K/Pg
P. tenuiculus type 2
P. tenuiculus type 1
Between +0 and +0.9 Myr above the K/Pg
Neobiscutum
P. tenuiculus type 1
P. vegrandis
Futyania
Younger
Older

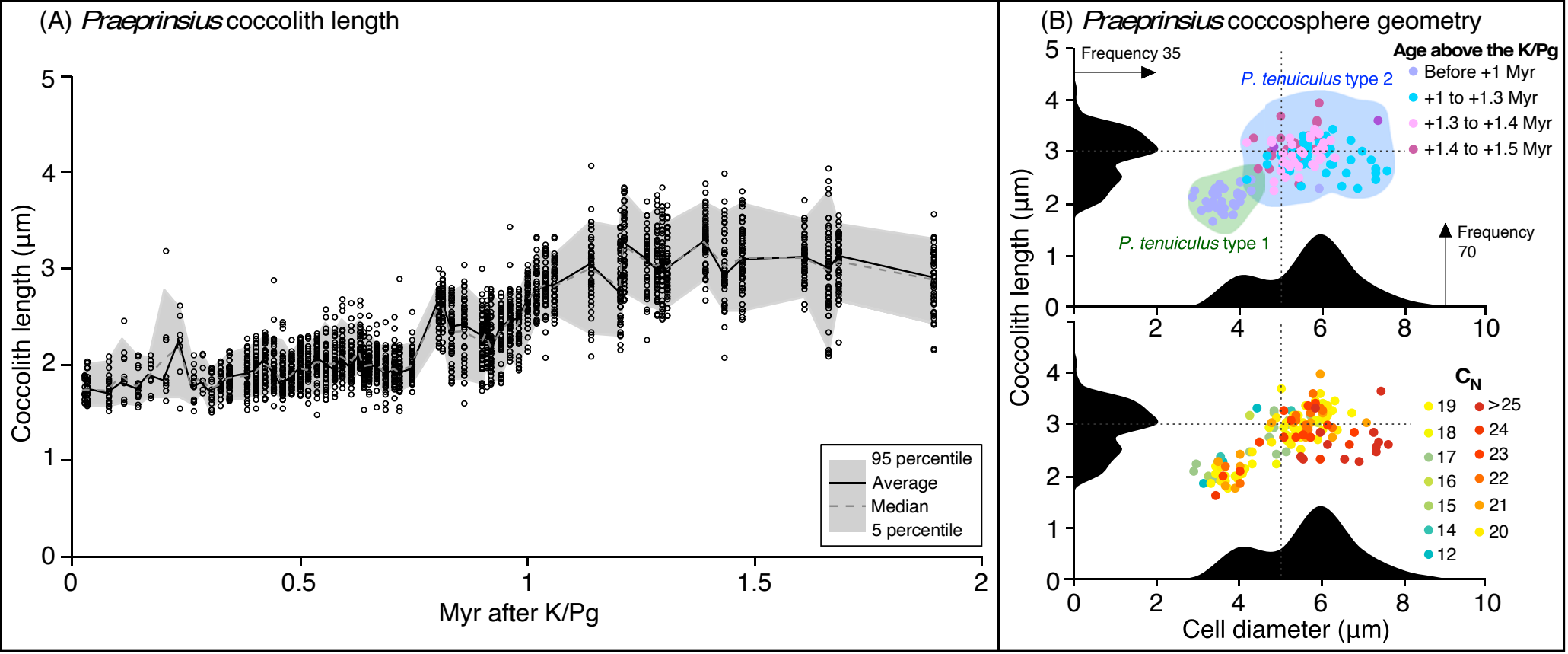
(A) Praeprinsius coccolith length
Coccolith length (µm)
Myr after K/Pg
95 percentile
Average
Median
5 percentile
(B) Praeprinsius coccosphere geometry
Frequency 35
Age above the K/Pg
Before +1 Myr
+1 to +1.3 Myr
+1.3 to +1.4 Myr
+1.4 to +1.5 Myr
P. tenuiculus type 2
P. tenuiculus type 1
Frequency 70
Coccolith length (µm)
Cell diameter (µm)
C_N
19
18
17
16
15
14
12
>25
24
23
22
21
20

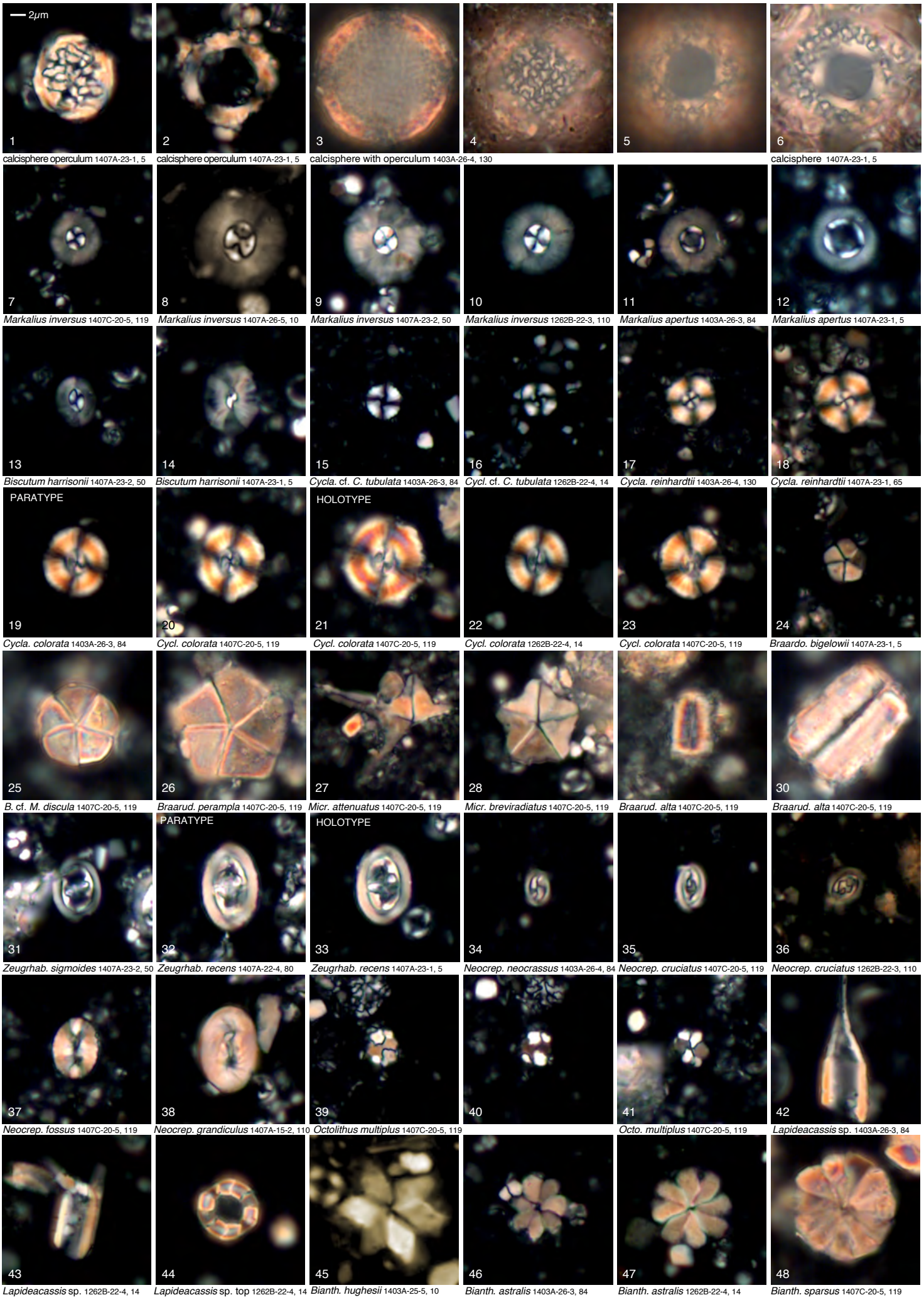
2μm
1
calcisphere operculum 1407A-23-1, 5
2
calcisphere operculum 1407A-23-1, 5
3
calcisphere with operculum 1403A-26-4, 130
4
5
6
calcisphere 1407A-23-1, 5
7
Markalius inversus 1407C-20-5, 119
8
Markalius inversus 1407A-26-5, 10
9
Markalius inversus 1407A-23-2, 50
10
Markalius inversus 1262B-22-3, 110
11
Markalius apertus 1403A-26-3, 84
12
Markalius apertus 1407A-23-1, 5
13
Biscutum harrisonii 1407A-23-2, 50
14
Biscutum harrisonii 1407A-23-1, 5
15
Cycla. cf. C. tubulata 1403A-26-3, 84
16
Cycl. cf. C. tubulata 1262B-22-4, 14
17
Cycla. reinhardtii 1403A-26-4, 130
18
Cycla. reinhardtii 1407A-23-1, 65
PARATYPE
19
Cycla. colorata 1403A-26-3, 84
20
Cycl. colorata 1407C-20-5, 119
HOLOTYPE
21
Cycl. colorata 1407C-20-5, 119
22
Cycl. colorata 1262B-22-4, 14
23
Cycl. colorata 1407C-20-5, 119
24
Braardo. bigelowii 1407A-23-1, 5
25
B. cf. M. discula 1407C-20-5, 119
26
Braarud. perampla 1407C-20-5, 119
27
Micr. attenuatus 1407C-20-5, 119
28
Micr. breviradiatus 1407C-20-5, 119
30
Braarud. alta 1407C-20-5, 119
Braarud. alta 1407C-20-5, 119
31
Zeugrhab. sigmoides 1407A-23-2, 50
PARATYPE
32
Zeugrhab. recens 1407A-22-4, 80
HOLOTYPE
33
Zeugrhab. recens 1407A-23-1, 5
34
Neocrep. neocrassus 1403A-26-4, 84
35
Neocrep. cruciatus 1407C-20-5, 119
36
Neocrep. cruciatus 1262B-22-3, 110
37
Neocrep. fossus 1407C-20-5, 119
38
Neocrep. grandiculus 1407A-15-2, 110
39
Octolithus multiplus 1407C-20-5, 119
40
41
Octo. multiplus 1407C-20-5, 119
42
Lapideacassis sp. 1403A-26-3, 84
43
Lapideacassis sp. 1262B-22-4, 14
44
Lapideacassis sp. top 1262B-22-4, 14
45
Bianth. hughesii 1403A-25-5, 10
46
Bianth. astralis 1403A-26-3, 84
47
Bianth. astralis 1262B-22-4, 14
48
Bianth. sparsus 1407C-20-5, 119

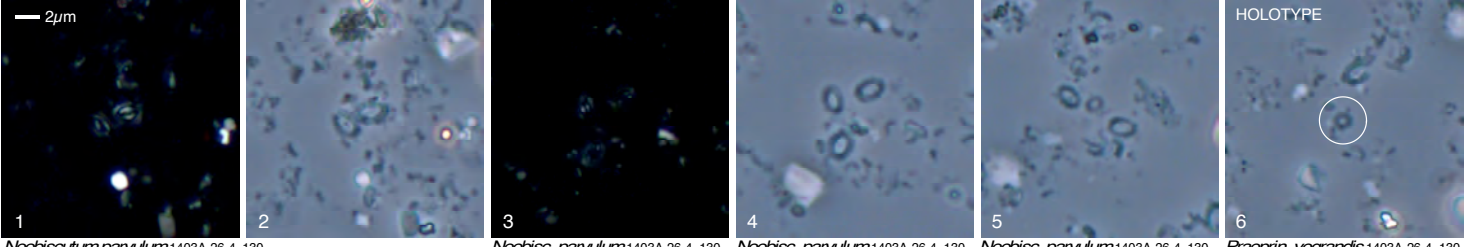

Neobiscutum parvulum 1403A-26-4, 130 | *Neobisc. parvulum* 1403A-26-4, 130 | *Neobisc. parvulum* 1403A-26-4, 130 | *Neobisc. parvulum* 1403A-26-4, 130 | *Praeprin. vegrandis* 1403A-26-4, 130

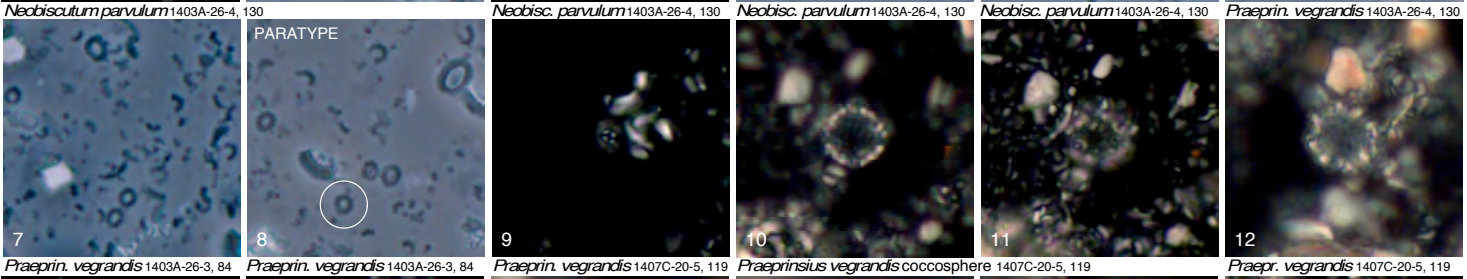

Praeprin. vegrandis 1403A-26-3, 84 | *Praeprin. vegrandis* 1403A-26-3, 84 | *Praeprin. vegrandis* 1407C-20-5, 119 | *Praeprinsius vegrandis* coccosphere 1407C-20-5, 119 | *Praepr. vegrandis* 1407C-20-5, 119

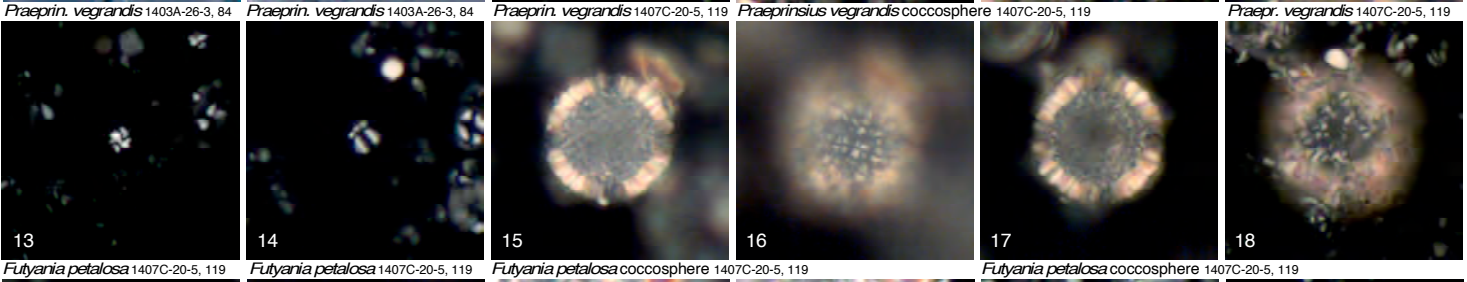

Futyania petalosa 1407C-20-5, 119 | *Futyania petalosa* 1407C-20-5, 119 | *Futyania petalosa* coccosphere 1407C-20-5, 119 | *Futyania petalosa* coccosphere 1407C-20-5, 119

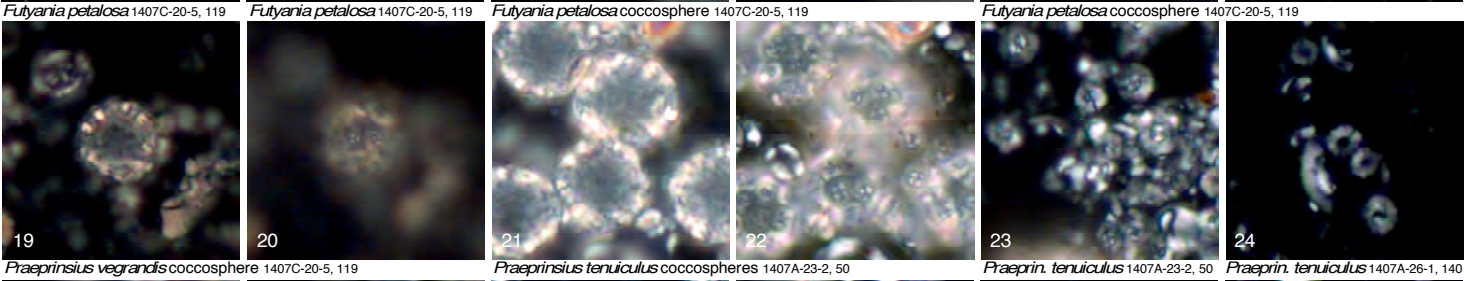

Praeprinsius vegrandis coccosphere 1407C-20-5, 119 | *Praeprinsius tenuiculus* coccospheres 1407A-23-2, 50 | *Praeprin. tenuiculus* 1407A-23-2, 50 | *Praeprin. tenuiculus* 1407A-26-1, 140

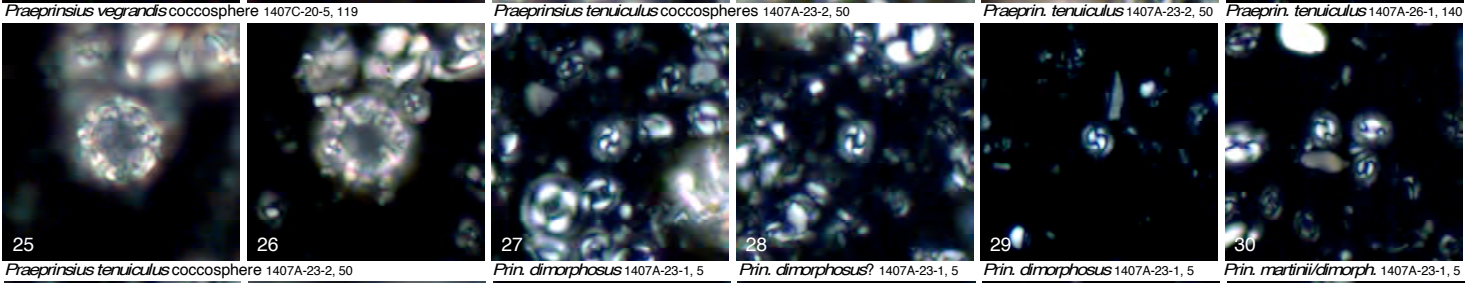

Praeprinsius tenuiculus coccosphere 1407A-23-2, 50 | *Prin. dimorphosus* 1407A-23-1, 5 | *Prin. dimorphosus*? 1407A-23-1, 5 | *Prin. dimorphosus* 1407A-23-1, 5 | *Prin. martinii/dimorph.* 1407A-23-1, 5

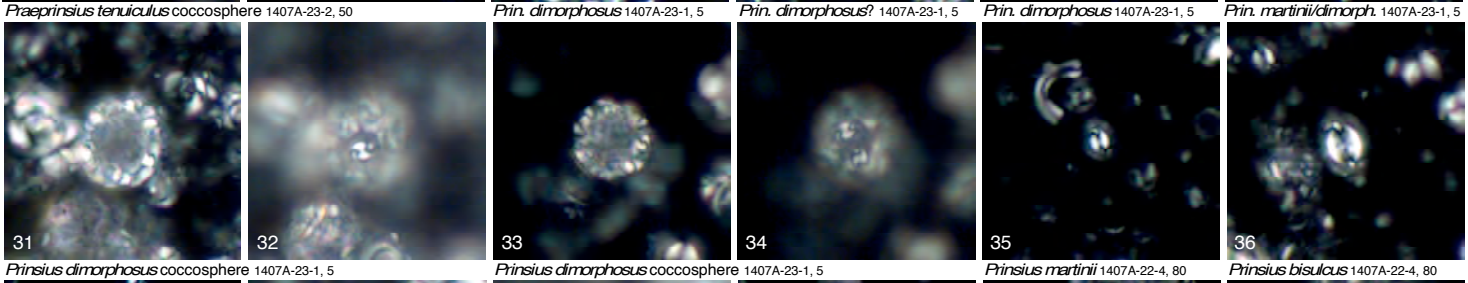

Prinsius dimorphosus coccosphere 1407A-23-1, 5 | *Prinsius dimorphosus* coccosphere 1407A-23-1, 5 | *Prinsius martinii* 1407A-22-4, 80 | *Prinsius bisulcus* 1407A-22-4, 80

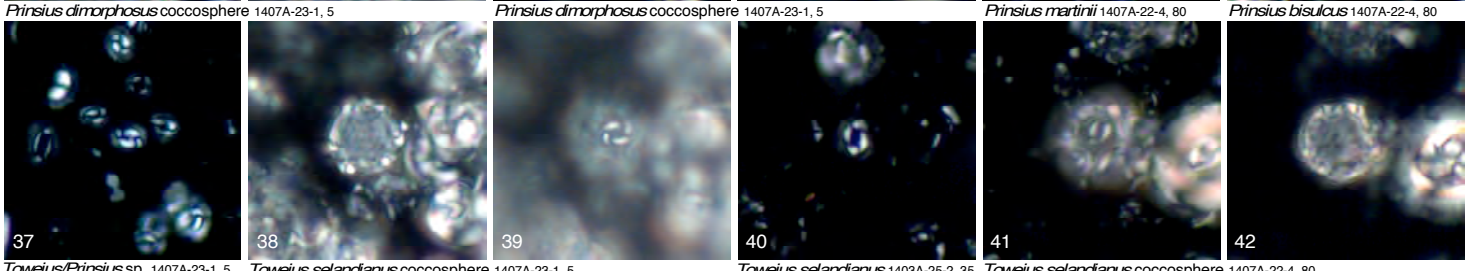

Toweius/Prinsius sp. 1407A-23-1, 5 | *Toweius selandianus* coccosphere 1407A-23-1, 5 | *Toweius selandianus* 1403A-25-2, 35 | *Toweius selandianus* coccosphere 1407A-22-4, 80

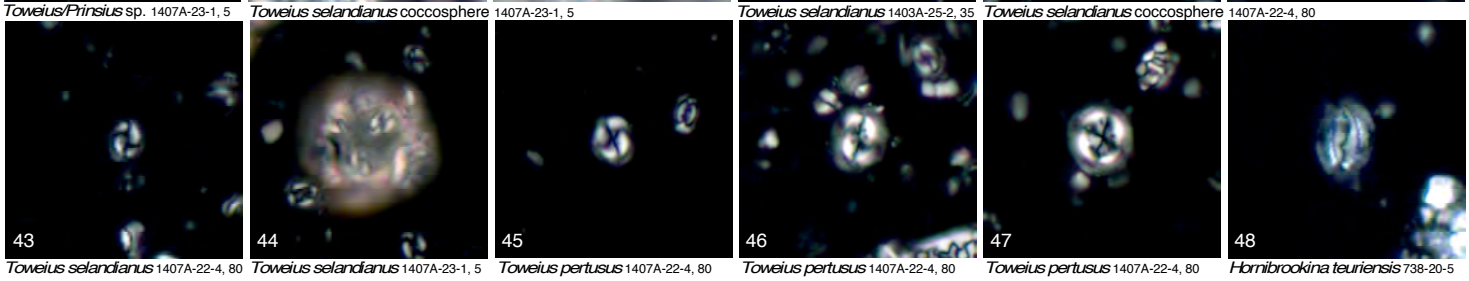

Toweius selandianus 1407A-22-4, 80 | *Toweius selandianus* 1407A-23-1, 5 | *Toweius pertusus* 1407A-22-4, 80 | *Toweius pertusus* 1407A-22-4, 80 | *Toweius pertusus* 1407A-22-4, 80 | *Hornibrookina teuriensis* 738-20-5

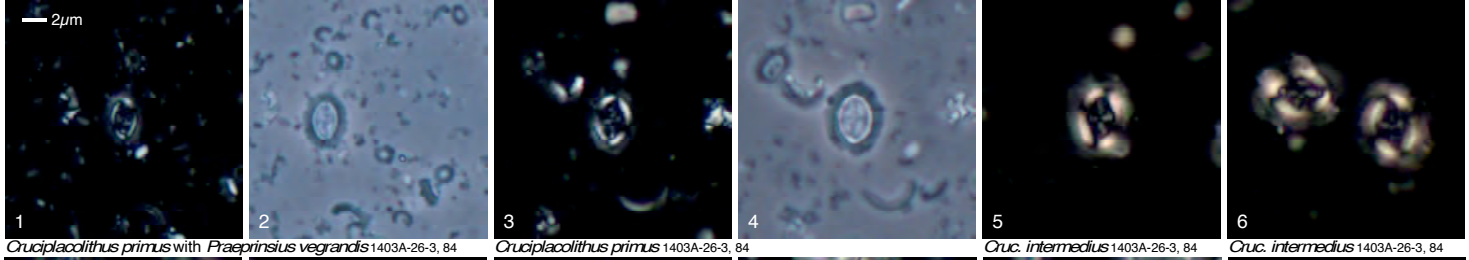

Cruciplacolithus primus with *Praeprinsius vegrandis* 1403A-26-3, 84 | *Cruciplacolithus primus* 1403A-26-3, 84 | *Cruc. intermedius* 1403A-26-3, 84 | *Cruc. intermedius* 1403A-26-3, 84

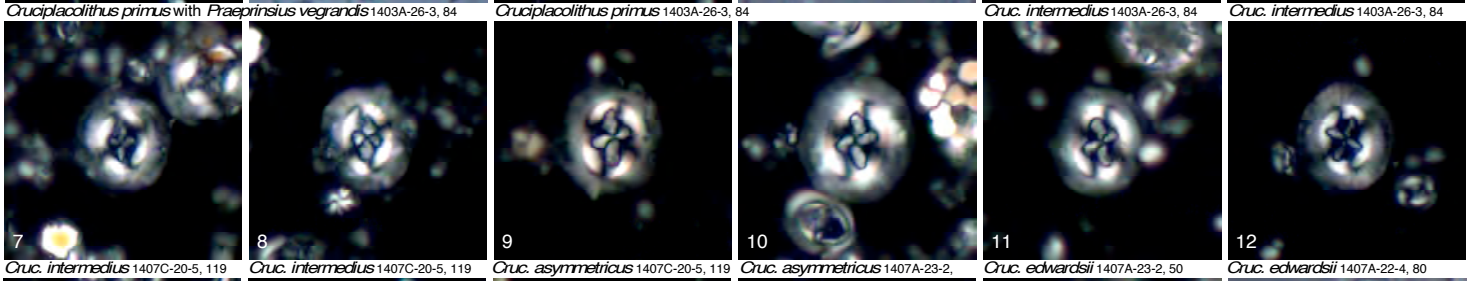

Cruc. intermedius 1407C-20-5, 119 | *Cruc. intermedius* 1407C-20-5, 119 | *Cruc. asymmetricus* 1407C-20-5, 119 | *Cruc. asymmetricus* 1407A-23-2, | *Cruc. edwardsii* 1407A-23-2, 50 | *Cruc. edwardsii* 1407A-22-4, 80

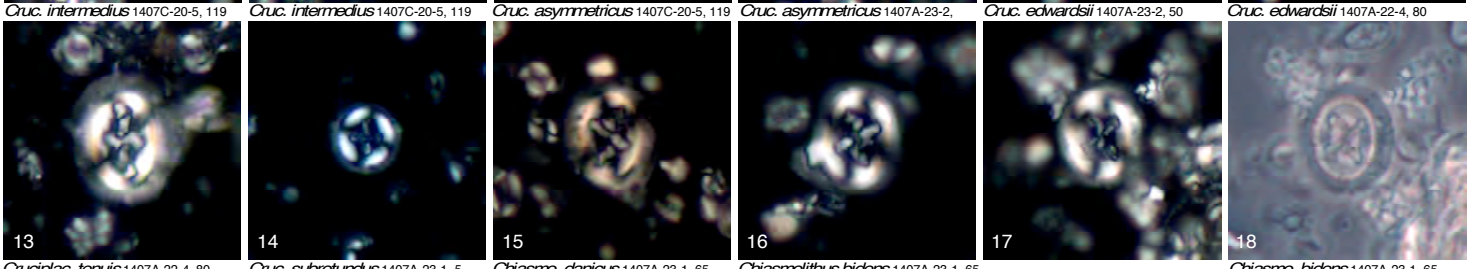

Cruciplac. tenuis 1407A-22-4, 80 | *Cruc. subrotundus* 1407A-23-1, 5 | *Chiasmo. danicus* 1407A-23-1, 65 | *Chiasmolithus bidens* 1407A-23-1, 65 | | *Chiasmo. bidens* 1407A-23-1, 65

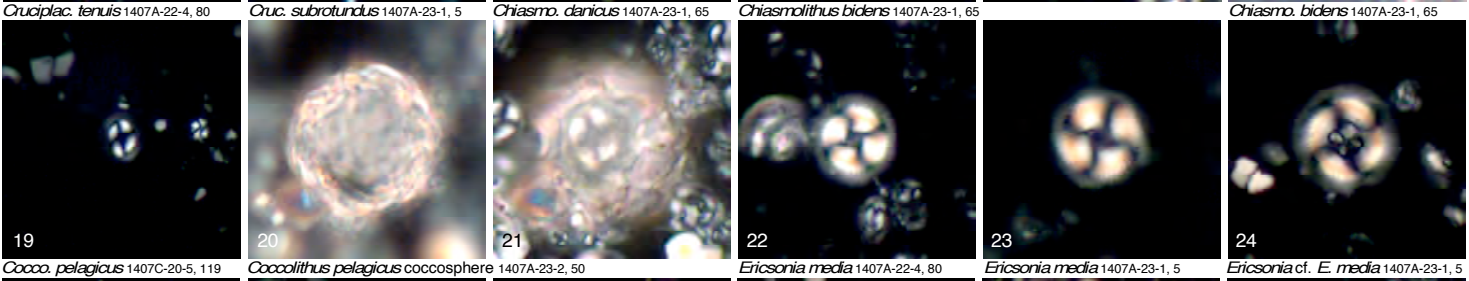

Cocco. pelagicus 1407C-20-5, 119 | *Coccolithus pelagicus* coccosphere 1407A-23-2, 50 | *Ericsonia media* 1407A-22-4, 80 | *Ericsonia media* 1407A-23-1, 5 | *Ericsonia* cf. *E. media* 1407A-23-1, 5

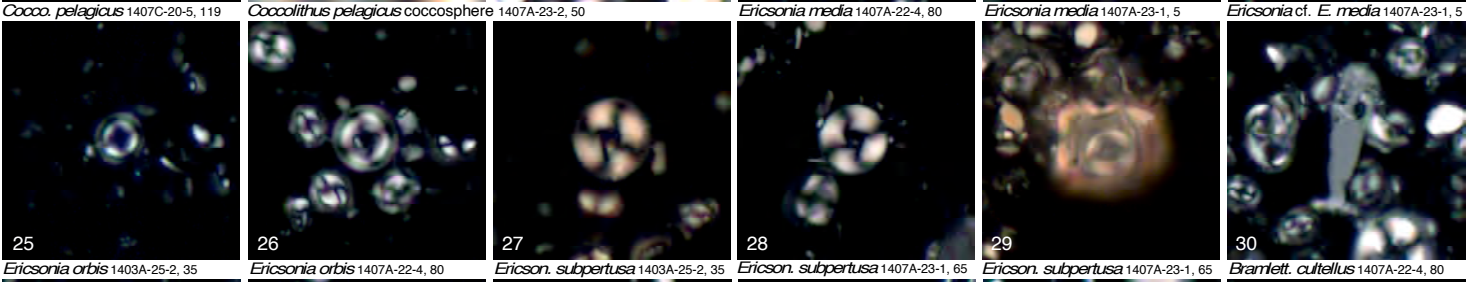

Ericsonia orbis 1403A-25-2, 35 | *Ericsonia orbis* 1407A-22-4, 80 | *Ericson. subpertusa* 1403A-25-2, 35 | *Ericson. subpertusa* 1407A-23-1, 65 | *Ericson. subpertusa* 1407A-23-1, 65 | *Bramlett. cultellus* 1407A-22-4, 80

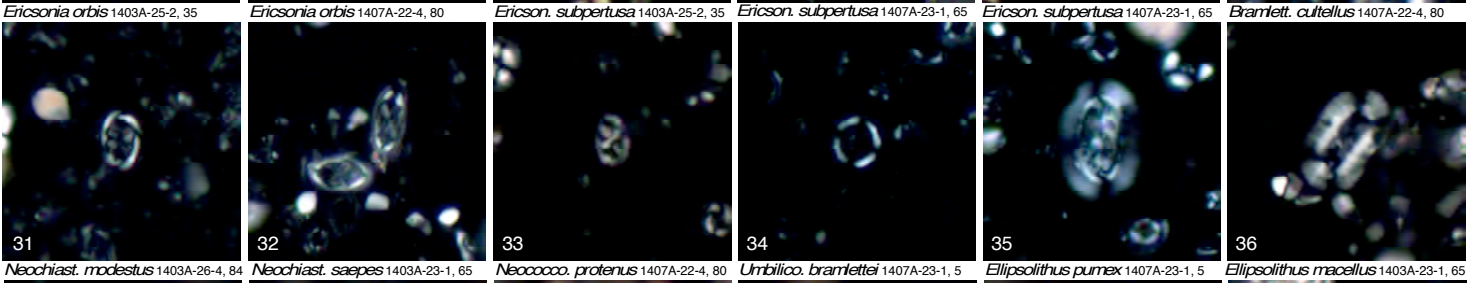

Neochiast. modestus 1403A-26-4, 84 | *Neochiast. saepes* 1403A-23-1, 65 | *Neococco. protenus* 1407A-22-4, 80 | *Umbilico. bramlettei* 1407A-23-1, 5 | *Ellipsolithus pumex* 1407A-23-1, 5 | *Ellipsolithus macellus* 1403A-23-1, 65

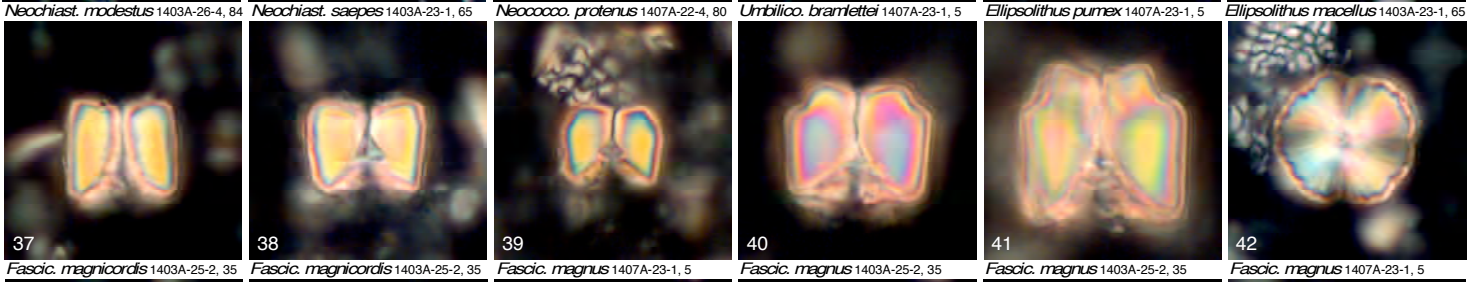

Fascic. magnicordis 1403A-25-2, 35 | *Fascic. magnicordis* 1403A-25-2, 35 | *Fascic. magnus* 1407A-23-1, 5 | *Fascic. magnus* 1403A-25-2, 35 | *Fascic. magnus* 1403A-25-2, 35 | *Fascic. magnus* 1407A-23-1, 5

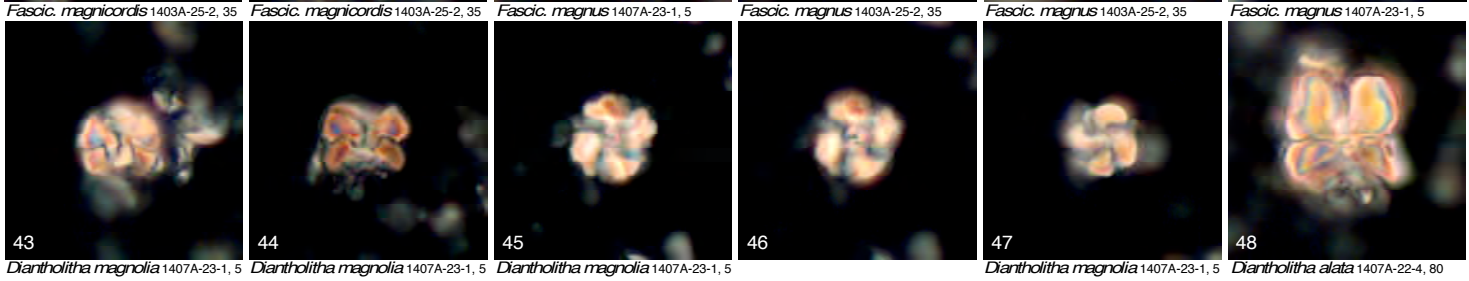

Diantholitha magnolia 1407A-23-1, 5 | *Diantholitha magnolia* 1407A-23-1, 5 | *Diantholitha magnolia* 1407A-23-1, 5 | | *Diantholitha magnolia* 1407A-23-1, 5 | *Diantholitha alata* 1407A-22-4, 80

Danian Prinsiaceae (*Neobiscutum–Praeprinsius–Futyania*)

1 μm

***Neobiscutum parvulum* – very small, elliptical, narrow central area**

1. *Neo. parvulum* El Kef +6.5m

2. *Neo. parvulum* El Kef +6.5m

3. *Neo. parvulum* El Kef +6.5m

4. *Neo. parvulum* El Kef +6.5m

5. *Neo. parvulum* El Kef +6.5m

***Praeprinsius vegrandis* – very small, circular-subcircular**

PARATYPE

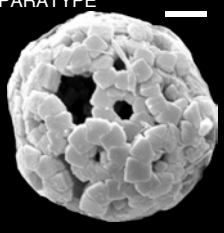

6. Praeprinsius vegrandis 1407C-20-4, 125

7. *Praeprinsius vegrandis* 1407C-20-4, 125

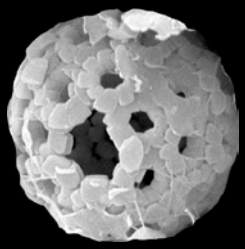

8. *Praeprinsius vegrandis* 1407A-23-1, 95

9. *Praeprinsius vegrandis* 1407C-20-4, 125

10. *Praeprin. vegrandis* 1407C-20-4, 125

***Praeprinsius tenuiculum* – circular-subcircular, one tube cycle**

Small, type 1 coccospheres

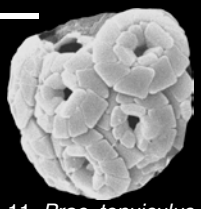

11. *Prae. tenuiculus* 1407A-23-1, 95

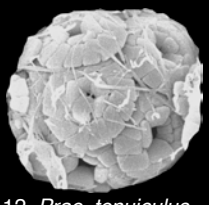

12. *Prae. tenuiculus* 1407C-20-4, 125

13. *Praeprinsius tenuiculus* 1407C-20-4, 125

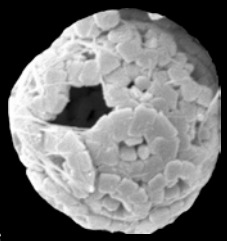

14. *Praeprinsius tenuiculus* 1407C-20-4, 125

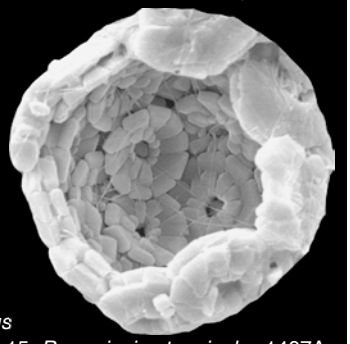

15. *Praeprinsius tenuiculus* 1407A-23-2, 50

Large, type 2 coccospheres

16. *Praeprinsius tenuiculus* 1407A-23-2, 50

17. *Praeprinsius tenuiculus* 1407A-23-2, 35

18. *Praeprinsius tenuiculus* 1407A-23-2, 50

19. *Praeprinsius tenuiculus* with raised tube 1407A-23-2, 50

***Futyania petalosa* – very small, circular-subcircular, one extended tube cycle**

1 μm

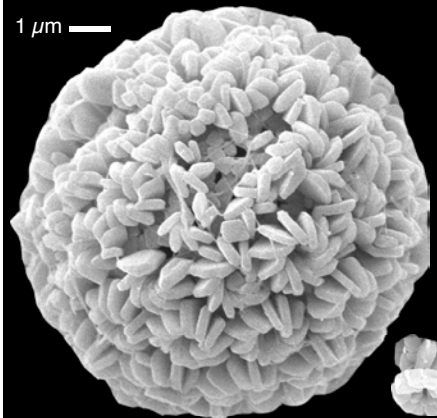

20. *Futyania petalosa* 1407C-20-4, 125

21. *Futyania petalosa* 1407C-20-4, 125

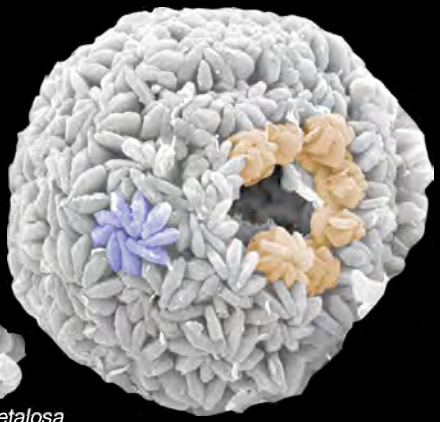

22. *Futyania petalosa* 1049C-8-5, 4

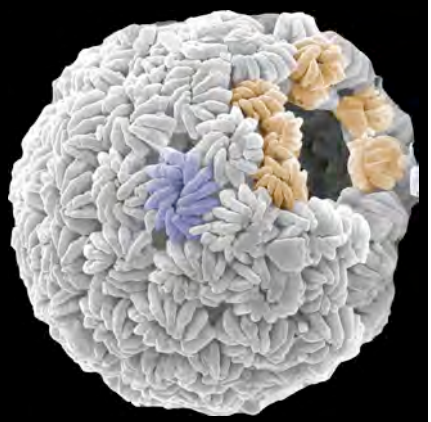

23. *Futyania petalosa* 1049C-8-4, 38

***Praeprinsius* – small, circular-subcircular , one or no tube cycle**

***Futyania petalosa* – very small, circular-subcircular extended tube cycle**

1 μm

1. *Praeprinsius vegrandis* 1407C-20-4, 125

2. *Praeprinsius tenuiculus* 1407A-23-2, 50

3. *Praeprinsius tenuiculus* with collar 1407A-23-2, 50

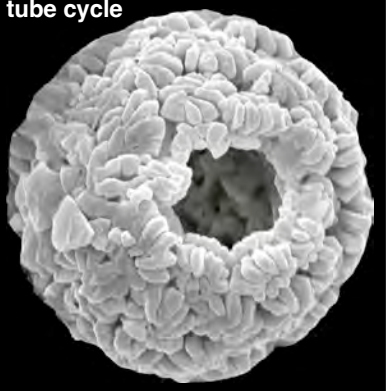

4. *Futyania petalosa* 1049C-8-4, 38

***Prinsius* – subcircular-elliptical, two tube cycles, narrow central area**

***Prinsius dimorphosus* – subcircular-subcircular, two tube cycles**

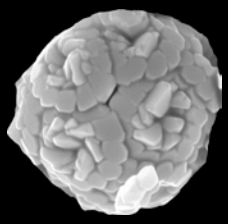

5. *Prinsius dimorphosus* North Sea

6. *Prinsius dimorphosus* North Sea

7. *Prinsius dimorphosus* North Sea

8. *Prinsius dimorphosus* North Sea

9. *Prinsius dimorphosus* North Sea

***Prinsius martinii* – elliptical, two tube cycles (~>4μm)**

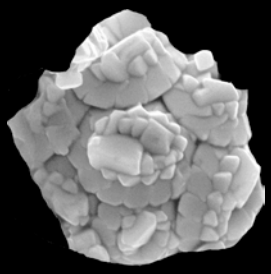

10. *Prinsius martinii* North Sea

11. *Prinsius martinii* North Sea

***Toweius* – subcircular-elliptical, two tube cycles, central area**

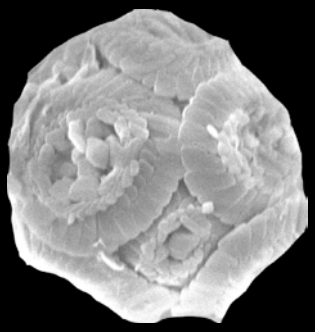

12. *Toweius pertusus* 1407A-23-1, 35

***Prinsius* – *Toweius* coccoliths**

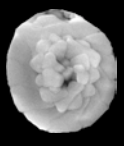

13. *Prinsius dimorphosus* 1407A-23-1, 5

14. *Prinsius dimorphosus* 1407A-23-1, 5

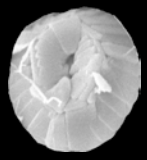

15. *Prinsius dimorphosus/martinii* 3.6μm 1407A-23-1, 95

16. *Prinsius martinii* 3.5μm 1407A-23-1, 5

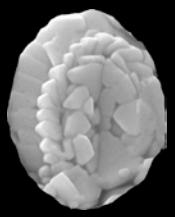

17. *Prinsius martinii* North Sea

18. *Prinsius martinii* 4.9μm 1407A-22-1, 80

19. *Prinsius martinii* 5.3μm 1407A-22-1, 80

1 μm

20. *Toweius selandianus* 1407A-22-4, 80

21. *Toweius selandianus* 2.9μm 1407A-22-4, 80

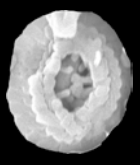

22. *Toweius selandianus* 1407A-23-1, 5

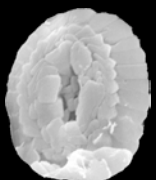

23. *Toweius selandianus* 1407A-23-1, 5

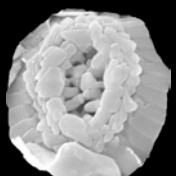

24. *Toweius selandianus* 1407A-23-1, 5

25. *Toweius selandianus* 1407A-23-1, 5

26. *Toweius pertusus* 1407A-23-1, 5

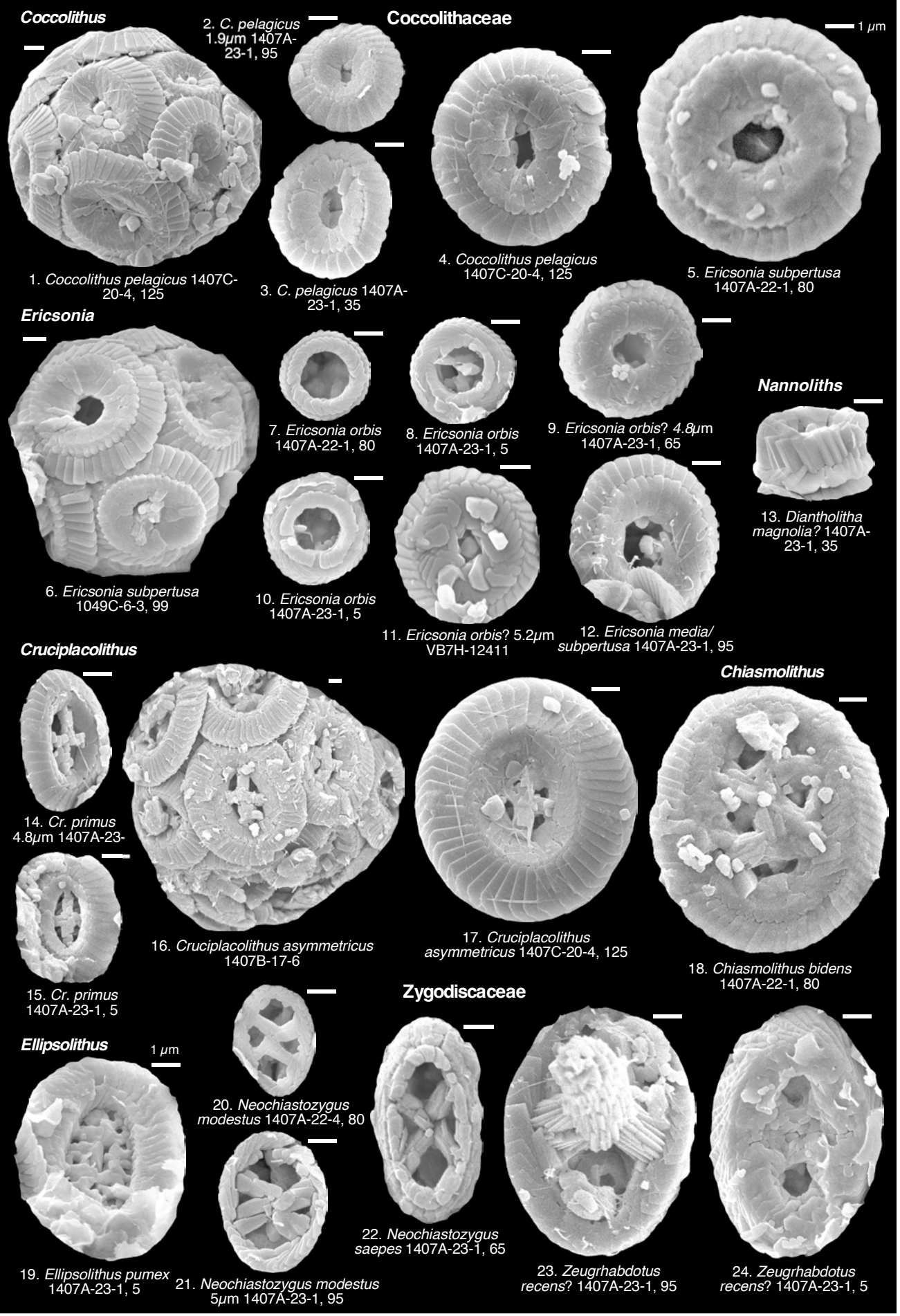
Coccolithus
Coccolithaceae
1 μm
2. C. pelagicus 1.9μm 1407A-23-1, 95
1. Coccolithus pelagicus 1407C-20-4, 125
3. C. pelagicus 1407A-23-1, 35
4. Coccolithus pelagicus 1407C-20-4, 125
5. Ericsonia subpertusa 1407A-22-1, 80
Ericsonia
Nannoliths
7. Ericsonia orbis 1407A-22-1, 80
8. Ericsonia orbis 1407A-23-1, 5
9. Ericsonia orbis? 4.8μm 1407A-23-1, 65
13. Diantholitha magnolia? 1407A-23-1, 35
6. Ericsonia subpertusa 1049C-6-3, 99
10. Ericsonia orbis 1407A-23-1, 5
11. Ericsonia orbis? 5.2μm VB7H-12411
12. Ericsonia media/subpertusa 1407A-23-1, 95
Cruciplacolithus
Chiasmolithus
14. Cr. primus 4.8μm 1407A-23-
16. Cruciplacolithus asymmetricus 1407B-17-6
17. Cruciplacolithus asymmetricus 1407C-20-4, 125
18. Chiasmolithus bidens 1407A-22-1, 80
15. Cr. primus 1407A-23-1, 5
Zygodiscaceae
Ellipsolithus
1 μm
20. Neochiastozygus modestus 1407A-22-4, 80
22. Neochiastozygus saepes 1407A-23-1, 65
19. Ellipsolithus pumex 1407A-23-1, 5
21. Neochiastozygus modestus 5μm 1407A-23-1, 95
23. Zeugrhabdotus recens? 1407A-23-1, 95
24. Zeugrhabdotus recens? 1407A-23-1, 5